Enabling High Wind Penetration in Electrical Grids

by

Mohab Elnashar

A thesis
presented to the University of Waterloo
in fulfillment of the
thesis requirement for the degree of
Doctor of Philosophy
in
Electrical and Computer Engineering

Waterloo, Ontario, Canada, 2011

AUTHOR'S DECLARATION

I hereby declare that I am the sole author of this thesis. This is a true copy of the thesis, including any required final revisions, as accepted by my examiners.

I understand that my thesis may be made electronically available to the public.

Abstract

Wind generation has become one of the most popular choices of technology for adding new generation capacity to power systems worldwide. Several factors have contributed to the increased integration of wind generation, including environmental concerns and the continual increase in fossil fuel prices. As well, recent regulations have moved toward limitations on greenhouse gases, especially in the European Union (EU). Similar laws are currently under consideration in the US and other parts of the world. Other factors have also promoted the use of wind energy, such as advances in manufacturing and control technology and the attractiveness of wind as a "green" source of energy.

The large-scale integration of wind power into an electricity system introduces planning and operational challenges because of the intermittent nature of wind speed and the difficulty involved in predicting it. For these reasons, wind energy is often considered an unreliable energy source. Additional problems are associated with the integration of large-scale wind farms into an electrical grid, among which wind power fluctuation is the most challenging. To maximize the penetration level of wind energy in a grid, a reliable technology must be developed in order to eliminate or at least decrease wind power fluctuation.

The primary goal of this thesis was to develop methods of maximizing the penetration level of wind energy conversion systems (WECSs) into a grid, which requires mitigating wind power fluctuation. A robust control technique has therefore been developed for mitigating wind power fluctuation. This control technique exploits historical environmental data collected over a number of years in order to evaluate the profile of the output power of a variety of wind energy conversion systems (WECSs). The developed control technique was applied to Types A and C WECSs modifying the pitch angle controller of Type A WECS and the back-to-back converter control of Type C WECS. The Attachment of a storage device to the WECSs after the control technique is applied was investigated from both an economic and a technical point of view. The optimum sizing and siting of the wind energy conversion system equipped with the proposed control technique was also studied.

This research is expected to contribute to the advancement of WECS technology by presenting a feasible solution to the problems associated with the integration of large-scale WECSs into electrical grids.

Acknowledgements

I thank God for helping me achieve this work.

I then would like to thank my supervisors, Professor Magdy Salama and Professor Ramadan El Shatshat for their continuous guidance throughout the period of my PhD studies. Their valuable suggestions and discussions were always helpful and inspiring. Also, their support and encouragement were my greatest motive to aim for the best.

I would also like to thank my Ph.D. committee members: Professor Mehrdad Kazerani, Professor Ehab El Saadany, Professor Tarek Hegazy, and the external examiner Professor Osama Mohamed from Florida International University.

My appreciation is also extended to my colleagues in the power group for their help and support. Also, many thanks to my colleagues in the PAMI research group.

I would like to show my deepest gratitude and respect to my family, especially my parents, the ones to whom I owe all the success in my life. I pray God to bless them and reward them. A final word to my wife; without you I could have never been able to achieve this work. Your patience and encouragement were always a source of strength for me.

Table of Contents

List of Figures

List of Tables

Chapter 1
Introduction

1.1 General

The approaching depletion of fossil fuels, environmental regulations due to the increase in the greenhouse effect, the rapid advancement of control and power electronics technology, and the new deregulated electricity market structures are the main factors that have led to an increasingly widespread use of renewable energy sources, which include wind, photo-voltaic, tidal, and geothermal. When these types of renewable energy are used as electrical energy sources in distribution systems, they are known as distributed generation (DG) [1-5]. In addition to renewable energy, micro-turbines, fuel-cells, and conventional diesel generators are also used in DG systems (DGs). DGs can relieve transmission congestion, reduce power losses, and maintain voltage levels within acceptable ranges. In addition, renewable energy DGs have the advantage of providing customers with clean energy.

Of the previously mentioned types of renewable energy systems, wind energy conversion systems have become the most popular choice for new generation installations in power systems worldwide. At the beginning of 2006, the estimated capacity of installed wind generation reached 60,000 MW, which corresponds to energy generation of 120 TWh per year [6]. Since large wind farms are now connected to transmission systems, wind energy is considered “utility scale” and can affect utility system planning and operations for both distribution and transmission systems. Wind energy has therefore received considerable public attention and has become the fastest-growing energy source in the last decade. The global installed wind capacity is expected to increase rapidly over the next decade because many governmental regulators around the world have implemented or are in the process of implementing policies to encourage this growth.

The operational difficulties introduced because of the stochastic nature of wind power have been recognized for some time and have been the subject of a number of studies that address this topic. However, the impact on power systems the uncertainty associated with

will become more fundamental when wind generation contributes a more significant portion of the total power generated.

1.2 Motivations

One of the problems associated with the large-scale integration of wind energy is the intermittent nature of wind and its effects on the operation of a power system and on the electricity market. The intermittency of the wind is defined as continuous variations in wind speed that result in lower power controllability and predictability and higher power variability compared to those associated with conventional power generation. The integration of intermittent wind power into existing power systems may affect the technical operation of the system. Hence, utility managers might become more reluctant to increase the integration of wind energy into a grid over time [7]. The following subsections introduce the most common challenges that are created by the intermittent nature of wind power and that are encountered during its integration into electrical grids.

1.2.1 Power Fluctuations

Wind power is proportional to the cube of the wind speed which is stochastic in nature, i.e., continuously changing from minute to minute, hour to hour, and even from season to season. Small variations in wind speed result in large wind power fluctuations, which are considered the main problem associated with wind power generation and the main barrier to increasing the integration of wind power into an electrical grid [8-15].

The undesirable effects of wind power fluctuations on power systems can be divided into their technical and economic impact. From a technical prospective, wind power fluctuations cause frequency deviation [9, 16-18] and, especially in remote areas, bus voltage fluctuations [13-15]. They also influence the stability and security of the power system [19]. Economic factors include the impact on the required spinning reserve capacity [15], the unit commitment and dispatch [20], and the market price of electricity [21-23].

1.2.2 Penetration Level

The determination of the penetration level, which is the amount of wind power that can be connected to a grid without violating the grid codes, is one of the most difficult challenges facing a power system operator. Grid codes are defined as the rules, standards, and guidelines that are set by national agencies or associations and that must be followed by power system participants [24, 25]. The difficulty in determining the penetration level results from its dependence on many factors, such as the total system losses, the voltage profile, the reactive power support, and the protective device settings. The stiffness ratio of a system, which is the short circuit capacity of the grid divided by the summation of the short circuit capacities of the wind farm and the grid at the point of common coupling [26], is considered another important factor that can be used to determine the maximum capacity of the wind power that is integrated into a grid at a specific point.

1.2.3 Storage Devices

Because wind energy is not dispatchable, a number of storage systems have been introduced in order to convert the wind energy into dispatchable energy. DC batteries, hydrogen, and hydro-storage are examples of storage systems employed in conjunction with wind power generation. Using one of these storage systems helps stabilize the output power of wind generation, i.e., reduce power fluctuation [27]. During periods of high generation and low consumption, the storage device is charged, and when consumption increases and/or wind generation decreases, the storage device boosts the power in the electric grid. Storage systems are classified according to their storage capacity, i.e., long term or short term, or according to their design technology, i.e., chemical, electromechanical, etc.

Selecting the appropriate type and choosing the optimum size of the storage device are important considerations in addressing the challenges of increasing the penetration level of wind energy. Technical and economic studies are key factors in such decisions [28, 29].

1.2.4 Trading Wind Power in a Liberalized Electricity Market

Due to the uncertainty and uncontrollability of wind speed as well as the difficulty of predicting it, forecasting generated power is a challenge for both the wind farm owner and

the system operator. Even with state-of-the-art forecasting methods, the short-term generation produced by wind farms cannot be predicted with a high degree of accuracy. In a liberalized market situation, forecasting errors lead to commercial risk because of imbalance costs imposed on wind power generation through in-advance contracting [23]. In addition, in order to increase the penetration level of wind energy, the system operator is forced to allocate greater spinning and supplemental energy reserves in order to keep the system balanced, which causes the total price of electricity to rise [15].

A variety of pricing schemes for generated wind power have been introduced for different utilities. In some markets, such as the United Kingdom [21], this type of power is treated in the same manner as traditional power; however, in others, more flexibility is employed in pricing wind generation in order to encourage this type of clean renewable energy, as happens in North American markets [30].

1.3 Research Objectives

This research focuses on the development of a comprehensive study for the purpose of enabling high wind penetration levels in electrical grids, and hence, improving system performance. This study has addressed the challenges mentioned and developed new and effective solutions for addressing them.

The main objectives of the research can be summarized as follows:

1) Model Type A and Type C wind energy conversion systems (WECSs) and simulate their output power based on real-time data.

2) Introduce a new control technique for overcoming the power fluctuation problem, and hence, maximizing the penetration level of wind energy and improving the performance of power systems.

3) Apply this new control technique to fixed-speed wind generation (Type A WECS) by modifying the existing pitch-angle controller in order to enable the dispatching of the wind energy.

4) Apply an optimization technique for selecting an adequate type and optimum size of storage device to be connected to Type A WECS. The purpose of this storage device is to compensate for the energy lost due to the application of the control technique mentioned. The application of this technique will increase the overall efficiency of a wind farm.

5) Develop a new wind energy conversion system configuration based on variable-speed wind generation with a doubly fed induction generator (Type C). The developed system introduces a storage system connected between two back-to-back converters with a novel control technique based on artificial intelligence. This system will increase the market share of this type of wind energy in the grid.

6) Apply an optimization technique for selecting an adequate type and optimum size of storage device associated with the proposed Type C wind energy conversion system configuration. This technique will increase system efficiency.

7) Conduct technical and economic studies in order to validate the improvements gained by applying the developed control methodology.

8) Apply an optimization technique for selecting the optimum size and site of a large wind energy conversion system after the new control technique has been applied.

1.4 Thesis Outline

The research based on the objectives listed is presented in this thesis, which is organized as follows:

1. Chapter 2 presents an overview of the types of wind energy conversion systems. This chapter focuses on Type A and Type C WECSs because of the popularity and the high market shares of these two types. The overview is supported by models and governing equations for each type of WECS and the associated control strategies.
2. Chapter 3 discusses the technical and economic impact of connecting large-scale wind energy conversion systems to the grid. This chapter concentrates on wind power

fluctuations because they are considered to be the main challenge in and barrier to increasing wind power penetration into electric networks.

3. Chapter 4 presents the new control technique to be applied in a WECS in order to reduce wind power fluctuations. The proposed control technique relies on wind power leveling. The power levels were calculated using data clustering and wind energy maximization.
4. The application of the developed control technique to a Type A wind energy conversion system is described in Chapter 5. The application was achieved by modifying the pitch angle controller associated with Type A WECS. An optimization technique was also applied for selecting an adequate type and optimum size of storage device to be connected to Type A WECS. The purpose of this storage device is to compensate for the energy lost due to the application of the control technique.
5. In Chapter 6, the application of the control technique presented in Chapter 4 to Type C WECS is explained. The application required the developed of a new configuration of Type C WECS with a storage device connected between the two back-to-back converters and the converter controller modified to accommodate the new configuration.
6. Chapter 7 presents the investigation of the optimum size and site of large-scale wind-based distributed generation (WBDG) to be connected to the grid. The optimization process considers that the WBCS runs under the developed control technique described in Chapter 4. An IEEE 24-bus meshed system used for reliability test assessment was also used in this research to test the new method.
7. Chapter 8 outlines the contributions of the presented research and includes the future work.

Chapter 2
Wind Energy Conversion Systems: An Overview

2.1 General

In recent decades, grid-connected wind turbines have gradually been enhanced until they have become MW-size power generation units. These units are usually accompanied by advanced control systems. Wind farms are generally equipped with two types of control systems: wind turbine and central automatic [31]. A wind turbine control system performs several control actions, such as turbine operation and grid connectivity, based on the information received about wind speed, generator voltage, and utility operating conditions. A central control and monitoring system that uses a supervisory control and data acquisition (SCADA) system is also required for wind farms, particularly large farms with a large number of wind turbines. A central control system monitors and sends control signals to each turbine in order to fully control the entire wind farm operation.

This chapter presents brief background information about wind energy conversion systems (WECSs) and a detailed survey of the literature related to the control techniques applied to a variety of types of WECSs.

2.2 Wind Turbine Characteristics

Wind turbine output power is proportional to the cube of the input wind speed. Fig. 2.1 shows typical wind turbine characteristics [32]. As wind speed increases, turbine output power also increases. Unfortunately, the peaks of different wind speed curves are not coincident. Therefore, to obtain the maximum allowable output power for every wind speed level, the rotor speed should track the peaks of the wind speed levels. This process is called the maximum power tracking method.

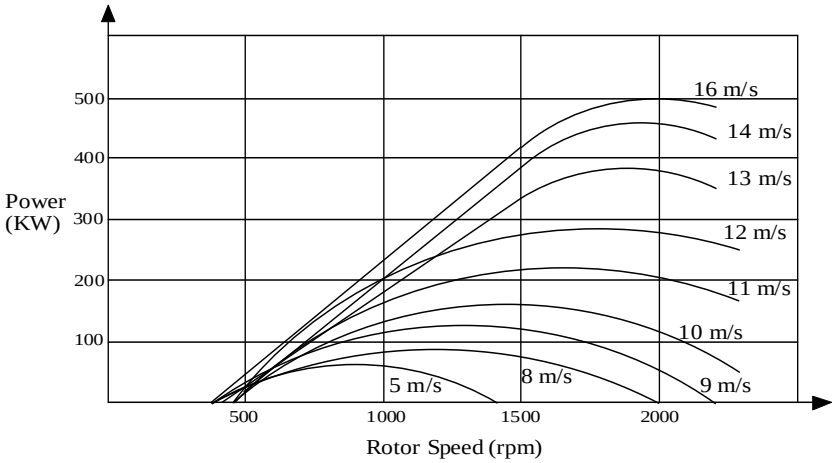

Fig. 2.1: Wind turbine characteristics [32]

The power output from a wind turbine can be expressed according to its rated power (P_{rated}), cut-in speed (V_{cut-in}), rated speed (V_{rated}), and cut-out speed ($V_{cut-out}$). Fig. 2.2 depicts the typical wind power-speed characteristics of a wind turbine [33].

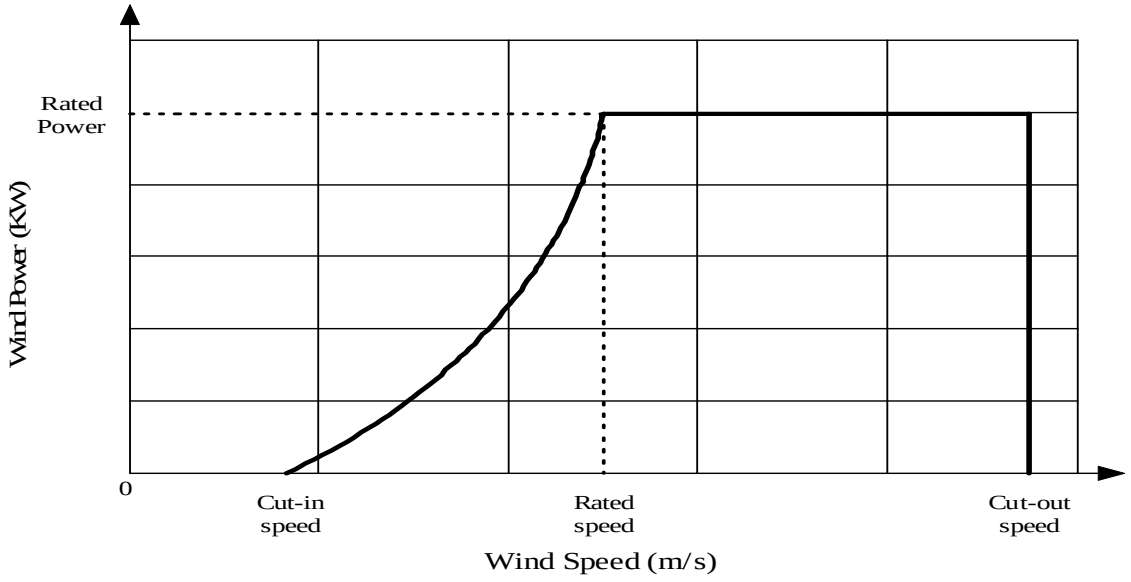

Fig. 2.2: Wind power-speed characteristics of a wind turbine

The mathematical function that relates the power output from a wind turbine to wind speed can be written as follows [34]:

$$P_{out}(V) = \begin{cases} 0 & 0 \le V \le V_{cut-in} \\ (a + bV + cV^2) P_{rated} & V_{cut-in} \le V \le V_{rated} \\ P_{rated} & V_{rated} \le V \le V_{cut-out} \\ 0 & V \ge V_{cut-out} \end{cases} \quad (2.1)$$

where

$P_{out}(V)$ is the power output from a wind turbine,

V is the wind speed in m/s,

$a, b, and\ c$ are constants, and

P_{rated} is the turbine rated output power.

The constants $a, b, and\ c$ can be expressed by V_{cut-in} and V_{rated} in order to represent the cubic relation between the wind power output and the wind speed and can be obtained from the following relations [34]:

$$a = \frac{1}{(V_{cut-in} - V_{rated})^2} [V_{cut-in}(V_{cut-in} + V_{rated}) - 4 V_{cut-in} V_{rated} \left(\frac{V_{cut-in} + V_{rated}}{2 V_{rated}} \right)^3] \quad (2.2)$$

$$b = \frac{1}{(V_{cut-in} - V_{rated})^2} [4(V_{cut-in} + V_{rated}) \left(\frac{V_{cut-in} + V_{rated}}{2 V_{rated}} \right)^3 - 3(V_{cut-in} + V_{rated})] \quad (2.3)$$

$$c = \frac{1}{(V_{cut-in} - V_{rated})^2} \left[2 - 4 \left(\frac{V_{cut-in} + V_{rated}}{2 V_{rated}} \right)^3 \right] \quad (2.4)$$

2.3 Wind Turbine Generators

Wind energy conversion systems (WECSs) are divided into four categories according to their construction: Type A, B, C, and D. Type A WECS belongs to the fixed-speed class of wind turbine generators, and Types B, C, and D are variable-speed wind turbine generators. In fixed-speed wind turbine generators, the generator is connected directly to the grid, and hence, the frequency of both the grid and the machine are coupled; i.e., the machine rotates at a constant speed regardless of the wind speed. On the other hand, the power converter in variable-speed wind generators enables the system frequency and the rotating speed of the machine to be decoupled. Figs. 2.3.a to 2.3.d show the configuration of fixed- and variable-speed wind turbine generators. In this research, only Types A and C wind energy conversion systems were considered because of the high market share of these two types: approximately 30 % and 45 % of market capacity, respectively [35].

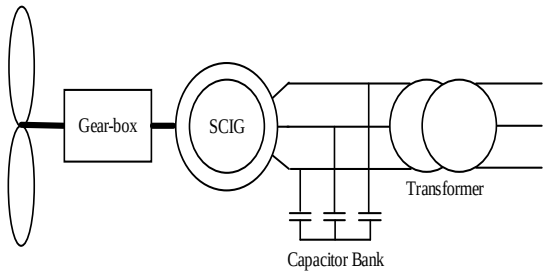

Fig. 2.3.a: Type A wind energy conversion system

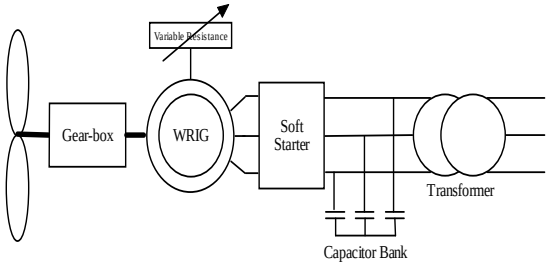

Fig. 2.3.b: Type B wind energy conversion system

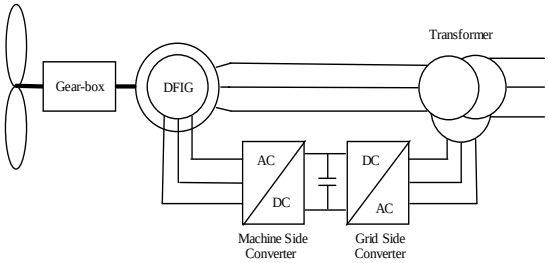

Fig. 2.3.c: Type C wind energy conversion system

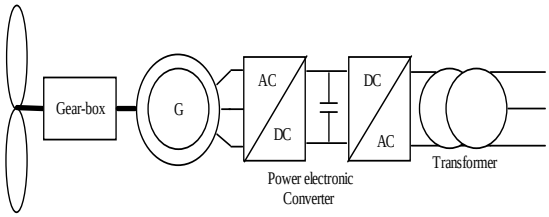

Fig. 2.3.d: Type D wind energy conversion system

2.4 Fixed-Speed Wind Energy Conversion System

Type A wind power generation consists of a wind turbine, a gearbox, and a squirrel cage induction generator (SCIG) whose terminals are connected directly to the grid. The direct connection of the SCIG terminals to the grid causes the rotor to be coupled with the grid frequency so that it operates at a fixed speed. Fig. 2.4 shows the characteristics of a fixed-speed WECS. The rotor speed is selected so that it aligns with the peaks of commonly occurring wind speeds. Observation of the power curve of a fixed-speed generator reveals that as wind speed increases, output power also increases until the generator reaches its rated output power. An increase in the supplied output power appears as an increase in the generator torque because the rotor speed is always fixed. After the rated generator output power is reached, the pitch angle control starts to increase the pitch angle, i.e., the angle of attack of the wind to the blades, in order to reduce any extra increase in the effective wind speed. If the wind speed reaches the cut-out speed, i.e., the maximum allowable wind speed, the stall control applies the brakes to the blades while the pitch angle control increases the pitch angle to the maximum.

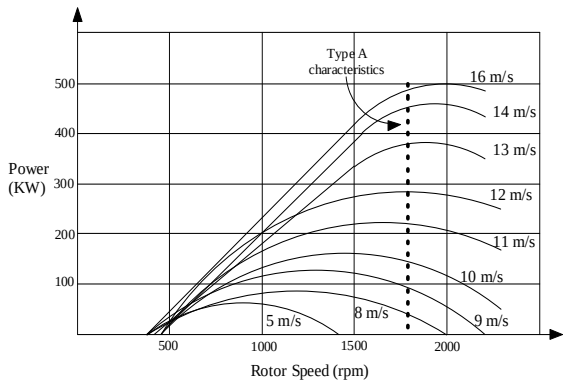

Fig. 2.4.a: Type A WECS characteristics [32]

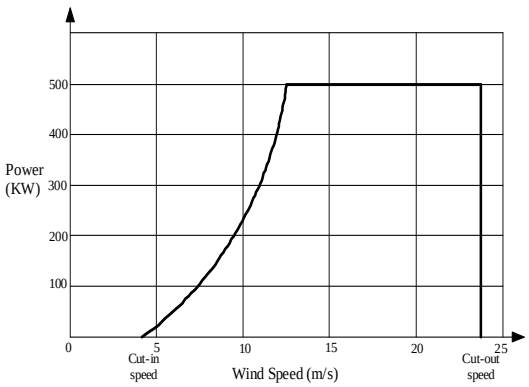

Fig. 2.4.b: Power curve for a fixed-speed generator

2.4.1 Pitch Angle Control

Employing blade pitch angle control is considered the most effective and reliable method of controlling the mechanical input power of a wind turbine. A blade pitch is similar to the

throttle valve in conventional steam turbines; however, a pitch angle control is much faster than a governor control in a steam turbine [27, 36, 37]. This kind of control methodology is implemented in medium-sized and large wind energy conversion systems in order to regulate the mechanical input power and hence the electrical power output of the wind turbine generator. A blade pitch angle control is also the usual method for controlling the output power at wind speeds above the rated wind speed [13, 38-40]. A description of a pitch angle control and the associated equations are as follows:

The control quantity of a pitch angle $G(\beta)$ is given by [12]

$$G(\beta)=\frac{\Delta\beta}{\Delta P}=\frac{1}{A_1+A_2V^2} \tag{2.5}$$

for

$$\begin{aligned} A_1 &= a_{12}+2a_{13}\beta+3a_{14}\beta^2 \\ A_2 &= a_{22}+2a_{23}\beta+3a_{24}\beta^2 \end{aligned} \tag{2.6}$$

where $a_{12}-a_{24}$ are constants; v is the wind speed; and ΔP and $\Delta\beta$ are small-signal state variables of the generator output power (P_g) and the pitch angle (β), respectively.

As shown in Fig. 2.5, $G(\beta)$ in Equation (2.5) depends on the wind speed (v), which varies from the cut-off wind speed to the rated wind speed. A pitch angle control follows the turbine output power curve, as shown in Fig. 2.6. For example, in region (a) in Fig. 2.6, the wind speed is lower than the cut-in speed, and the available power is minimal ($P=0$ p.u.) therefore, the pitch angle controller sets the pitch angle β to 90°, i.e., zero output power. In region (b), however, where the output power varies from $P=0$ p.u. to $P=1$ p.u., the blade angle is set to its minimum value, typically 5° to 10°. In region (c), the pitch angle varies

between its minimum and 90° in order to keep the output turbine power at P=1 p.u. Finally, in region

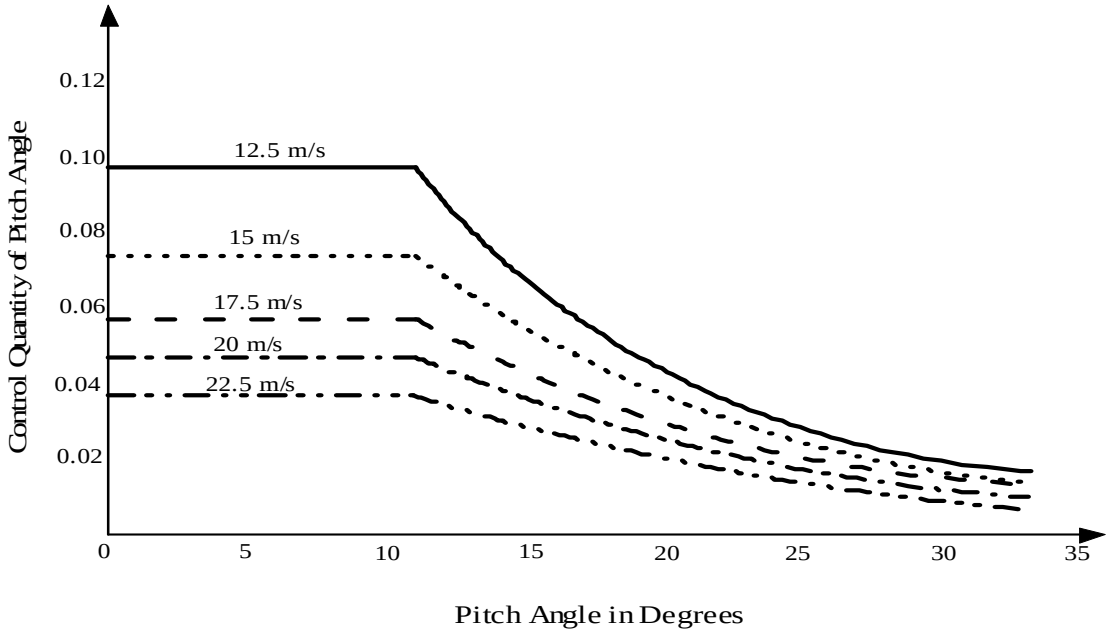

Fig. 2.5: Control quantity of the pitch angle

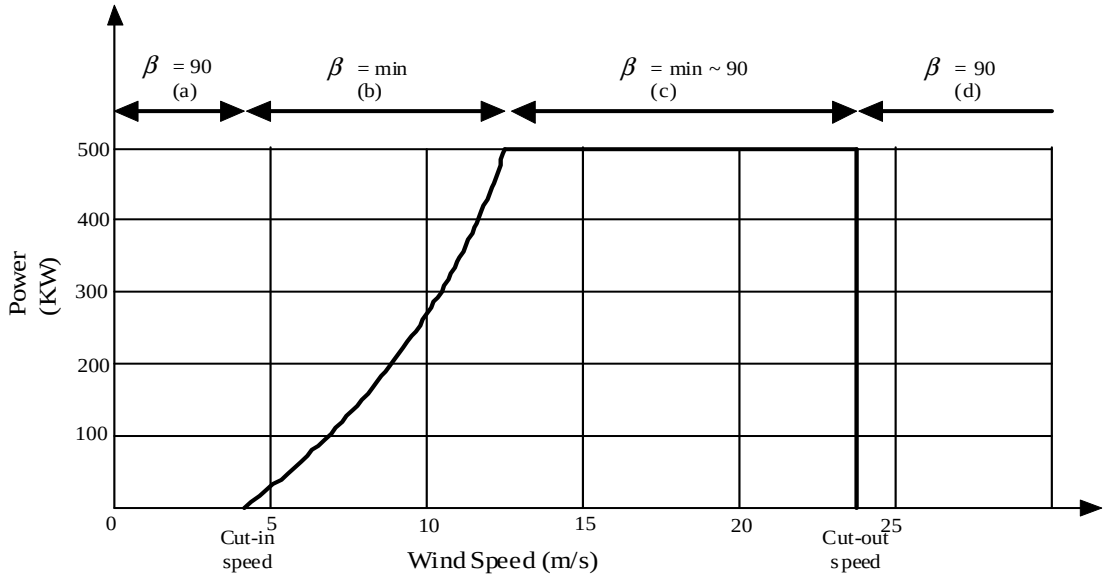

Fig. 2.6: Wind turbine output power curve

(d), for safety reasons, the pitch angle β is set at 90° in order to keep the output power at $P=0$ p.u.. Fig. 2.7 shows a block diagram for the pitch angle controller that resolves the pitch angle output β_{output} , where the output power error e is used as input into the lead-lag controller. The pitch angle variable $\Delta\beta$ is obtained by multiplying the output power signal ΔP of the PD controller and $G(\beta)$ of (3.1). Then, from the addition of $\Delta\beta$ and β, the pitch angle output β_{output} can be obtained, as shown in Fig. 2.7.

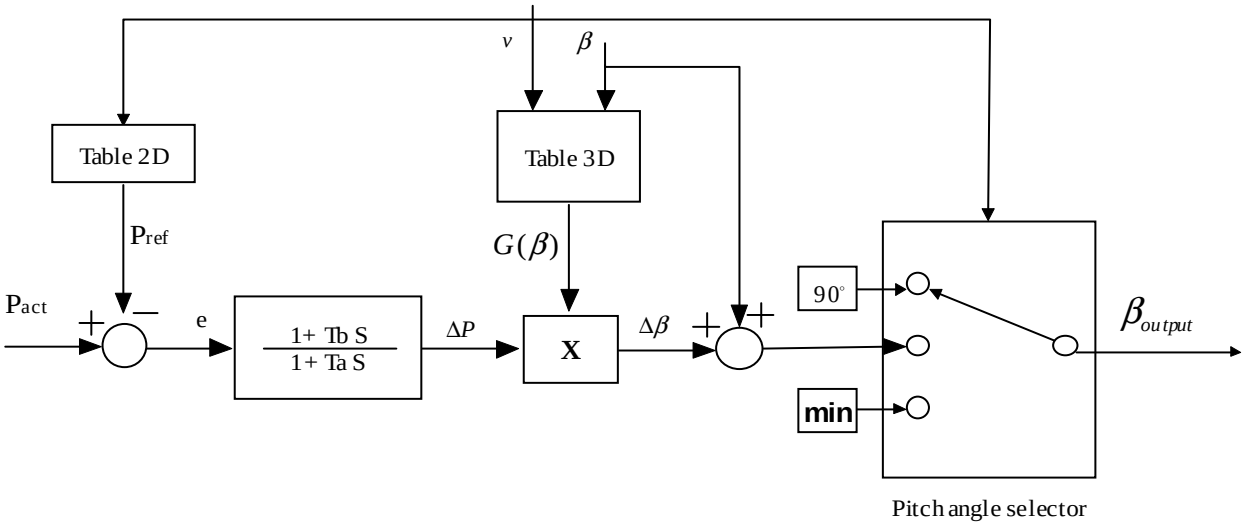

Fig. 2.7: Pitch angle control system

2.4.2 Stall Control

Two basic types of stall control are used to control and protect a wind turbine: passive and active. In passive stall-controlled turbines, the inherent aerodynamic properties of the blade determine the power output without any change in blade geometry. The twist and thickness of the rotor blade vary along its length in such a way that turbulence occurs behind the blade when the wind speed becomes too high. This turbulence means that less of the energy in the air is transferred, minimizing power output at higher speeds. On a passive stall-regulated

wind turbine, the process is very similar to the operation of a pitch angle controller except that the blades move in the opposite direction. Rather than decreasing the angle of attack of the wind on the blades, the stall controller increases the angle of attack in order to send the blades into a deeper stall, thus wasting the excess energy in the wind. An important advantage of active stall control over pitch angle control is that the blade remains essentially stalled at wind speeds above the rated wind speed, so that wind gusts result in much smaller cyclic fluctuations in blade loads and power output.

2.5 Variable Speed Wind Energy Conversion Systems

2.5.1 Type B WECS

Type B wind power generation consists of a wind turbine, a gearbox, a wound rotor induction generator (WRIG), a soft starter, a capacitor bank, and an interface transformer. The WRIG is equipped with a resistor controlled via a power electronics circuit that consists of a diode bridge and a DC chopper. Both the resistor and the power electronics circuit are connected to the rotor winding and are usually mounted on the rotor to eliminate the slip rings and hence minimize the maintenance cost. The duty ratio of the DC chopper is controlled to adjust the effective value of the resistor which allows the rotor to vary its rotational speed up to ± 10% of its rated speed in order to enhance the power quality and reduce the mechanical loading of the turbine components. This type of control is known as OptiSlip. In addition to the OptiSlip, the wind turbines of Type B WECS are equipped with an active blade pitch control system as well as passive stall control. The generator is connected directly to the grid. A capacitor bank provides the reactive power compensation. A smoother grid connection is achieved through the use of a soft-starter.

The wind turbine generates power when the rotor speed exceeds the generator's synchronous speed. As the wind speed increases, the power input to the generator increases, the rotor slip increases, and hence the electrical output power increases. As long as the input power from the wind turbine is below the rated power, the external rotor resistors are short circuited (duty ratio = 1). However, when the input power to the generator begins to exceed

the rated power, the external rotor resistance is adjusted to keep the output of the turbine constant. Analysis of Type B WECS is beyond the scope of this research.

2.5.2 Type C WECS

Type C wind power generation consists of a wind turbine, a gearbox, and a doubly fed induction generator (DFIG) with its stator terminals connected directly to the grid. The DFIG rotor terminals are also connected to the grid through an AC/DC/AC converter which allows a complete decoupling between the rotor speed and the grid frequency; i.e., the rotor speed can be easily changed without being affected by the grid frequency. Fig. 2.8.a and Fig. 2.8.b show the characteristics of a variable-speed WECS. As the wind speed increases, the output power increases, and the rotor speed also increases in order to keep tracking the peak points of the wind speed curves. When either the rated power or the cut-out speed is reached, the same procedures described for a Type A WECS are take effect in a Type C WECS; i.e., the pitch angle controller is activated.

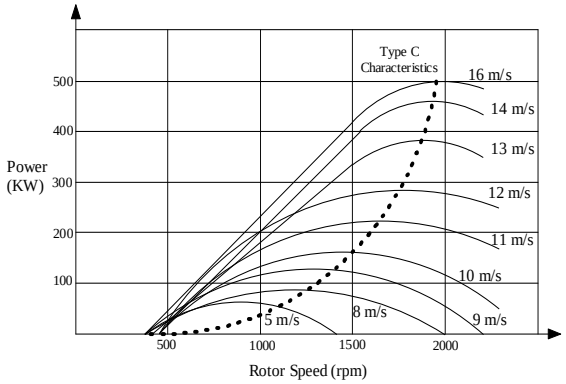

Fig. 2.8.a Characteristics of Type C WECS [32]

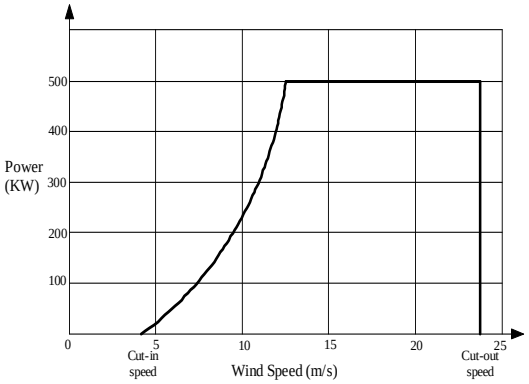

Fig. 2.8.b Power curve for a variable speed turbine

Type C WECS has two modes of operation: sub-synchronous and super-synchronous. In sub-synchronous mode, when the wind speed is low, the generator speed is lower than the synchronous speed, and most of the power is transmitted through the stator while part of the power is circulated in the rotor circuit. On the other hand, in super-synchronous mode, when

the wind speed is high, the generator speed exceeds the synchronous speed, and the power is transmitted through both generator circuits. The converter in the rotor circuit allows the distribution of power between the two circuits.

2.5.2.1 Doubly Fed Induction Generator Control

Doubly fed induction generators (DFIGs) were successfully used in the wind energy conversion systems in the early 1990s. To control both the mechanical parameters (torque and speed) and the electrical parameters (active and reactive power delivered to the grid) of the machine, two back-to-back voltage source converters are connected in the rotor circuit. The machine-side converter, which is connected directly to the rotor's terminals, is responsible for controlling the DFIG parameters, such as DFIG speed, torque, and currents. On the other hand, the grid-side converter, which is connected to the grid's terminals, is responsible for controlling the active and the reactive power delivered from the rotor to the grid. The machine-and grid-side converters are discussed in the next subsections.

DFIG-based wind energy conversion systems are variable-speed wind generators in which the speed is controlled mainly to maximize the amount of power captured from the wind (maximum power tracking) [41]. The DFIG stator and rotor voltage equations are as follows:

$$V_{sabc} = R_s I_{sabc} + \frac{d\lambda_{sabc}}{dt} \tag{2.7}$$

$$V_{rabc} = R_r I_{rabc} + \frac{d\lambda_{rabc}}{dt} \tag{2.8}$$

Transforming Equations (2.7) and (2.8) to the synchronously rotating reference frame allow them to be written as [42, 43]

$$V_{sd} = R_s I_{sd} - \omega_s \lambda_{sq} + \frac{d\lambda_{sd}}{dt} \tag{2.9}$$

$$V_{sq} = R_s I_{sq} + \omega_s \lambda_{sd} + \frac{d\lambda_{sq}}{dt} \tag{2.10}$$

$$V_{rd} = R_r I_{rd} - (\omega_s - \omega_r)\lambda_{rq} + \frac{d\lambda_{rd}}{dt} \quad (2.11)$$

$$V_{rq} = R_r I_{rq} + (\omega_s - \omega_r)\lambda_{rd} + \frac{d\lambda_{rq}}{dt} \quad (2.12)$$

where ω_s is the angular speed of the synchronous *dq* reference frame, and ω_r is the angular speed of the rotor. The stator and rotor flux linkages are given by

$$\lambda_{sd} = L_{ls} I_{sd} + (I_{sd} + I_{rd}) L_m = L_s I_{sd} + L_m I_{rd} \quad (2.13)$$

$$\lambda_{sq} = L_{ls} I_{sq} + (I_{sq} + I_{rq}) L_m = L_s I_{sq} + L_m I_{rq} \quad (2.14)$$

$$\lambda_{rd} = L_{lr} I_{rd} + (I_{sd} + I_{rd}) L_m = L_r I_{rd} + L_m I_{sd} \quad (2.15)$$

$$\lambda_{rq} = L_{lr} I_{rq} + (I_{sq} + I_{rq}) L_m = L_r I_{rq} + L_m I_{sq} \quad (2.16)$$

where $L_s = L_{ls} + L_m$ and $L_r = L_{lr} + L_m$ are the stator and rotor inductances, and L_{ls}, L_{lr} and L_m are the stator leakage, rotor leakage, and mutual inductances, respectively. The electromagnetic torque can be written as

$$T_{em} = p\,(\lambda_{sq} I_{sd} - \lambda_{sd} I_{sq}) = p\,L_m\,(I_{sd} I_{rq} - I_{sq} I_{rd}) \quad (2.17)$$

where *p* is the number of pole pairs.

The typical stator and rotor resistances, especially in large induction machines, are very small and could be neglected. Hence, the stator active and reactive powers can be expressed as follows [43]:

$$P_s = 1.5\,(V_{sd} I_{sd} + V_{sq} I_{sq}) \quad (2.18)$$

$$Q_s = 1.5\ (V_{sq}I_{sd} + V_{sd}I_{sq}) \tag{2.19}$$

Similarly, the active and reactive rotor powers are expressed as follows:

$$P_r = 1.5\ (V_{rd}I_{rd} + V_{rq}I_{rq}) \tag{2.20}$$

$$Q_r = 1.5\ (V_{rq}I_{rd} + V_{rd}I_{rq}) \tag{2.21}$$

The following subsections briefly describe the two voltage source converters connected in the rotor circuit.

2.5.2.2 Machine-Side Converter

Three control loops in the machine-side converter control four parameters in the DFIG: rotor current, output torque, rotor speed, and stator DFIG reactive power. With respect to the current controller, the rotor current is decoupled into *d* and *q* components; the *q* component of the rotor current largely determines the torque produced while the *d* component can be used to control the reactive power at the stator terminals. The governing equations of the controller of the machine-side converter are explained in Chapter 6.

Since the stator flux ψ_s is almost fixed to the stator voltage, torque can be controlled by the *q* component of the rotor current, I_{rq}. Since it is difficult to measure torque, it is most often controlled in an open-loop manner. Therefore, the *q* component of the reference current can be determined from the reference torque, T_{ref}.

However, the current dynamics should be set to be much faster than the speed dynamics so that the speed can be controlled in cascade with the current.

Finally, since the flux for a DFIG system can be considered to be constant, the relationship between the reactive power and the *d* component of the rotor current is static.

The *d* component of the rotor current can therefore be used to control the reactive power of the DFIG, which is usually set to operate the machine at a unity power factor.

2.5.2.3 Grid-Side Converter

The main purpose of a grid-side converter is to control the dc-link voltage. Control of the grid-side converter consists of a fast inner current control loop, which controls the current through the grid, and an outer, slower, control loop that controls the dc-link voltage. The reference frame of the inner current control loop is aligned with the grid flux, which means that the *q* component of the grid current controls the active power delivered from the converter and that the *d* component of the grid current, accordingly, controls the reactive power. This arrangement implies that the outer dc-link voltage control loop must act on the *q* component of the grid current. The governing equations of the controller of the grid-side converter are included in Chapter 6. The block diagram of the DFIG controller is shown in Fig. 2.9.

2.5.3 Type D WECS

Type D wind turbine generator, in its simplest form, consists of a gearbox, a generator, and an AC-to-AC full power converter. Various types of generators are being used, such as synchronous generators, permanent magnet generators, and squirrel cage induction generators. Because it is completely decoupled from the grid, it can provide a wider range of operating speeds than the Type C and has a larger range of reactive power and voltage control capacities. Its main disadvantage is the cost of the full-size power converter. However, recent advances and the relatively lower cost of power electronics components make it feasible to build variable-speed wind turbines with power converters that have the same rating as the turbines. The control strategy for a Type D WECS is very similar to that of a Type C WECS. The examination of a Type D WECS is beyond the scope of this research.

Many studies have compared different types of generators used in wind energy conversion systems with respect to performance, cost, power quality issues, and control complexity [44, 45]. These studies showed that although a constant-speed SCIG is more rigid and easier to control, it produces power with a higher level of fluctuation [44]. However, compared to both

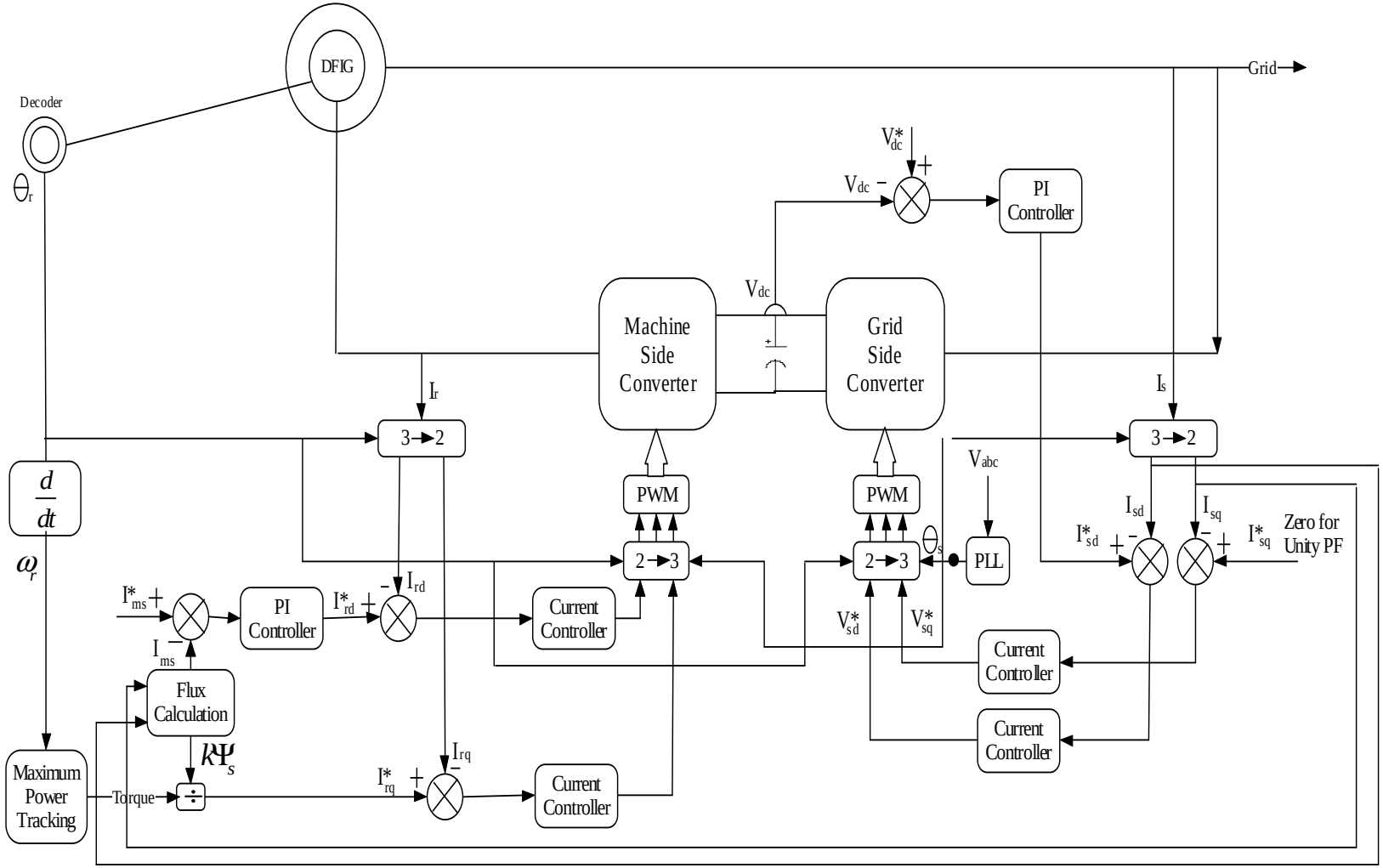

Fig.2.9 Block diagram of the DFIG controller

constant-speed and full-converter SCIGs, the extra cost of the slip rings in a DFIG are compensated for by the smaller converter and the energy captured during the super-synchronous mode. Regarding power quality issues, the performance of a DFIG is much better than that of the SCIG during 80 % of the symmetrical and asymmetrical voltage sags [45].

2.6 Storage Systems

The variability in and difficulty of predicting generated wind power has created significant interest in adding a storage system to wind generation. Energy storage systems, such as DC batteries, compressed air, hydro-storage, hydrogen-based systems, and flywheels, can offer sufficient flexibility for operation in connection with the stochastic generation of wind energy [46]. In areas where expansion of the transmission capacity is undesirable due to environmental, economic, or technical restrictions, energy storage connected to wind generation terminals can increase the exploitation of the energy source in order to supply local loads with constant power.

Generally, storage systems can be classified either according to their technology, as electrical and electromechanical, or according to their conducting period, as short or long term. The following subsections introduce energy storage systems that are classified as short or long term.

2.6.1 Short-Term Energy Storage Systems

Short-term storage systems are characterized by their ability to supply the required level of energy for a short period of time, i.e., for seconds or perhaps a few minutes, and by their corresponding relatively low prices compared to long-term storage systems. Short-term storage systems are integrated into wind energy conversion systems mainly to mitigate high-frequency variations in wind power, i.e., flickers. They can also be used to enhance the low-voltage ride-through capability of wind generators. The ride-through capability of a WECS is defined as the ability of a power source to deliver usable power for a limited time during a power loss [47].

2.6.1.1 Flywheel Energy Storage

One of the oldest and most reliable energy storage devices is the flywheel. It is often employed in small wind energy conversion system applications and can be used to eliminate short-term (seconds to minutes) power fluctuations [48].

In previous studies, flywheel energy storage (FES) has been integrated into wind energy conversion systems (WECSs) in order to enhance power quality [49-51]. The problem of voltage sags and sudden changes in load demand in a stand-alone system has been investigated with respect to constant- and variable-speed WECSs. FES has been proven to enhance the power smoothing of a constant-speed WECS [50, 51]; however, in variable-speed WECSs, FES allows control of the DC-link voltage of the grid-side power converter and hence the power flow from the variable-speed WECS to the grid [49]. The main drawbacks of FES are its extra size and weight, and the limited durability of the stored energy. From an economic point of view, a case study has shown that for a 1 MW capacity wind turbine, connection with a 15.9 KWhr FES that can store energy for a maximum of 10 min produces a gain of about $30,000 per year [52].

2.6.1.2 Super-Capacitor Energy Storage

In addition to flywheel storage devices, super-capacitor storage is considered one of the most promising short-term energy storage systems. Super-capacitor storage has recently been shown to have higher efficiency and a longer life cycle than batteries [53].

Super-capacitor energy storage has recently become one of the most attractive alternatives for enhancing the performance of wind energy conversion systems through the mitigation of high-frequency wind power fluctuations [53, 54]. A super-capacitor is applied in a constant-speed WECS through a DC-DC converter in order to control active and reactive power, thus compensating for power fluctuations [54]; however, super-capacitors fail in the case of low-frequency fluctuations. They have also been integrated into a doubly fed WECS at the DC-link in order to compensate for rapid power variations and to enhance the fault ride through capability of the wind turbine [53].

2.6.2 Long Term Energy Storage Systems

Unlike short-term energy storage systems, long-term storage systems are characterized by their ability to store energy for very long periods, which might reach several months in the case of pumped hydro storage. However, they have the disadvantage of higher capital investment and running costs. For example, building a reservoir for pumped hydro storage with a 2100 MW generating capacity costs about $ 1.7 billion [55].

Long-term energy storage systems were implemented in power systems even before the integration of renewable resources into the networks. They are used in substations in order to enhance the stability, reliability, security, and power quality of the power system. However, when they are attached to a renewable energy resource, they are used to convert a stochastic renewable energy source into a dispatchable one. The use of storage systems is consequently included in power system planning operations as well as in daily power scheduling.

2.6.2.1 Battery Energy Storage

Compared to other types of storage systems, a battery storage device has a number of attractive features. They are able to store a large quantity of energy, and they can deliver this energy in the form of transferred power at either slow or extremely high rates without being damaged. They are also rugged and reliable and provide a source of constant power. For these reasons, a battery storage system is a well-proven storage technique for wind energy conversion systems [56-58].

Connecting battery storage to a wind turbine generator enhances the combined system's participation in unit commitment and scheduling. Studies have included the considerations of wind speed and load uncertainties but have not addressed real-time wind speed or load data [57]. Nevertheless, actual wind speed and irradiance data have been applied in order to investigate a wind/photovoltaic system combined with battery storage [58]. To increase the penetration level of wind energy, to address power quality issues, and to improve stability margins, a combination of battery storage and a reactive power support device such as a static Var compensator or a static synchronous compensator has been proposed in several

studies in the literature [59, 60]. However, the cost of combined systems is impractically high.

2.6.2.2 Pumped Hydro Energy Storage

Pumped hydro storage is the process of pumping water into large barriers constructed at a higher level and then retrieving it later. This type of storage system is considered the most reliable but also the most expensive. Some areas, however, have natural reservoirs, in which case, this solution can be both economical and environmentally friendly. The recovery of the stored energy is controlled by the release of the required amount of pumped water through a turbine [61, 62].

Since cost is the main different to the use of pumped hydro as a storage system, the literature examines the effect of attaching a pumped hydro storage system to a wind energy conversion system with respect to operating costs, optimum sizing, and spinning reserve [15, 61]. One method of reducing the total operational cost is to minimize the share of conventional generators in the delivered power [61], but this method might also affect the system reliability. Another method is to minimize the spinning reserve and hence the use of must-run generators, which are usually characterized by low no-load efficiency [15]. The optimum sizing of various types of storage systems is discussed in later subsections.

2.6.2.3 Compressed Air Energy Storage

As with pumped hydro storage, a compressed air storage system stores energy in mechanical form but with greater system flexibility and lower system costs. Implementing a compressed air storage system in a power system has had limited use thus far. Few studies of this topic have been conducted, and most address only the economic aspects. In [63], the author proposed an electricity market model for investigating the economics of a compressed air energy storage system in a system with a high level of wind energy penetration. A variety of parameters were included in the study, such as load characteristics, wind power plant characteristics, energy prices, and generation/transmission system capabilities.

2.6.2.4 Hydrogen Energy Storage

While wind energy can be stored in mechanical form, it is also possible to store it in chemical form by using the electrical output of the wind turbine generator to produce hydrogen and oxygen in an electrolytic cell [62, 64]. The oxygen is traded directly in the oxygen market, while hydrogen can either be traded in the market or used to produce electric power through fuel cells [65].

Both technical and economic studies have been carried out in order to investigate the viability of introducing hydrogen as a storage system and as an end product [65-67]. The technical studies have examined the optimum operational planning for a system consisting of wind generation and a hydrogen storage system that generates hydrogen as a fuel and as electric power through stationary fuel cells. A day-ahead electricity market was selected as a mean of examining the proposed strategy [67]. The disadvantages of the proposed scheme are its exclusion of the consideration of load uncertainty, its use of a dump load, and the fact that the capital cost of the system is ignored. Energy storage in the form of hydrogen combined with renewable energy sources that have different voltage/current characteristics was assessed in order to test the reliability of a system that uses the proposed control methodology. The simulation results indicated that safe and reliable operation is possible with enhanced energy management [66]. The proposed configuration was tested for a stand-alone system without any indication of the consequences of applying it in a grid-connected system.

The economic studies, however, led to different conclusions. On one hand, the studies show that buying electricity from the market at low prices during the off load periods and converting it into hydrogen to either sell or convert back to electricity has been proven to be a source of considerable profit [67]. On the other hand, those who consider wind their only energy source found hydrogen to be an infeasible system [65].

2.6.3 Thermal Energy Storage

Thermal energy storage is the latest development in storage system technology. The basic concept is either to store energy in thermal reservoirs or to use it in a different application. The thermal reservoir may be maintained at a temperature above or below that of the ambient environment. The topology proposed in the literature is to combine a wind energy conversion system with thermal energy storage. During periods of low power demand, the unused wind energy is converted to thermal energy that is then used to convert a hydrocarbon fuel to a liquid or gas fuel [68]. The proposed strategy showed very low efficiency; however, the author's opinion was that wind energy is free energy.

2.6.4 Combined Energy Storage

Several studies have proposed a combination of two or more storage devices; in most cases, short-and long-term energy storage systems are combined. Short-term storage is exploited in order to mitigate rapid (high-frequency) power variations. However, a long-term storage system is utilized for low-frequency power variations in order to convert a renewable energy source into a dispatchable one, which could help enhance system reliability and increase the participation of renewable energy sources in the electricity market.

The first combination proposed consisted of a flywheel and a battery storage device, which were applied to an autonomous system [69]. The goal of the proposed configuration is to investigate the deviations in frequency when a renewable energy source supplies a stand-alone system. The simulation results proved that the frequency deviation is very small and that the system can perform adequately. If the proposed system were connected to a grid, however, the control strategy might be completely different.

Another study combined compressed air and super-capacitor energy storage devices [70] in order to ensure a smooth power transition between power levels in a maximum power tracking based on fixed speed wind energy conversion system. This solution seems to require an uneconomical investment.

2.6.5 Sizing of Storage Devices

Economic studies can determine the optimum size of storage device that can be attached to a renewable energy source [28, 29, 64, 65]. The main goal of these studies was to enhance the energy management of the renewable energy source in order to develop better performance and to allow suppliers to bid more flexibly in the energy and ancillary service markets. Different criteria have been used to determine the optimum size of a storage device. These criteria depend on the type of storage device, the type of system (autonomous or grid connected), and the variables included in the optimization function, such as capital cost. The global optimization function of all the studies is either to minimize the total cost [28, 29] or to maximize the system profit [64, 65].

In [28], the optimum size of a pumped hydro storage device combined with a renewable energy source was determined from the identification of the expected price of energy, the costs of the storage unit (fixed and running costs), and the round-trip efficiency of the storage technology. The objective function to be minimized was the expected daily cost of operation and amortization. The capacity of a battery storage device is normally specified in terms of power and energy capacity [46]. The energy capacity describes the amount of energy that can be drawn from or stored in the battery. The power rating determines the power that can be supplied or stored by the battery under the rated discharge/charge time interval. The capital cost of a battery is also determined based on its power and energy capacities [71]. The main drawback of this methodology is that the author assumed that the capital cost of the wind turbine and the power converters are constant [29].

The storage system that causes the most debate with respect to its economic effect is hydrogen energy storage because many alternatives can be taken into account in the optimization function, such as whether to trade hydrogen in the hydrogen market, whether to import (buy) electricity from the market in off-peak periods in order to develop hydrogen for later use, and whether to develop power from the hydrogen using a low-efficiency (maximum of 45 %) fuel cell or to sell all the hydrogen production directly. To investigate the implementation of hydrogen storage systems in a power system, consideration should be

given to the costs of the plant, including the storage system, as well as the additional margins obtainable from the sale of the stored energy [64]. Combining a hydrogen storage system with a base power generator, e.g., a nuclear power generator, has been recently discussed in the literature [65]. The main purpose of the base power was to assure a high level of reliability and continuity of supply; however, the reason for selecting nuclear power specifically was the emerging nuclear electrolyzer technology which has increased efficiency. The results show that for the given realistic assumptions, hydrogen is not a viable option for electricity storage for the current electricity market and pricing. The drawback of this study is the omission of the fixed cost of the proposed system.

2.7 Summary

This chapter has presented brief background information about the components of the wind energy conversion systems (WECSs) and a detailed survey of the literature related to about the control techniques applied to a number of types of WECSs. As previously mentioned, the following chapters will consider only Types A and C wind energy conversion systems because of the high market share of these two types.

Attaching storage devices to wind energy conversion systems has recently received a considerable attention. These devices can be used to reduce fluctuations in the output power of WECSs; to shift the overnight peak wind generation to match the load peaks; and to provide reactive power support. However, the main challenge still involved in the use of storage devices is the high cost associated with their installation. Thus, studying the economic aspect of installing these devices is of great importance. The investigation of this factor is presented in the following chapters.

Chapter 3
Impact of WECSs on Electrical Grids

3.1 General

A typical problem with wind energy conversion systems is the continual variations in the power they produce that result from the direct relationship between the generated power from wind and wind speed, which is random in nature. The main aim of this chapter is to explain the process used to accurately evaluate the technical and economic impact on the performance of the grid that results from the installation of wind energy conversion systems. This chapter also presents a detailed description of the specific power fluctuation problem, its technical and economic impact on power systems, and the solutions proposed in the literature.

3.2 Technical and Economic Impact of WECSs

Wind power fluctuates over time, mainly as a result of changes in meteorological conditions. These power variations occur for all time scales: seconds, minutes, hours, days, months, and seasons. Understanding these variations and the level of their predictability is a critical step in any attempt to increase the penetration of wind generation into and the optimal operation of power systems. Electric power systems are inherently variable because of continual variations in the load and supply but they are well designed to deal efficiently with these changes. The system operator must manage both predictable and unpredictable events in the grid, including scheduled equipment maintenance; line contingencies; sudden loss of a large load/generation; load variations; and, of course, wind power fluctuations.

The short-term variability of wind power (in the order of minutes to hours) is important because it affects the operational scheduling of the generation units, the balancing of demand/load power, and the determination of the amount of reserves needed. Many models have been developed as a means of predicting short-term variations in wind power such as time series models and geographical spreading models.

The long-term variability of wind power (months and years) which is determined by seasonal meteorological patterns and by inter-annual variations in wind speed [31] affects operational and long-term planning for power systems. However, long-term variations can be predicted more accurately than short-term variability.

The ability to obtain power from wind energy sources over the long term is called wind power capacity factor, which is defined as the yearly average wind power divided by the rated power of the wind turbine/farm. A typical value of the wind power capacity factor is 35 %. This capacity factor greatly affects the economics of the wind industry. For example, some countries (e.g., Canada) provide substantial incentives to wind generation so that utilities are obliged to buy all generated power at a high price. On the other hand, countries such as the United Kingdom force wind generators to bid in the market in the same way as conventional generators, and penalties are applied for forecasting errors.

In general, the technical difficulties associated with the integration of wind energy conversion systems into electrical grids are largely due to but not limited to power fluctuations, voltage fluctuations/flickers, the operation and scheduling of generators, system security, and errors in the prediction of wind power generation. On the other hand, the economic difficulties include the high cost of wind turbine generators compared to the annual developed energy, the cost of reserves, storage device costs, and the costs associated with prediction errors.

3.3 Wind Power Fluctuations

It is obvious that the main challenge with integrating wind power in electrical grids is the wind power fluctuations, which sometimes also cause other wind integration difficulties. Wind power fluctuations have other possible causes other than variations in wind speed, such as a blade passing in front of the tower, an imbalance in the rotor turbine, and rotational sampling, and these types of power fluctuations are more severe when the power is delivered by an asynchronous generator coupled directly to the electric grid. The remainder of this chapter therefore focuses mainly on this problem.

Two terms are commonly associated with wind power variations: power fluctuations and flickers. Power fluctuations are slow power variations, in the range of 0.01 Hz; flickers, however, have higher frequency variations, in the range of a few hertz. A flicker is defined as "the impression of fluctuating brightness or color, occurring when the frequency of observed variation lies between a few hertz and the fusion frequency of images, according to the IEEE standard dictionary of electrical and electronic terms" [72].

The difference between flickers and fluctuations is explained in the following descriptions: "Flicker and voltage changes are due to rapid changes in the load, generation output or to the switching operations in the network." "Fluctuations of active and/or reactive power of wind turbines are due to the effects of random wind fluctuation, tower shadow, yaw error, misalignment, wind gusting and wind shear, which cause flickers" [10].

3.3.1 Impact of Power Fluctuations on Power Systems

The fluctuating nature of wind speed and, hence, wind-generated power imposes a number of technical and economical restrictions on a power system. In weak networks as well as strong networks that have large wind energy penetration levels, continuous variations in wind power cause the system voltage to fluctuate, the system frequency to deviate from the nominal frequency, and the generation to be insufficient to feed the loads. With respect to the economic difficulties, the inability of wind farms to supply the power scheduled in a contract results in the imposition of specific penalties, which increases the gross cost of wind generation.

3.3.1.1 Technical Impact

The following subsections explain the technical impact on the operation of the power system of the fluctuations in power produced by wind energy sources.

3.3.1.1.1 Voltage Fluctuations

Some problems, such as small voltage variations and flicker might arise from individual wind turbines or wind farm generation, when variations in wind speed produce mechanical power fluctuations, which cause speed changes in the turbine rotor, leading in turn to variations in

current and voltage in the generators. Voltage flicker can become a factor that discourages utilities from allowing wind turbines to be connected to weak networks, and even prevents integration with relatively strong networks in the case of large amount of wind power being connected [72].

It has been shown that flicker emission from variable-speed turbines is relatively low [7, 10, 14, 73, 74], which means that studying flicker emission from constant-speed turbines has greater value. In variable speed wind energy conversion systems, incoming power fluctuations can be reduced by changing the turbine rotor speed slightly, and the power electronic converters in the wind turbine systems provide the possibility of reducing dynamic voltage fluctuations. Rather than maintaining the reactive power at zero, i.e., unity power factor operation, the reactive power can also be controlled in order to minimize voltage fluctuations caused by wind power fluctuation.

3.3.1.1.2 Frequency Deviation

Only the probabilistically firm component of wind power is traded in the hourly electricity markets [18]. The system operator deducts the forecasted firm component of wind power from the forecasted demand. However, the power required in order to cap the difference between the demand and the wind power is scheduled every hour from conventional power plants in order to maintain a balance between the power supply and the forecasted demand. Power plants handle deviations between actual and forecasted demand and actual and forecasted wind generation by means of an automatic governor control (AGC), which continuously adjust their real power references in order to regulate the system frequency.

Variations in wind speed cause the turbo alternators in power plants to accelerate and decelerate, and consequently, cause the system frequency to deviate from the 50 Hz or 60 Hz standard [16]. Since the under/over frequency relays protect the system against large frequency swings and sustained frequency errors, the frequency deviation caused by wind power fluctuations can falsely trip the frequency protection relays. Tripping of the protective relays of a large wind farm in order to isolate it from the network can apply more stress on

the power system, consequently causing the system operator either to shed some loads or to introduce expensive power generators to the network.

3.3.1.1.3 Power System Stability

There are two types of power system stability: transient and steady state, also called dynamic stability. A fault on a high-voltage transmission network or the loss of a major generating unit is considered a major impact on the power system and might lead to system instability. During such a period, the study of the system dynamics is defined as a transient stability study. Stability depends strongly on the magnitude and location of the disturbance and to a lesser extent on the initial state or operating condition of the system. However, the problem of studying the stability of power systems that are undergoing small load/generation changes has been called a steady-state or dynamic stability problem. Since wind power is known to fluctuate continually, studying system stability with wind generation imbedded in the system is always a dynamic stability problem.

A major issue related to the control and stability of electric power systems is the maintenance of the balance between generated and consumed power. Because of the fluctuating nature of wind speeds, the continual growth of wind power generation in power systems has caused the system operator to focus more on the fluctuations in the power production of wind turbines, especially when the wind turbines are concentrated geographically in large wind farms.

3.3.1.1.4 Power System Security

Power system security analysis is the process of detecting whether the power system is in a secure or an alert state. A secure state implies that the load is satisfied and that no limit violations will occur under present operating conditions or in the presence of unforeseen contingencies. The alert state implies that particular limits have been violated and/or that the load demand cannot be met and that corrective actions must be taken in order to bring the power system back to a secure state.

On small island power systems, wind power fluctuations may have even more severe consequences for the operation and security of the system [19]. An example of such a system is the one on the island of Hawaii, which is not connected to other systems. The ability to integrate wind power into the system on the island is also limited by the generation mix, which includes a relatively large number of non-regulated generating units [75]. Wind power fluctuations are also considered to be a security issue in networks with very weak interconnections. The island of Ireland has a good example of such a system, which has only a very weak connection to the system in Scotland.

3.3.1.1.5 Unit Commitment and Dispatch

The optimal selection of on-line units (unit commitment) and optimal output levels of committed units (dispatch procedures) for conventional generation is considered a serious problem for the system operator and needs to be continually to compensate for any integration of large amounts of wind energy into the electrical networks [20].

Since unit commitment deals with the balance between generated power and loads, wind power fluctuations should be combined with load variations when a unit commitment problem is considered. In other words, the total regulated power from conventional generators at any moment depends on the sum of the wind power and load variations. Wind power fluctuations could counterbalance [76] or amplify load variations [77].

3.3.1.2 Economic Impact

The following subsections explain the economic impact on the operation of power systems due to the fluctuations in power caused by wind energy sources.

3.3.1.2.1 Spinning Reserves

The power generated from wind energy conversion systems is intermittent, which increases the consideration of uncertainty with respect to system reserve. Reserve is defined as the regulated power generators allocated to meet imbalances between the predicted and actual demand. The scale of the wind forecast times is important for determining reserve requirements. For times from several seconds to a few minutes, the overall output fluctuation

in wind generation is small, given the considerable diversity of the output from individual wind farms. Reserve requirements deal with the uncertainty in wind forecasts over periods of minutes to hours.

If wind fluctuations were perfectly predictable, system operating costs would be relatively small for systems with considerable wind power, provided that their conventional power generation has enough flexibility to handle the changes. In reality, forecasting wind power generation is strongly related to the forecasting of multiple atmospheric variables, e.g., wind speed and direction, air density, and spatial scales of atmospheric motion. These difficult wind forecasting uncertainties are considered an additional balancing requirement which can be fairly significant. Wind fluctuations generally follow a normal distribution but with longer tails, which indicate a need for more reserve in order to capture the majority of the imbalances [15]. On the other hand, the reserve allocation affects the system's ability to accept wind generation. A high spinning reserve allocation requires the running of a large number of partly loaded generators; therefore, the total system energy is accompanied by reserve provisions. This "must-run" reserve generation leaves less room for wind power generation.

3.3.1.2.2 Unit Scheduling

Unit scheduling is somewhat similar to unit commitment but is related to an economic perspective. Current short-term power markets are designed for trading conventional (dispatchable) generation. The time span from aftermarket clearing until delivery can be up to 36 h (Scandinavia) or up to 38 h (Spain); any deviations from the submitted production plan are penalized. The penalty associated with imbalances due to wind power is termed the imbalance cost, and it increases the cost of running a wind energy conversion system. At wind penetrations of up to 20 % of the peak demand of a system, it has been also found that the increase in system operating costs that results from wind variability and uncertainty has amounted to about 10 % or less of the wholesale value of the wind energy [78].

3.3.1.2.3 Liberalized Electricity Market

The structure of most deregulated electricity markets is either day-ahead or hour-ahead. In both structures, generators may have to buy or sell energy to cover deviations due to prediction errors. To increase the penetration of wind energy conversion systems (WECSs) in the grid, the large prediction errors that occur with most prediction methods must first be reduced.

An additional point of concern is that in the presence of imbalance costs and uncertain wind generation, a method is required for determining the optimum level of contracted energy that should be sold on the advance markets. To maximize the profits produced by wind power that is traded in a deregulated electricity market, several factors must be considered, e.g., wind power forecasting, wind generation modeling, and optimization.

3.3.2 Proposed Solutions in the literature for the Fluctuation Problem

Many solutions have been proposed for solving the fluctuation problem. One is to keep a minimum level of thermal plant generation in order to maintain an adequate operating reserve and to keep system-control capabilities at about 30 % to 50 % of the capacity of the utility [76]. Below this range, problems begin to arise; however, lower ranges could probably be achieved if the design were modified. This solution is completely specific to the system configuration and parameters and does not take into account the required system reserve.

Another solution [79] is to reduce the bus voltage fluctuation in a variable-speed wind energy conversion system if wind farm converters are used to enhance the reactive power compensation, i.e., to generate reactive power during low system voltage and absorb reactive power during high system voltage. However, this method reduces the amount of active power generated and complicates converter control. It has also been proven that a wind turbine should be connected to a grid with a short-circuit capacity of 50 times the rating of the turbine in order to minimize the flicker emission of the turbine [7], which in most cases is impractical.

Another solution to power fluctuation was proposed in [9], in which it was shown that the generator rotating shafts in thermal and hydro power plants could be modified to make use of inherent inertia and to act as energy storage devices. This solution could provide significant help with the filtering of power fluctuations produced by the wind turbines; however, the dynamic behaviour of the network might be affected.

As previously mentioned in Section 3.3.4.1.2, wind power fluctuation could force the frequency relays to trip, and it has been estimated that if the under/over frequency relay allows a deviation of 1 % of 60 Hz, the peak power fluctuation produced by a single wind frequency could reach 5 % of the total power ratings of thermal plants [14, 16]. This recommendation relates only to grid codes and is not a real solution for wind power fluctuation.

The most common solution to power fluctuation is to attach a type of storage system to either each individual wind turbine or to the aggregated wind turbines at a wind farm [15, 48, 56-59, 61, 63, 64]. Storage is the only device that has the ability to stock generated excesses during high-wind/low-demand periods and then subsequently discharge this energy as needed. Since wind power fluctuations are expected to become more pronounced due to the increase in the wind capacity connected to a grid, the value of storage systems has become more obvious because of the amount of wind energy installed and the inelasticity of some generation systems. From a technical point of view, this solution is almost perfect. However, from an economic perspective, adding a storage system to wind power generation imposes an extra cost, which reduces the gross revenue.

To reduce the output power fluctuations of wind farms, [11, 12] have presented a control strategy of leveling the output power from wind farms. Based on both the average output power of the wind farm and its standard deviation, a control strategy and pitch angle control that uses a generalized predictive controller in all operating regions were implemented. In the proposed strategy, the wind speed is first measured, and the corresponding available average wind farm output power and its standard deviation are then calculated. Next, according to the system operator’s power command, the output power of each wind turbine generator at the

farm is determined, depending on the available (ready) number of wind turbine generators. This solution would affect the amount of energy produced by the wind farm, which might be an economic disincentive.

In [73], the design of an electrical filter suitable for avoiding the flicker effect was proposed. The main problem was the low frequency of the torque oscillation of the wind turbine, which may reach 1 Hz at low rotational speeds. This very low frequency could not be filtered by either the turbine or electrical generator inertia, which causes an oscillation in the generator current. Filtering the flicker is difficult because of its very low frequency, and the technical implementation of this control strategy could be impractical.

3.4 Summary

This chapter has presented a literature survey of the technical and economic impact on the performance of the grid when wind energy conversion systems are installed. Particular emphasis is on the power fluctuation problem associated with wind power generation. The main finding revealed by this survey is the lack of a technically and economically comprehensive solution for power fluctuation. Addressing this issue is the main motivation behind this research.

Chapter 4
The Leveling Technique

4.1 General

The main objective of this chapter is to present a novel control technique that can overcome the main problem associated with the integration of a wind energy conversion system, which is power fluctuation, and hence reduce the associated negative impact discussed in the previous chapter. The general concept of the control technique is presented in the following section, and the application of the stages involved in the method is discussed in detail in the sections that follow.

4.2 The Leveling Technique

The main goal of the developed leveling control technique is to mitigate the power fluctuation that occurs due to the continual variations in wind speed and hence in wind output power. The proposed control methodology relies on wind speed (power) leveling, i.e., selecting a fixed number of wind power levels for a specific time period (day, season, or year) at which the wind turbine will operate. If the wind power is between any two levels, the wind energy conversion system (WECS) controller adjusts the output power to ensure that the effective wind power generated is held steady at the lower level selected.

The scheme for selecting power levels is as follows: first, wind speed data are collected from a candidate site for a specific period of time; the more data collected, the better the control efficiency. Second, the wind speed data are input into a suitable clustering technique which will determine the number of speed levels (clusters) and their values (centroids). Third, the values of the speed levels (power levels) are adjusted in order to maximize the total energy captured based on the number of speed levels and the wind speed data. Finally, the corresponding speeds (power levels) that maximize the total energy captured are applied to the controller of Type A and Type C wind energy conversion systems.

For example, let the output of the clustering technique and the optimization algorithm, for the wind speed curve shown in Fig. 4.1, be three optimum speeds of 6 m/s, 8 m/s, and 10.5 m/s. If the wind speed is lower than 6 m/s, the wind turbine generator produces power corresponding to the cut-in speed. If the wind speed is greater than 6 m/s but lower than 8 m/s, the controller adjusts the WECS to produce power that corresponds to a wind speed of 6 m/s. The same procedure is applied to the other two levels. Fig. 4.2 shows a sample power output of WECS after the leveling technique has been applied.

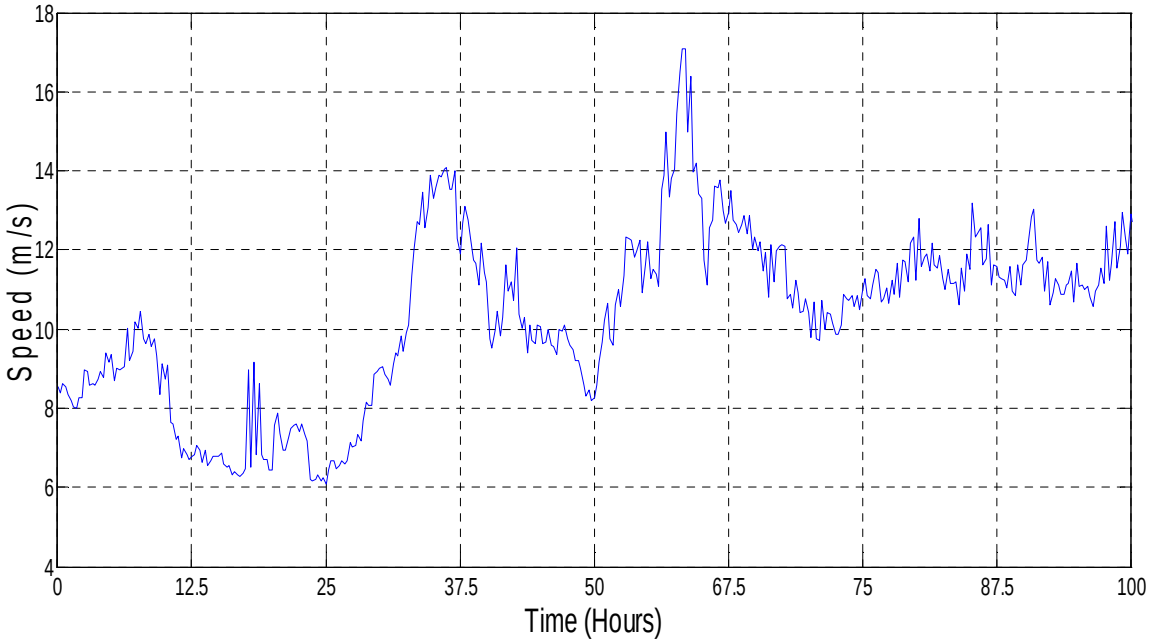

Fig. 4.1: Wind speed before the leveling technique is applied

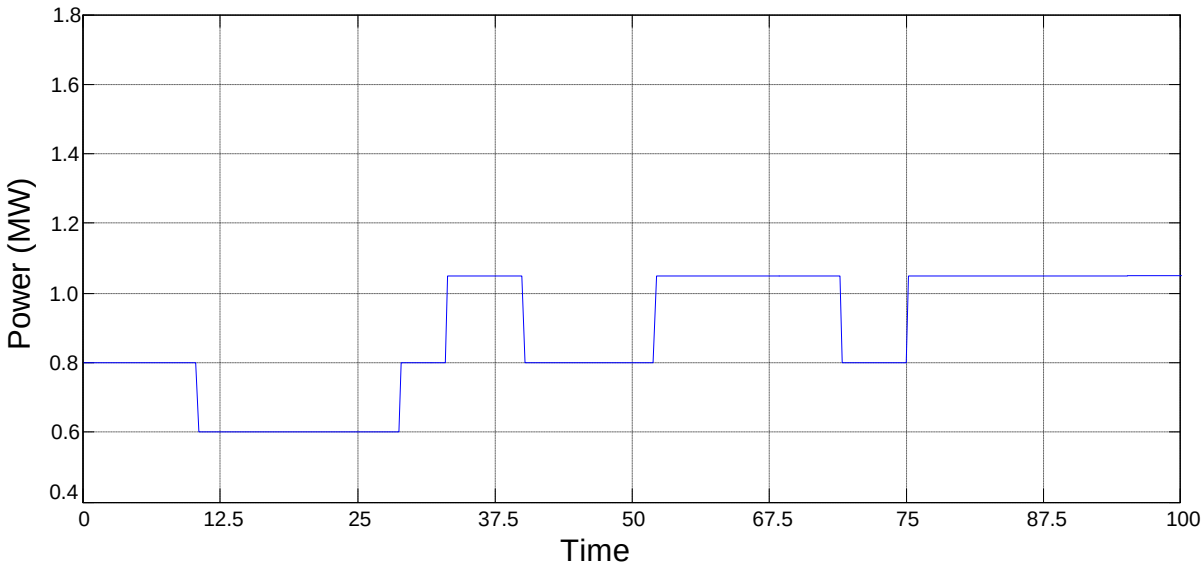

Fig. 4.2: Generated power after the leveling technique is applied

4.3 Wind Speed Data

Many mathematical representations of wind speed were proposed in the literature, two of which have attracted the most attention due to their accuracy and suitability for simulation techniques: probabilistic and chronological representation. The following subsections present a brief description of these mathematical representations of wind speed data.

4.3.1 Probabilistic Wind Data

A typical expression often recommended for modeling the behaviour of wind speed is the Weibull probability density function (pdf), which is a Gaussian density function with a longer tail. This representation uses the Weibull pdf to compare the actual wind speed profile at different sites and the estimated wind speed profile [9].

$$f(v) = \frac{k}{c}\left(\frac{v}{c}\right)^{k-1} \exp\left[-\left(\frac{v}{c}\right)^{k}\right] \qquad \text{Weibull pdf} \qquad (4.1)$$

where k is called the shape index and c is called the scale index. As the shape index k changes, the shape of the pdf changes accordingly, as shown in Fig. 4.3.a. However, Fig.4.3.b shows the effect on the pdf of changing the scale index C. When the shape index k equals 2, the pdf is known as a Rayleigh pdf, which mimics most wind speed profiles. Therefore Equation (4.1) can be written as

$$f(v) = \left(\frac{2v}{c^2}\right)\exp\left[-\left(\frac{v}{c}\right)^2\right] \qquad \text{Rayleigh pdf} \qquad (4.2)$$

where $c \approx 1.128 V_m$ and V_m is the mean wind speed.

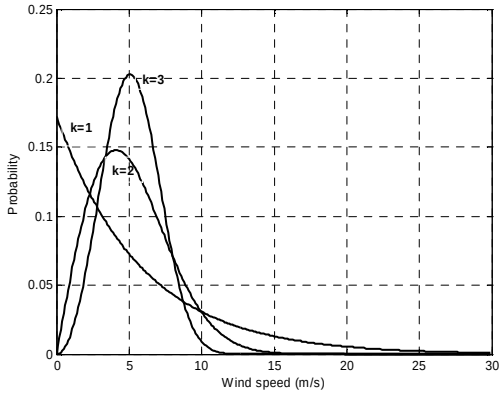

Fig. 4.3.a: Weibull probability density functions with different values of shape index k

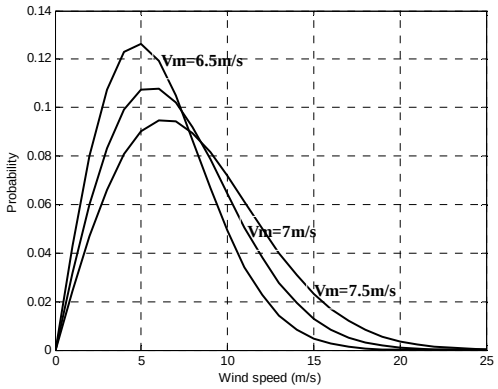

Fig. 4.3.b: Rayleigh probability density functions with different values of scale index c

4.3.2 Chronological Wind Data

Estimating the profile of the output power of the wind energy conversion systems using long historical time series of wind speed and wind direction data is known as chronological simulation. The main advantage of chronological simulations is their ability to include temporal information in the analysis, i.e., time-to-time variations. However, the main drawback of these simulations is that they should be carried out over extensive periods of time in order to provide an accurate evaluation of the performance of the system by including

all possible patterns that can be extracted from the WECSs. Such a study requires collecting historical time series wind speed and direction data at the location where the WECSs are to be installed. The time resolution of the data collected should be suitable for taking into account short-term, i.e., minute-to minute, variations in the wind speed and hence in the generated wind power.

In summary, since the main goal of this thesis is to determine a method of reducing the power fluctuations generated from WECSs and because these power fluctuations involve time-to-time wind speed variations, a chronological representation of the wind speed data was the method considered for this research, and the discussion in the remainder of the thesis is based on this consideration.

4.4 Wind Speed Clustering

Wind speed is stochastic in nature and is closely related to a number of atmospheric variables, such as wind direction, air density, and to spatial/temporal scales of atmospheric motion. For this research, a clustering technique was chosen as the method of determining the most likely wind speed that can occur in a given set of wind data. These most likely wind speeds represents the centroids of the clusters of data and in the developed algorithm these centroids were utilized to minimize fluctuations in the output power.

Cluster analysis is the organization of a collection of patterns, or data points, into clusters based on similarity. Patterns within any given cluster are more similar to each other than they are to a pattern belonging to a different cluster. A simple distance measure such as the Euclidean distance can often be used to reflect the dissimilarity between two patterns [80]. The clustering output can be hard (the data is partitioned into groups) or fuzzy (each pattern has a variable degree of membership in each of the output clusters).

4.4.1 Clustering Techniques

Clustering techniques can be divided into two major categories: supervised and unsupervised. In supervised clustering, the number of clusters as well as the data to be clustered are provided as an input to the clustering algorithm, which assigns each unit of the data entered

to the cluster that has the best fit. On the other hand, unsupervised clustering techniques do not require the number of clusters as input. The number of clusters is determined by the clustering algorithm which makes the clustering algorithm, a longer complicated and requires more run time. The varied approaches to clustering data can be described as shown in Fig. 4.4.

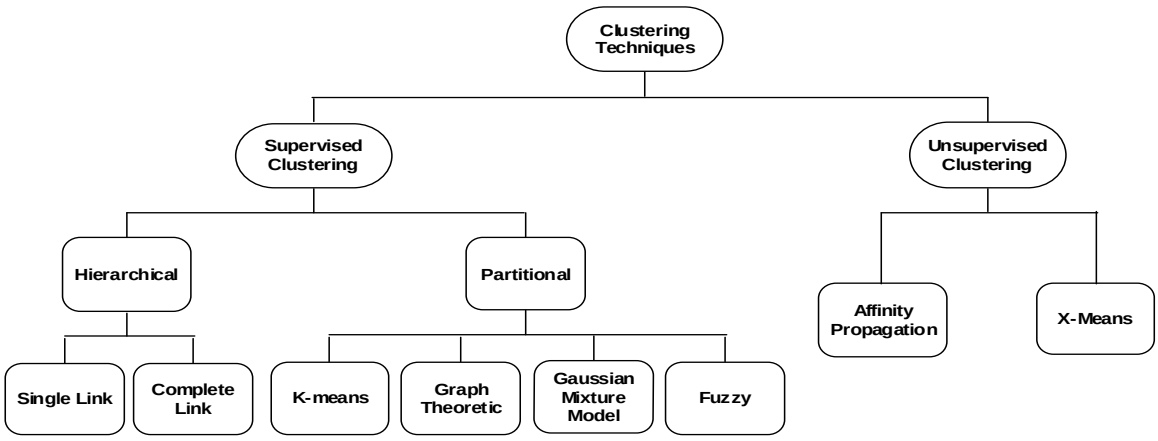

Fig. 4.4: Clustering techniques

4.4.1.1 Supervised Clustering Techniques

Supervised clustering techniques, which require in addition to the number of clusters (i.e., the number of levels) the data entry (i.e., the wind speed data), can be classified as hierarchical, partitional, k-means, graph-theoretic, Gaussian mixture model, or fuzzy.

4.4.1.1.1 Hierarchical Techniques

Most hierarchical clustering algorithms are either single-link [81] or complete-link [82]. These two algorithms differ in the way they characterize the similarities between a pair of clusters. In the single-link method, the distance between two clusters is the minimum of the distances between all pairs of patterns drawn from the two clusters (one pattern from the first cluster, the other from the second). In the complete-link algorithm, the distance between two clusters is the maximum of all pair distances between patterns in the two clusters. In both cases, two clusters are merged to form a larger cluster based on minimum distance criteria.

The clusters obtained by the complete-link algorithm are more compact than those obtained by the single-link algorithm.

4.4.1.1.2 Partitional Techniques

Partitional methods have advantages in applications involving large data sets. The main problem accompanying the use of a partitional algorithm is the need to verify the number of desired output clusters. Reference [83] provides guidance with respect to this key design decision. Partitional techniques usually produce clusters by optimizing a criterion function, such as distance function, defined either locally, based on a subset of the patterns, or globally, defined over all of the patterns. In practice, the algorithm is typically run multiple random times with different starting states, and the best configuration obtained from all of the runs is used as the output clustering.

4.4.1.1.3 K-Means Clustering Technique

The K-means is the simplest and most commonly used algorithm and employs a squared error criterion [84]. It starts with a random initial partition and keeps reassigning the patterns to clusters based on the similarity between the pattern and the cluster centres until the squared error stops decreasing significantly after a number of iterations. The objective it tries to achieve is to minimize the total variance:

$$V = \sum_{i=1}^{k} \sum_{x_j \in S_i} \left(x_j - \mu_i \right)^2 \tag{4.3}$$

where k is the number of clusters; $S_i = 1, 2, ..., k$; and μ_i is the centroid (mean point) of all the points.

A major problem with this algorithm is that it is sensitive to the selection of the initial partition and may converge to a local minimum of the function value of the criterion if the initial partition is not chosen accurately.

4.4.1.1.4 Graph-Theoretic Clustering Technique

The best-known graph-theoretic clustering algorithm is based on the construction of a minimal spanning tree (MST) of the data [85], followed by the deletion of the MST edges with the largest lengths in order to generate clusters.

4.4.1.1.5 Gaussian Mixture Model Clustering Technique

The basic assumption in the Gaussian mixture model technique is that the patterns to be clustered are drawn from one of several distributions, and the goal is to identify the parameters of each distribution (means and variance). Most of the work in this area has assumed that the individual components of the mixture density are Gaussian, and if so, the parameters of the individual Gaussians are to be estimated.

The procedure for this clustering technique is as follows: after the number of clusters is determined, the initial Gaussian means and variances for each cluster are initialized using the K-means algorithm and the distance to the nearest cluster, respectively. The probability of each pattern (data point) belonging to each cluster is then calculated. Based on the probability calculated in the previous step, each point is assigned to the appropriate cluster. All the data points within each cluster are then used to construct new Gaussian probability density functions with new means and variances. If there are major changes in the means and variances, the whole process is repeated; otherwise, the means are considered the optimum centres of the clusters.

4.4.1.1.6 Fuzzy Clustering Technique

Traditional clustering approaches generate partitions; in a partition, each pattern belongs to one and only one cluster. Hence, the clusters in a hard clustering are disjointed. Fuzzy clustering extends this concept to associate each pattern with every cluster using a membership function [86].

4.4.1.2 Unsupervised Clustering Techniques

As previously mentioned, unsupervised clustering techniques do not require the number of clusters to be entered as input. These kinds of clustering algorithms are therefore able to determine the number of clusters (i.e., power levels) as well as the centre of these clusters (i.e., the initial values of the power levels).

The affinity propagation technique and the x-means tecnique are the most popular two types of unsupervised clustering technique and are discussed in the next subsections.

4.4.1.2.1 Affinity Propagation Technique

Affinity propagation is a new technique that takes as input measures of similarity between pairs of data entries and simultaneously considers all data entries as potential exemplars (i.e., number of clusters). Real-value messages are exchanged between data entries until a high-quality set of exemplars and corresponding clusters gradually emerges. Rather than requiring that the number of clusters be entered into the algorithm, affinity propagation takes as input a real number x(k, k) for each data entry k so that data entries with larger values of x(k, k) are more likely to be chosen as exemplars. These values are referred to as “preferences.” The number of identified exemplars (number of clusters) is subjected to the values of the input preferences, but it also emerges from the message-passing procedure.

4.4.1.2.2 X-Means Clustering Technique

K-means is a very popular technique for general clustering. However, it suffers from three major drawbacks: it scales poorly computationally; it might stick in a local minimum; and because it is a supervised clustering technique, the number of clusters must be entered into the algorithm. Recently, a more accurate and efficient technique has been developed. It is based on the k-means but has the ability to self-guess the number of clusters. X-means is a new algorithm that efficiently searches the space of cluster locations and the number of clusters in order to optimize the Bayesian information criterion (BIC) or the Akaike information criterion (AIC) measure.

The x-means algorithm works in the following way. Initially, the lower and upper boundaries of the number of clusters are provided as input to the algorithm. The x-means process begins with the application of a k-means algorithm to the data points with number of clusters is equal to the lower boundary. It then increases the number of clusters by splitting each cluster into halves. The quality of each half is then evaluated against the original cluster by computing the BIC of the split relative to that of the original cluster. If the BIC score increases after splitting, the cluster is replaced by its halves; otherwise, the split is ignored. The splitting process continues until either the upper boundary is reached or no more splits are available. A flowchart of an x-means algorithm is shown in Fig. 4.5. Experiments show that this technique reveals the true number of clusters in the fundamental distribution and that it is much faster than repeatedly using an accelerated k-means for different values of K.

In summary, the main disadvantage of supervised clustering algorithms is that the number of clusters is known initially; i.e., the number of clusters is an input value required by the clustering algorithm. However, unsupervised clustering algorithms can cluster the data into initially unknown clusters. Unsupervised clustering algorithms were determined to be more suitable for this research and were used in the developed control technique. The x-means clustering algorithm is a good unsupervised clustering technique that is efficient and produces reliable results for highly scattered types of data sets[87, 88]. The x-means clustering algorithm was therefore used in this study in order to determine the number of wind speeds (power levels) and the values of these wind speeds (centroids).

The main author of the x-means clustering technique provided an online executable file that includes the code of the algorithm free of charge for users. This code requires as input the data points along with the upper and lower boundaries of the number of clusters, and it has been used in this thesis in order to determine the optimum number of clusters.

4.5 Values of Power Levels

For this research historical wind speed data were used and the number of wind speed levels was determined using the x-means clustering technique. The number of wind speed levels

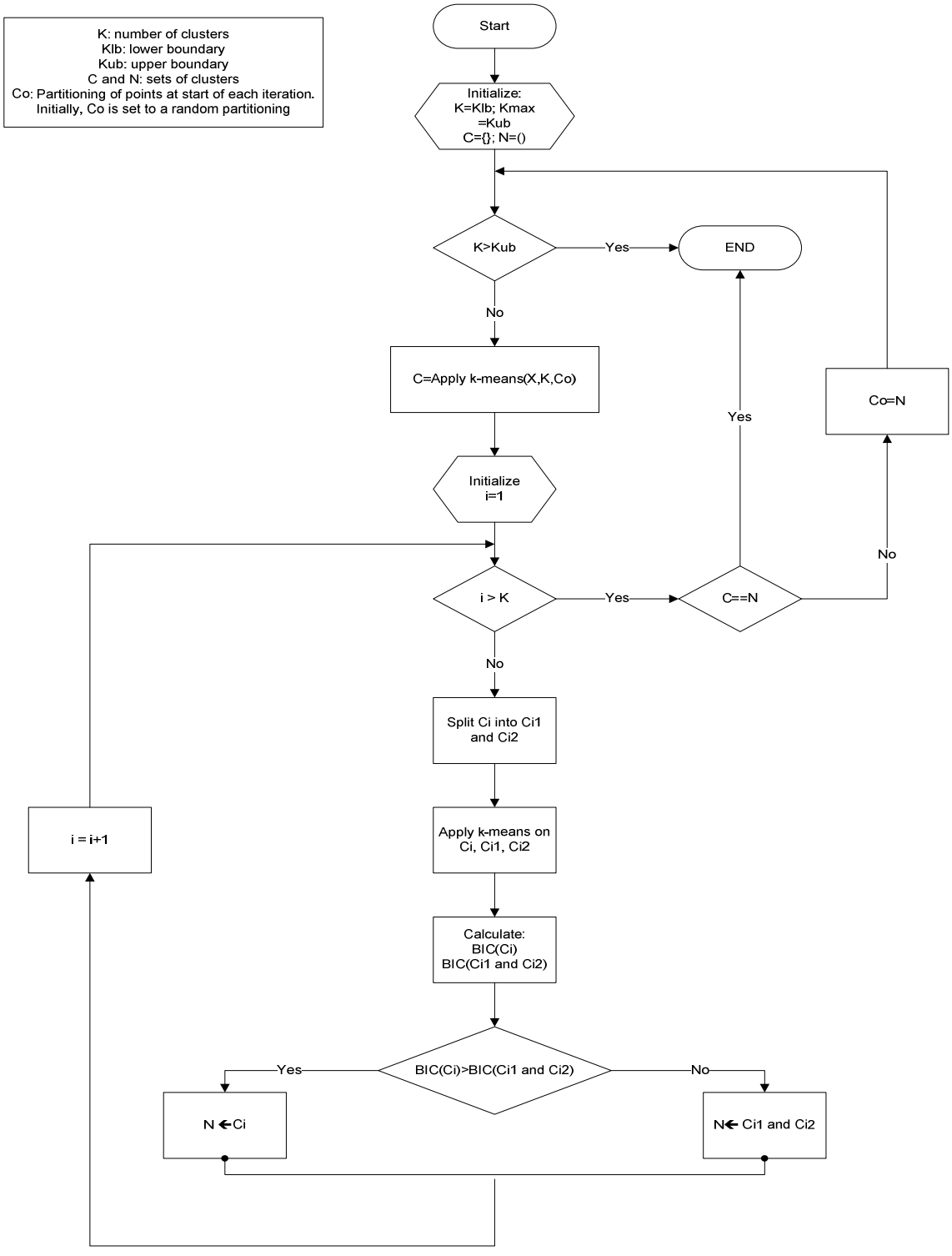

Fig. 4.5: The x-means algorithm

obtained from the x-means clustering algorithm and the wind speed data were applied to the optimization model on an hourly basis in order to determine the values of the power output levels that corresponded to that set of wind speed data records. The objective function of the optimization model is to maximize the energy captured from the available wind speed data by selecting the appropriate speed values; the more data collected, the better the model efficiency. The formulation of the objective function for selecting the appropriate values of power levels can be written as follows:

$$\max \quad \sum_{i=1}^{N} \sum_{j=1}^{K} \alpha_j(i) \left(a + b V_j + c V_j^2\right) P_{rated} \quad \Delta t \tag{4.4}$$

s.t.

$$\alpha_1(i) + \alpha_2(i) + ... + \alpha_{k-1}(i) + \alpha_k(i) = 1 \tag{4.5}$$

$$\begin{aligned}
&V_1 - m\left(\alpha_2(i) + \alpha_3(i) + ... + \alpha_k(i)\right) \le \alpha_1(i) V(i) \le V_2 \\
&V_2 - m\left(\alpha_1(i) + \alpha_3(i) + ... + \alpha_k(i)\right) \le \alpha_2(i) V(i) \le V_3 \\
&\qquad\qquad\qquad\qquad \vdots \\
&V_{k-1} - m\left(\alpha_1(i) + ... + \alpha_{k-2}(i) + \alpha_k(i)\right) \le \alpha_{k-1}(i) V(i) \le V_k \\
&V_k - m\left(\alpha_1(i) + \alpha_2(i) + ... + \alpha_{k-1}(i)\right) \le \alpha_k(i) V(i)
\end{aligned} \tag{4.6}$$

$$V_1 < V_2 < \ldots < V_{k-1} < V_k \tag{4.7}$$

$$V_1 = V_{cut-in} \tag{4.8}$$

$$V_k = V_{rated} \tag{4.9}$$

where N is the number of available wind speed data points, K is the number of power levels obtained by the x-means; $V(i)$ represents wind speed data points, $\alpha_1, \alpha_2, ..., \alpha_k$ are binary

variables, m is a number greater than the cut-out speed, Δt is the sampling time, and $V_1, V_2, ..., V_k$ are the optimum values of the speed levels, i.e., the output of the optimization model.

The non-linear objective function and the binary variables $\alpha_1, \alpha_2, ..., \alpha_k$ make this model a mixed integer non-linear programming (MINLP) model. Equation (4.4) activates only one part of the objective function per wind speed data point; i.e., if the data point lies between V_1 and V_2, then α_1 will be equal to one in order to activate the first part only $\left(a + bV_1 + cV_1^2\right)$, and the rest of the objective function will be equal to zero; hence, the energy will be calculated assuming $V(i) = V_1$, and so on. Equations (4.5) to (4.7) describe the constraints used for determining which level the data point belongs to. Finally, (4.8) and (4.9) set the minimum and maximum levels for the cut-in speed and rated speed, respectively.

4.6 Summary

This chapter has introduced the idea of the novel control technique for reducing wind power fluctuations and hence decreasing the negative impact of large wind energy conversion systems on the performance of the electric network. One of the advantages of the new control technique is its ability to use a long historical time series of data in an efficient and intelligent way in order to maintain temporal information in the wind speed data. The main concept of the developed method is to 1) collect wind speed data from the candidate site; 2) to apply the x-means clustering technique to this wind speed data in order to determine the number of clusters (power levels) and the initial values of these power levels; 3) to use the estimated number of levels, the wind speed data, the cut-in speed, and the rated speed in the optimization algorithm in order to determine the exact values for the power levels that maximize the energy captured from the wind generation.

The following chapters describe the application of the new leveling technique to Types A and C wind energy conversion systems. The existing controllers of both types were modified to accommodate the new leveling technique.

Chapter 5
Applying the Leveling Technique in Type A WECS

5.1 General

This chapter explains how the new leveling technique was applied to Type A wind energy conversion system through the modification of the main controller, which is a pitch angle controller. A classical pitch angle controller basically adjusts the pitch angle to its minimum position when the wind speed lies in the interval between the cut-in speed and the rated speed. When the wind speed exceeds the rated speed, the controller varies the pitch angle to generate an effective power equivalent to the rated power. Since, most of the yearly wind speed belongs to the interval between the cut-in speed and the rated speed, at which point the pitch angle controller is inactive, and because wind power is proportional to the cube of the wind speed, wind power generation is considered one of the major sources of power fluctuation.

Based on the control technique explained in Chapter 4, the classical pitch angle control was extended to cover the interval between the cut-in speed and the rated speed. This interval was divided into small segments, each having upper and lower boundaries (the power levels). Within the segment boundaries, the pitch angle controller was used to control the pitch angle in order to develop a constant level of output power that corresponds to that segment.

The concept of extending the active region of the pitch angle control is not new. In [11, 12], the pitch angle control was extended to all operating regions. Based on both the average output power of the wind farm and its standard deviation, the master controller of the wind farm varies the set points of the pitch angles of each individual wind turbine in order to develop an aggregated power level that matches the power level required by the system operator, i.e., the system operator determines the value of the level at a certain instant and it can vary every dispatch interval. However, in the leveling technique developed in this research, the values of the levels are constant all over the year. The levels are based on the on-site wind speed data, they have optimum number, and they have optimum values.

5.2 Modification of the Pitch Angle Controller

As previously mentioned, the new algorithm was applied to Type A wind energy conversion system which has blade pitch angle controller as the main controller. As shown in Section 2.4.1, the pitch angle controller is effective only when the wind speed reaches or exceeds the rated value. However, in the developed control methodology, the pitch angle controller was modified so that it is active for all wind speeds. Two major modifications were applied to the controller in order to facilitate the application of the leveling methodology to a Type A WECS. These modifications were made in the two lookup tables circled in Fig. 5.1.

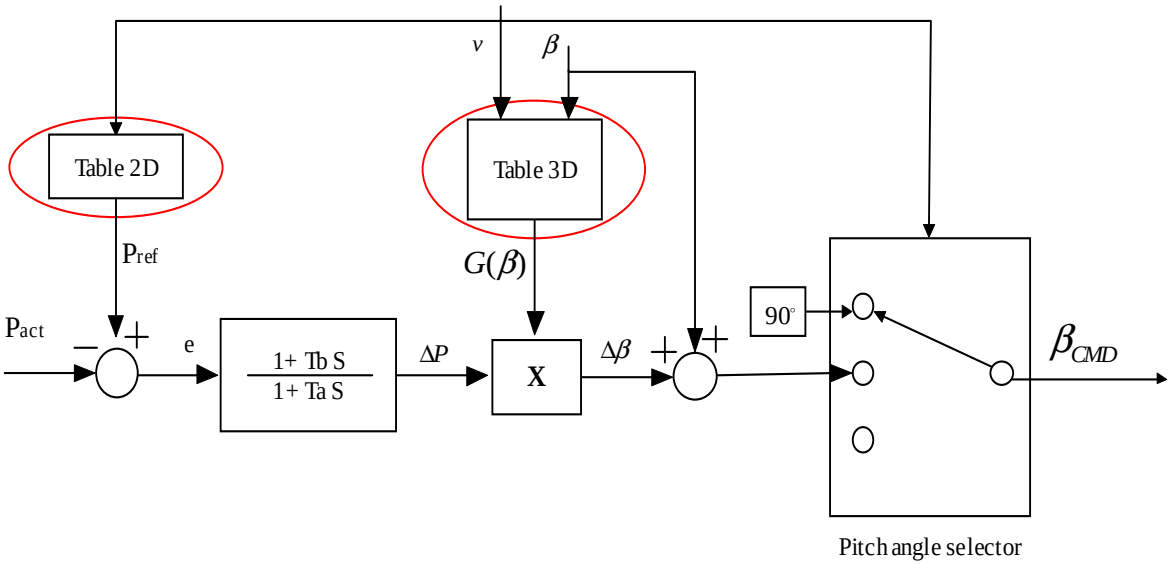

Fig. 5.1: Modified pitch angle control system

The first lookup table that provides the reference power (P_{ref}) is now fed only by the number of levels selected and their corresponding values. If the wind speed lies between any of the wind levels selected, the lookup table automatically selects the lower level, as previously mentioned. The reference power signal therefore always corresponds to one of the power levels selected.

On the other hand, the second lookup table, responsible for developing the control quantity signal, was modified to include all the available wind speeds, which covers the

whole range between the cut-in speed and the cut-out speed. Fig. 5.2 and Fig. 5.3 show the entries to the lookup table in both cases, i.e., before and after the application of the leveling methodology.

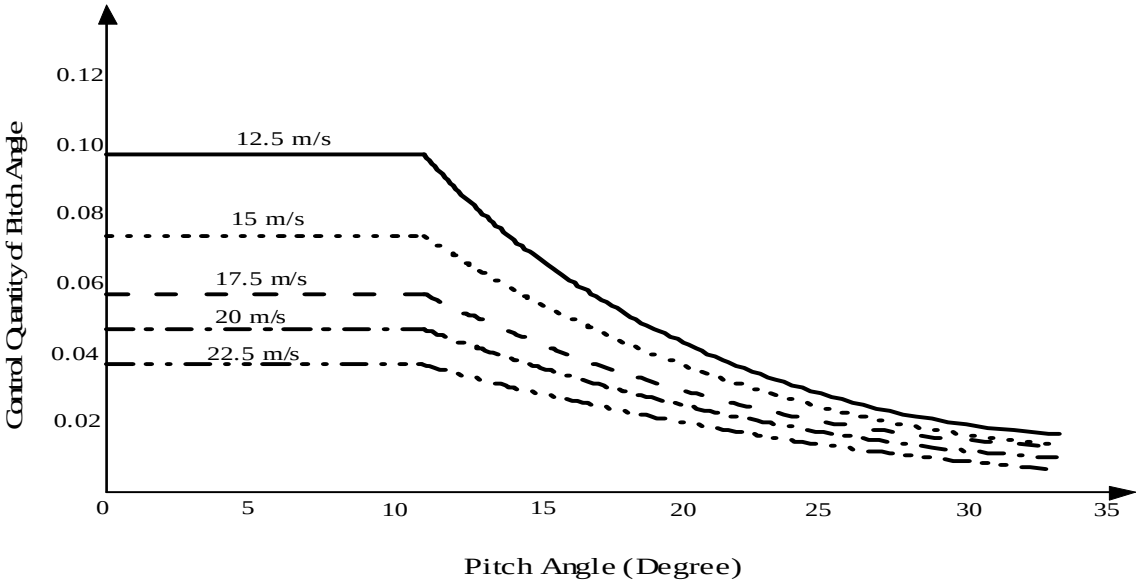

Fig. 5.2: Control quantity before the application of the leveling technique

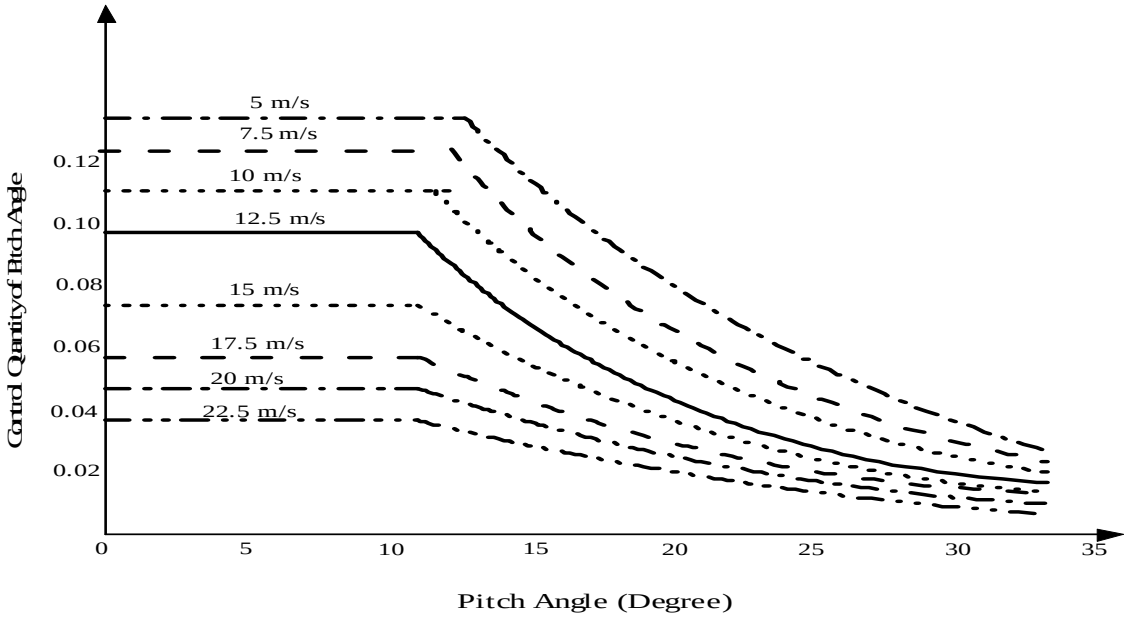

Fig. 5.3: Control quantity after the application of the leveling technique

Fig. 5.4 shows the wind turbine power curve after the application of the modifications to the reference power signal, i.e., after the application of the leveling technique. The region from the cut-in speed to the rated speed is now divided into sub-regions of constant power output. Fig. 5.4 also shows that the pitch angle control law has been extended to cover the region from the cut-in speed to the cut-out speed.

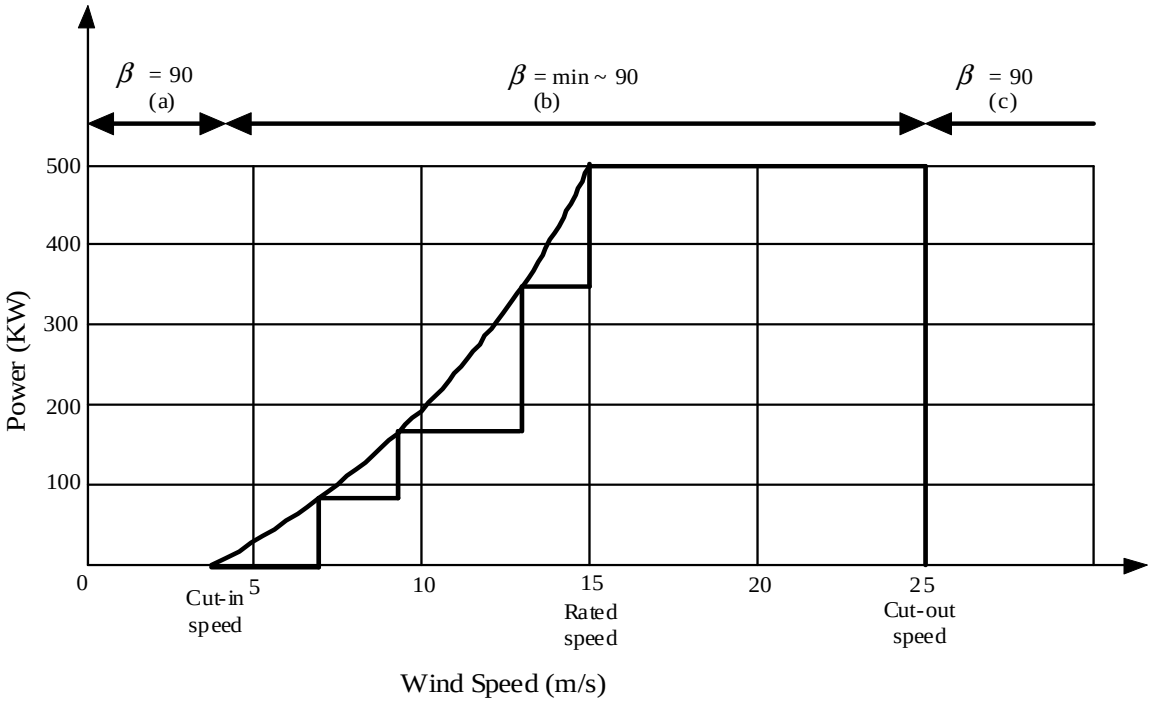

Fig. 5.4: Modifications to the reference power signal of the pitch angle controller

5.3 Simulation Results

Wind speed data for entire year were selected in order to include the seasonal effect. The wind speed data were collected from two sites for their consecutive years so that chronological simulations could be performed in order to verify the wind power leveling technique. Wind speed data were collected from Site A for 2005 and 2006, and data for year 2007 was collected from Site B. Two consecutive years were selected for Site A in order to compare the number of levels and the values in each year as a means of investigating the feasibility of using the levels of the current year in the next year. Wind speed for the whole

year data were recorded and tabulated on an hourly basis in order to increase the accuracy of the choice of levels. Figs. 5.5, 5.6, and 5.7 show the wind speed data collected from Site A for 2005 and 2006, and from Site B for 2007, respectively.

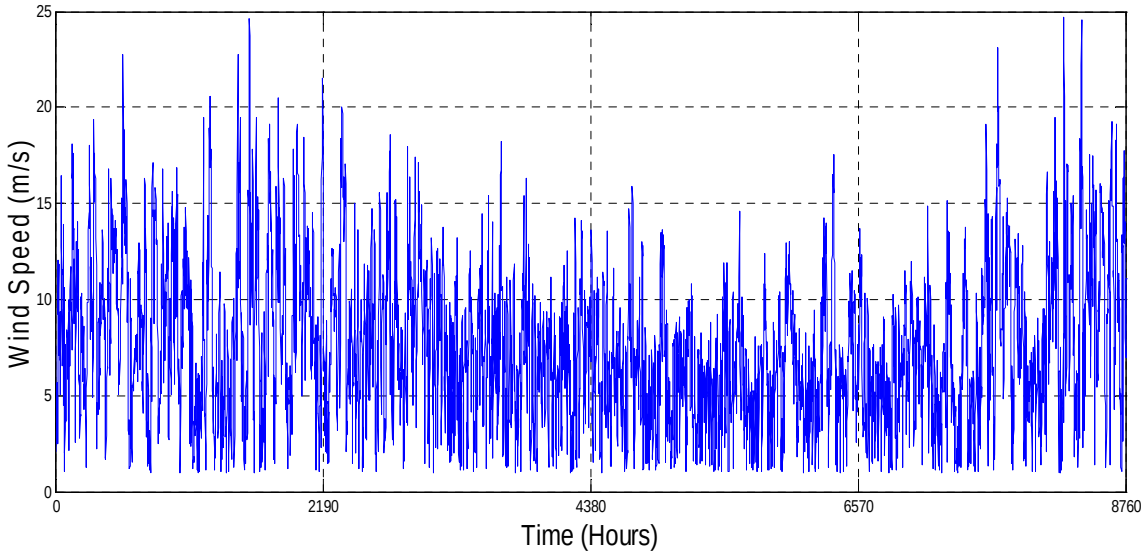

Fig. 5.5: Wind speed data for 2005 (Site A)

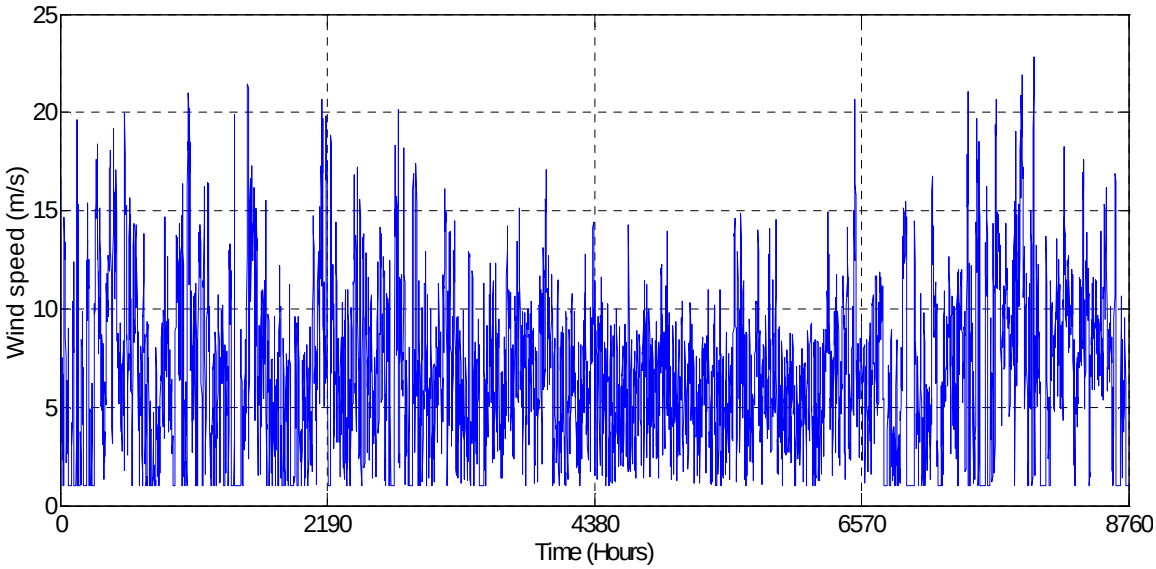

Fig. 5.6: Wind speed data for 2006 (Site A)

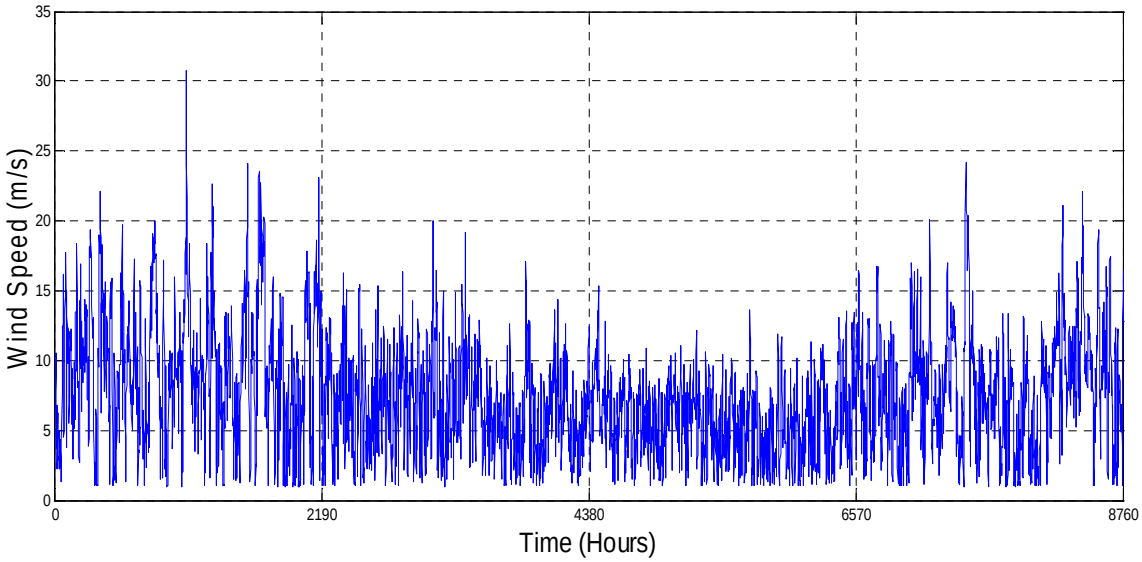

Fig. 5.7: Wind speed data for 2007 (Site B)

The technical specifications of the 2.0 MW wind turbine are listed in Table 5.1 and were used in the simulation.

TABLE 5.1: SPECIFICATION OF 2.0 MW WIND TURBINE

Rotor	Diameter	80 m
	Area swept	5027 m^2
	Nominal revolution	16.7 rpm
	Operational interval	9-19 rpm
	Number of blades	3
Tower	Hub height	60-100 m
Operational Data	Cut-in speed	4 m/s
	Rated speed	15 m/s
	Cut-out speed	25 m/s
Generator	Type	Asynchronous
	Nominal output	2000 KW
	Operational data	50/60 Hz, 690 v

Table 5.1 shows that the cut-in speed, rated speed, and cut-out speed are 4 m/s, 15 m/s, and 25 m/s, respectively. Hence, the first step before the wind speed data were applied to the clustering technique was to exclude all data less than 4 m/s and greater than 15 m/s. The following subsections present the simulation results of the clustering and optimization techniques for the Site A data of 2005 and 2006.

5.3.1 Simulation Results for Years 2005 and 2006 (Site A)

The wind speed data for 2005 and 2006 were applied to the x-means clustering technique in order to determine the number of power (speed) levels. The lower bound of the number of clusters was set to one cluster, while the upper limit was set to 15 clusters. The output number of clusters of the x-means for the wind speed data provided for the two years was six clusters for each year. Table 5.2 shows the mean of each cluster, i.e., the magnitude of each level, and the energy that would be captured if these values were applied directly to the controller of the WECS as a percentage of the case in which no power leveling is used.

TABLE 5.2: CENTRES OF THE OPTIMAL NUMBER OF CLUSTERS

CLUSTER	**2005**	**2006**
	Centre	**Centre**
1	4.907 m/s	4.787 m/s
2	6.612 m/s	6.802 m/s
3	8.361 m/s	8.178 m/s
4	10.168 m/s	9.863 m/s
5	12.24 m/s	11.897 m/s
6	14.607 m/s	14.721 m/s
ENERGY CAPTURED	**80.8 %**	**81.34 %**

The energy output by the clustering technique represents only the mean value for each cluster. The means of the clusters are the centres of the clusters, but they are not necessarily the wind speed values that can capture the maximum energy from the wind speed. To

determine the wind speeds that can capture the maximum energy, the optimization technique discussed below was used. Since the x-means clustering shows that there are six levels, the objective function and the constraints of the optimization model (Equations (4.4) to (4.9)) were modified to reflect the six levels, as follows:

$$\max \sum_{i=1}^{N} [\alpha_1(i)\left(a + bV_1 + cV_1^2\right) + \alpha_2(i)\left(a + bV_2 + cV_2^2\right) \\ \alpha_3(i)\left(a + bV_3 + cV_3^2\right) + \alpha_4(i)\left(a + bV_4 + cV_4^2\right) \\ \alpha_5(i)\left(a + bV_5 + cV_5^2\right) + \alpha_6(i)\left(a + bV_6 + cV_6^2\right)]P_{rated}\ \Delta t \tag{5.3}$$

s.t.

$$\alpha_1(i) + \alpha_2(i) + \alpha_3(i) + \alpha_4(i) + \alpha_5(i) + \alpha_6(i) = 1 \tag{5.4}$$

$$\begin{aligned} &V_1 - m\left(\alpha_2(i) + \alpha_3(i) + \alpha_4(i) + \alpha_5(i) + \alpha_6(i)\right) \le \alpha_1(i)V(i) \le V_2 \\ &V_2 - m\left(\alpha_1(i) + \alpha_3(i) + \alpha_4(i) + \alpha_5(i) + \alpha_6(i)\right) \le \alpha_2(i)V(i) \le V_3 \\ &V_3 - m\left(\alpha_1(i) + \alpha_2(i) + \alpha_4(i) + \alpha_5(i) + \alpha_6(i)\right) \le \alpha_3(i)V(i) \le V_4 \\ &V_4 - m\left(\alpha_1(i) + \alpha_2(i) + \alpha_3(i) + \alpha_5(i) + \alpha_6(i)\right) \le \alpha_4(i)V(i) \le V_5 \\ &V_5 - m\left(\alpha_1(i) + \alpha_2(i) + \alpha_3(i) + \alpha_4(i) + \alpha_6(i)\right) \le \alpha_5(i)V(i) \le V_6 \\ &V_6 - m\left(\alpha_1(i) + \alpha_2(i) + \alpha_3(i) + \alpha_4(i) + \alpha_5(i)\right) \le \alpha_6(i)V(i) \end{aligned} \tag{5.5}$$

$$V_1 < V_2 < V_3 < V_4 < V_5 < V_6 \tag{5.6}$$

$$V_1 = 4\ \ m/s \tag{5.7}$$

$$V_6 = 15\ \ m/s \tag{5.8}$$

Constants *a*, *b*, and *c* in (5.3) can be calculated using Equations (2.2) to (2.4), the cut-in speed, and the rated speed. The values of the constants are as follows:

$$\begin{aligned} a &= 0.12422 \\ b &= -0.06358 \\ c &= 0.008131 \end{aligned} \tag{5.9}$$

When (5.9) is substituted in (5.3) and the optimization model is run the values for the power (speed) levels that maximize the output power can be found. The platform used to run the optimization model is GAMS, and the solver selected is Baron which is able to solve mixed integer non-linear problems. Table 5.3 shows the values for the optimum levels as well as the percentage of energy captured after the leveling technique was applied to the wind speed data for 2005 and 2006. The percentage of energy captured was calculated by dividing the total annual energy capture after the application of the leveling technique by the total energy capture without the application of the leveling technique.

TABLE 5.3: OPTIMAL LEVEL VALUES AND ASSOCIATED PERCENTAGE OF ENERGY CAPTURED FOR 2005 AND 2006

LEVEL	**VALUE (2005)**	**VALUE (2006)**
1	4 m/s	4 m/s
2	6.6 m/s	6.4 m/s
3	8.51 m/s	8.2 m/s
4	9.9 m/s	10.5 m/s
5	12.3 m/s	12.2 m/s
6	15 m/s	15 m/s
ENERGY CAPTURED	**91.3 %**	**90.6 %**

It is interesting to note that the output of the x-mean clustering technique, i.e., the number of power levels, for 2006 is very close to that for 2005. This result proves that the wind speed

probability density functions generated from the wind speed data for the same site for two consecutive years are almost identical [89]. However, the level values differ slightly from those for 2005.

5.3.2 Simulation Results for Year 2007 (Site B)

The same procedure was applied to the wind speed data for 2007 that were collected from a different site. The optimum number of clusters output by the x-means for 2007 was five. The number of levels and the wind speed data were applied in the previously described optimization model. Equations (5.3) to (5.5) were adjusted to accommodate five levels. Table 5.4 shows 1) the optimum number of clusters; 2) the centroid of each cluster, i.e. the magnitude of each level; 3) the energy captured if these values are applied directly to the controller of the WECS; 4) the optimum level values as well as the percentage of energy captured after the leveling technique was applied to the wind speed data for 2007.

TABLE 5.4: OPTIMAL LEVEL VALUES AND ASSOCIATED PERCENTAGE OF ENERGY CAPTURED FOR 2007

LEVEL	**X-MEANS CENTRES**	**OPTIMIZED LEVELS**
1	5.33 m/s	4 m/s
2	6.82 m/s	7.156 m/s
3	11.14 m/s	10.04 m/s
4	12.79 m/s	12.44 m/s
5	15.93 m/s	15 m/s
ENERGY CAPTURED	**79.89 %**	**87.64 %**

It is interesting to note that since the number of levels (clusters) for Site B is less than for Site A, the percentage energy capture is also less. However, the power fluctuation at Site B is less than at Site A.

The results in Tables 5.2, 5.3, and 5.4 show an energy reduction of about 10 % due to the application of the power leveling technique to a Type A WECS. Operating wind farms at fixed levels for the entire year has several advantages. First, the error in the prediction of the output power will certainly be reduced because wind speed predictions will be made within the speed band. Second, with the power leveling technique, energy scheduling will allow the system operator to easily schedule the output power of the wind farm. The system operator will know the specific number of power levels generated from the wind farm which can then be used for scheduling the wind farm into the system; i.e., the wind farm can be semi-dispatchable. Finally, the power fluctuation and hence the voltage fluctuation, which is considered the main challenge in increasing the penetration level of wind power, will definitely be reduced. All of these advantages are believed to outweigh the cost of the loss of energy generation. Fig. 5.8, Fig. 5.9, and Fig. 5.10 show the wind power before and after the application of the leveling technique for the first day of 2005, 2006, and 2007, respectively.

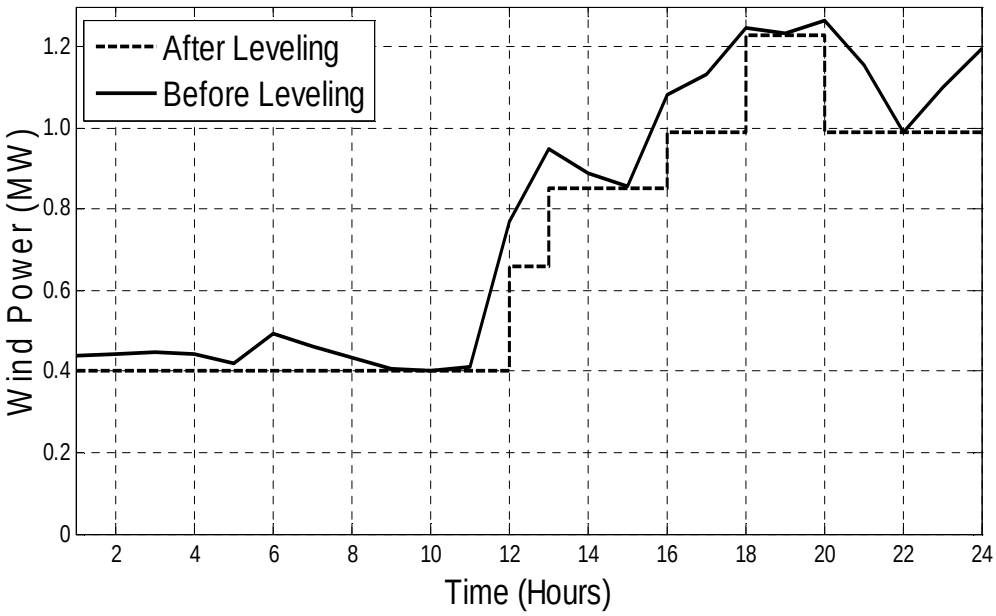

Fig. 5.8: Wind power before/after the application of the leveling technique for the first day of 2005

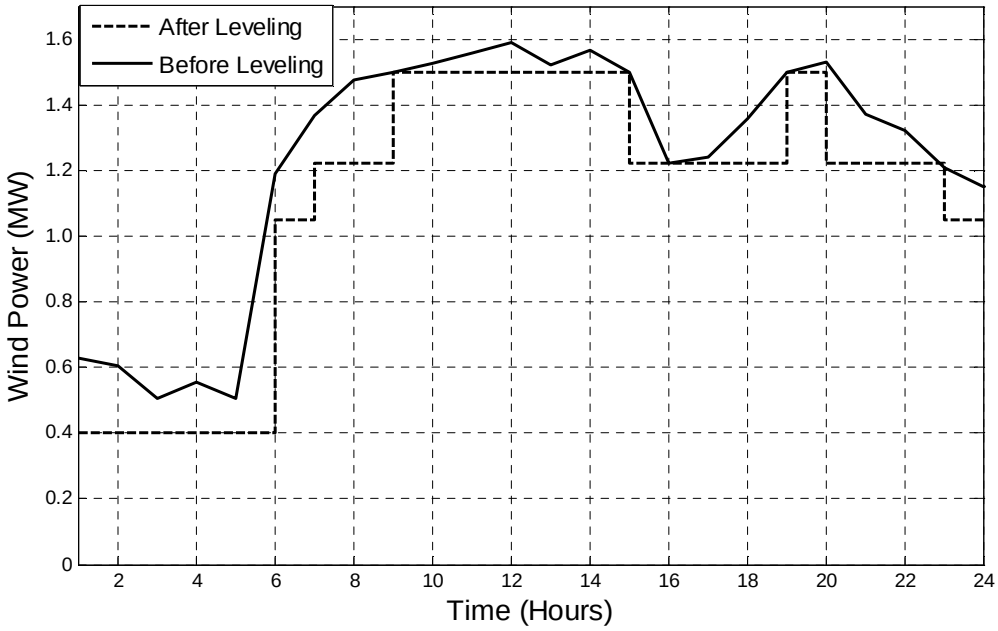

Fig. 5.9: Wind power before/after the application of the leveling technique for the first day of 2006

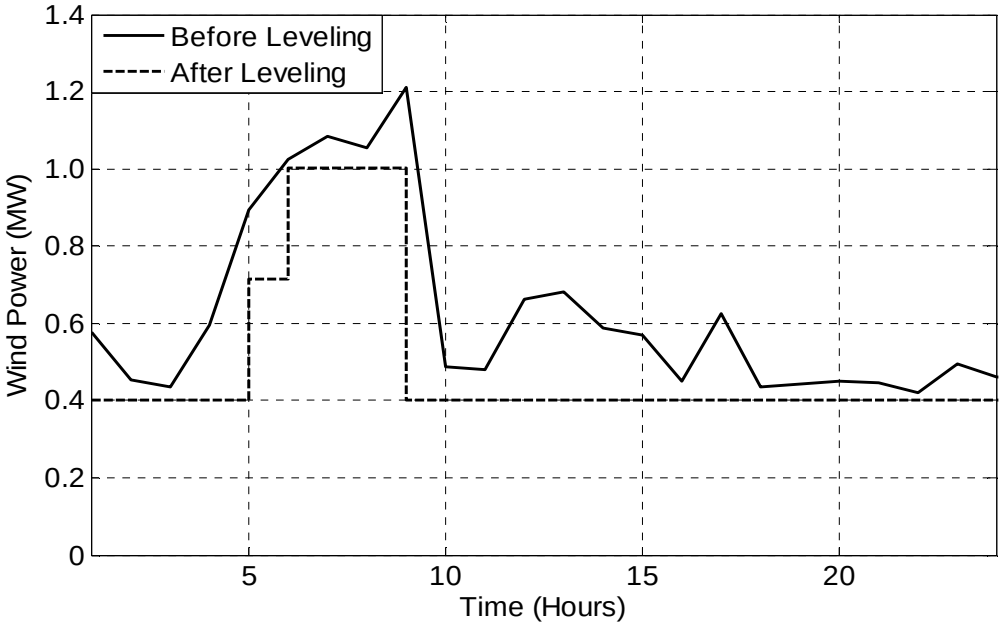

Fig. 5.10: Wind power before/after the application of the leveling technique for the first day of 2007

It is important to note here that the number of power levels that must be scheduled every day may be less than the number of clusters predicted by the solution, which makes the wind energy output more constant and more suitable for power system scheduling. The maximum number of levels in any given day is, of course, the number of clusters. The percentage of energy captured per day using the optimized power levels was calculated, and the average energy for the 365 days was found to be similar to the results listed in Tables 5.3 and 5.4 for the data from Sites A and B.

It is evident from Fig. 5.8, Fig. 5.9, and Fig. 5.10 that the continual variations in the output wind power have been greatly eliminated and that the output power is constant over a long period of time. The developed leveling technique reduces the wind power fluctuation and hence the voltage fluctuations. In order to prove the voltage fluctuation reduction due to the application of the leveling technique, a 100 MW wind farm is tested in a large mesh 24-bus transmission system (will be explicitly explained in Chapter 7) pre and post the utilization of the leveling technique. The wind power profile shown in Fig. 5.10 is used in the simulations and the voltage profile at the closest bus to the wind turbine generator is recorded. Fig. 5.11 and Fig. 5.12 show the voltage profile at the closest bus to the point of connection of the wind generator before and after the application of the leveling technique. It can be noted that there is continuous voltage variations before the application of the leveling technique which require continuous operational action to keep the voltage within the permissible range. However, after the application of the leveling technique very less frequent actions are required over time. For example, if a voltage regulator is used to control the voltage, it will adjust the taps less frequent after the application of the leveling technique compared to the case where the leveling technique is not utilized.

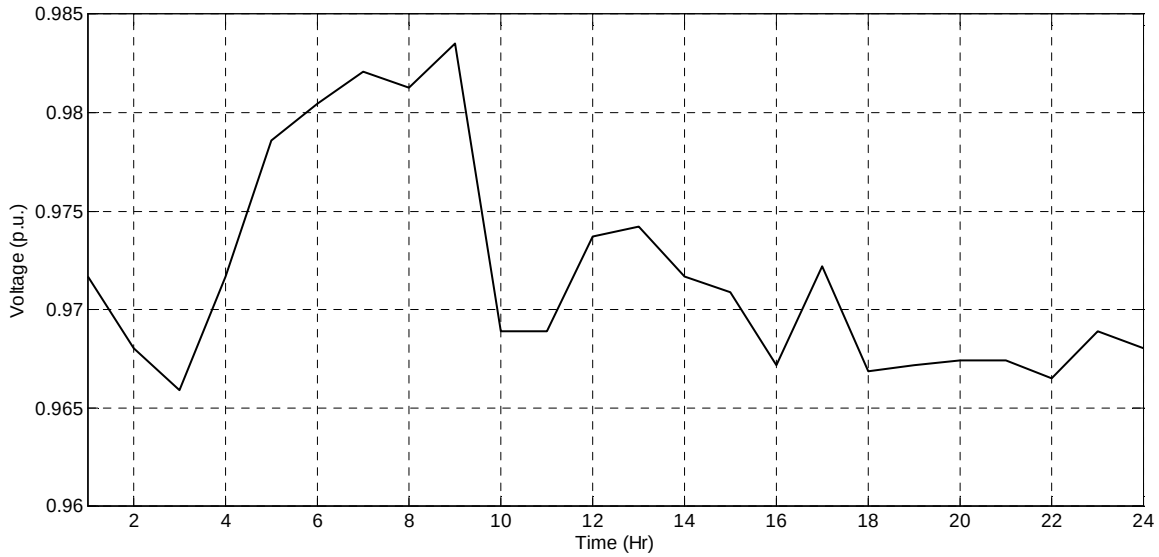

Fig. 5.11: Wind voltage fluctuations before the application of the leveling technique

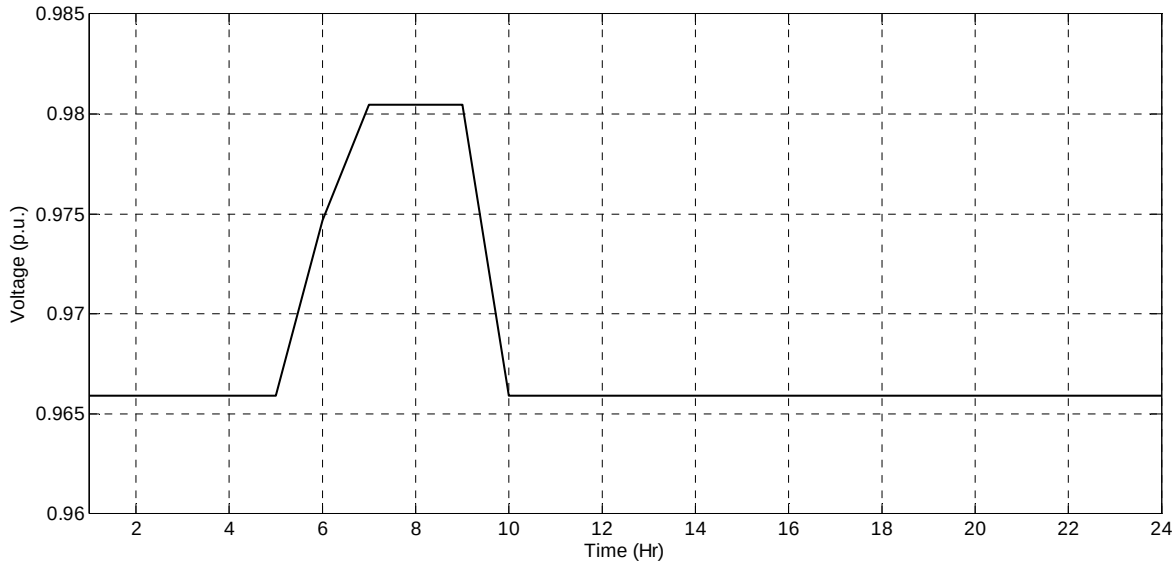

Fig. 5.12: Wind voltage fluctuations after the application of the leveling technique

5.4 Storage Device

This section explains the addition of a storage device to the terminal of the SCIG of Type A WECS.

5.4.1 System Description and Modeling

As explained in Chapter 2, the developed control technique was applied to Type A wind energy conversion system that consisted of a wind turbine, a gearbox, and a squirrel cage induction generator (SCIG) whose terminals were connected directly to the grid. The new component introduced in this section is the storage device whose terminal was connected across the SCIG's terminals. Fig. 5.13 shows the new system configuration with the old system drawn in gray.

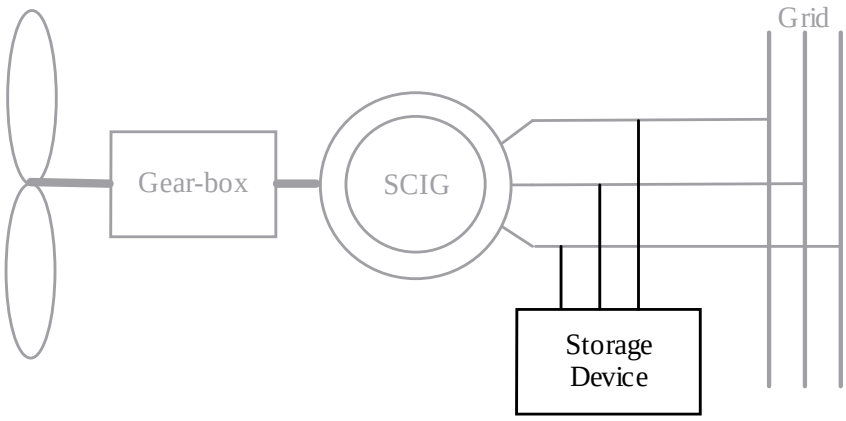

Fig. 5.13: Proposed system configuration

As discussed in Chapter 2, the characteristics of the energy storage device vary significantly as a function of the principal technology. For example, magnetic energy storage and the flywheel, which are both short-term energy storage solutions, are characterized by high efficiency (in the order of 90 %), a very high life cycle of charge and discharge operations, and fast access to the stored energy. However, their cost per unit of energy is relatively high [90]. On the other hand, battery storage systems (BSS) facilitate the storage of

energy at a low cost per unit of energy, especially the new BSS technologies. They are also able to store a large quantity of energy and can deliver this energy in the form of transferred power at either slow or extremely high rates without being damaged. They are also rugged and reliable and provide a source of constant power. For these reasons, a battery storage system is a well-proven storage technique for wind energy conversion systems [56-58]. For these reasons, a BSS was chosen as an appropriate type of storage device for this study.

The components of a BSS are a storage element (battery bank), a converter, a controller, and a transformer. Fig. 5.14 shows a schematic diagram of a BSS. The following subsections describe the modeling of each component of the BSS.

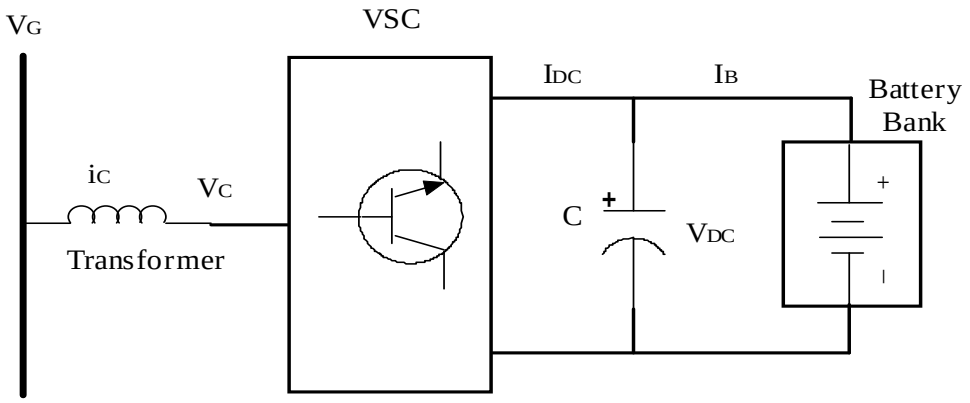

Fig. 5.14: Battery storage system (BSS)

5.4.1.1 Voltage Source Converter Model

In the developed model, it was assumed that the converter switches are ideal, and that the converter is fed from a balanced sinusoidal three-phase supply. The mathematical model of the voltage source converter in the dq reference frame is given as follows [91]:

$$L\frac{di_{cd}}{dt} = -Ri_{cd} + \omega Li_{cq} + V_{Gd} - V_{DC}S_d \tag{5.10}$$

$$L\frac{di_{cq}}{dt} = -Ri_{cq} + \omega Li_{cd} + V_{Gq} - V_{DC}S_q \tag{5.11}$$

$$C\frac{dV_{DC}}{dt} = \frac{3}{2}\left(i_{cd}S_d + i_{cq}S_q\right) - I_B \tag{5.12}$$

Where S_d and S_q are the constants of d-axis and q-axis dependent voltage sources.

5.4.1.2 Battery Model

The battery model selected is a double-layer capacitor model, which can be represented by the classical equivalent circuit shown in Fig. 5.15 [92].

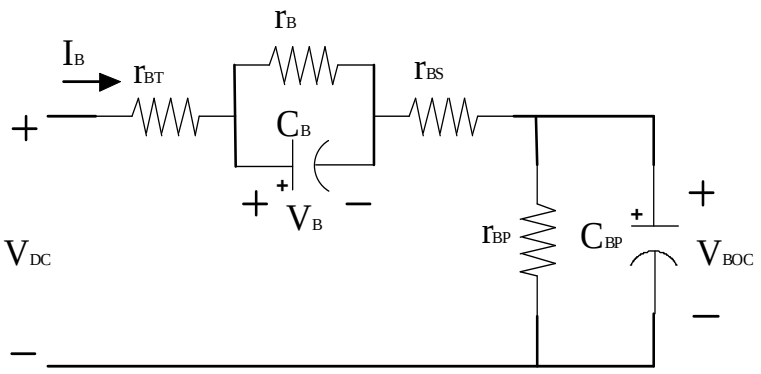

Fig. 5.15: Battery equivalent circuit

In the equivalent circuit shown, V_{BOC} is the open circuit voltage of the battery, V_B is the overvoltage of the battery, r_{BT} is the connecting resistance, r_{BS} is the internal resistance, I_B is the DC current flowing into the battery, r_B is the overvoltage resistance, r_{BP} is the self-discharge resistance, C_B is the overvoltage capacitance, and C_{BP} is the equivalent capacitance of the battery.

When KVL and KCL are applied to the equivalent circuit, the following equations can be derived:

$$I_B = \frac{V_{DC} - V_{BOC} - V_B}{r_{BT} + r_{BS}} \tag{5.13}$$

$$I_B = C_{BP}\frac{dV_{BOC}}{dt} + \frac{V_{BOC}}{r_{BP}} \tag{5.14}$$

$$I_B = C_B\frac{dV_B}{dt} + \frac{V_B}{r_B} \tag{5.15}$$

The power transmitted from the grid to the battery storage and vice versa is given by

$$P = \frac{V_G V_C \sin \emptyset}{X} \tag{5.16}$$

$$Q = \frac{V_G}{X}(V_G - V_C \cos \emptyset) \tag{5.17}$$

where X is the leakage reactance of the transformer, V_C is the terminal voltage of the converter, and V_G is the grid voltage.

The real and reactive power can be thus controlled through the adjustment of the phase angle between the grid voltage and the magnitude of the converter output voltage.

5.4.1.3 Controller Design

The developed controller provides an active and a reactive power signal in order to elicit the required system response. The controller converts these active and reactive signals into PWM switching signals that modulate the modulating index and the phase angle. The goal of good controller design is to achieve an independent active and reactive power control. The d-component of the current vector in a steady state is the active current component (d-current), while the q-component of the current vector becomes the reactive current component (q-current) [90].

To achieve this objective, a decoupled PI controller was developed, which produces the desired switching signals from independent active and reactive power signals. A schematic diagram of the developed controller is shown in Fig. 5.16.

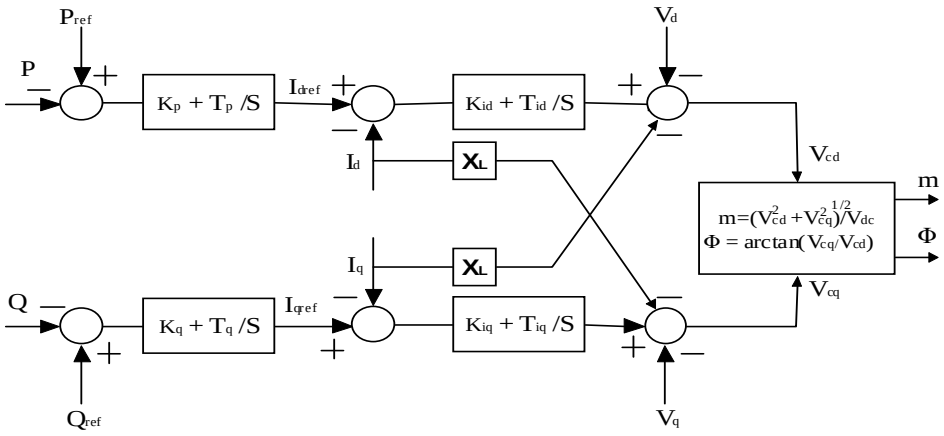

Fig. 5.16: BSS controller

In this simulation, the reactive power reference signal was set to zero so that reactive power is neither absorbed nor transmitted to the grid. The active power reference signal was set to the difference between the generated output power and the desired power level. The active power reference signal could be positive or negative, depending on the desired power level. If the desired power level is lower than the generated power, the active power signal is set to the positive absolute value of the difference between the desired level and the generated power (charging mode), and vice versa when the desired level is greater than the generated power (discharging mode).

5.4.2 Methodology

As previously mentioned, a storage device, i.e., the battery storage system (BSS), was utilized in order to maintain the power levels for longer periods and thus increase the benefits of the power leveling technique. In this study, the BSS was therefore not used as a backup energy source when there is no wind power nor was it used to generate constant power along

the WECS. This scenario led to the use of a smaller BSS, i.e., one with a fraction of the rated output power of the wind generator.

The modification to the pitch angle controller explained in Section 5.2 was not appropriate for this case because the pitch angle controller is applied to the WECS only when the available wind power is greater than the rated power of the wind turbine.

There are two modes of operation for a WECS when a BSS has been added to its terminals. In Mode I, the power generated from the WECS is divided into two parts: the power level transferred to the grid, and the difference between the generated power and the power level, which is transferred to the BSS. In this mode, the active power reference signal is set to the difference between the generated power and the transmitted power level (positive value).

In Mode II, all of the power generated from the WECS is transferred to the grid and the difference between the generated power and the next power level is supplied by the BSS. In this mode, the active power reference frame is adjusted to the negative of the difference between the generated power and the next power level. Fig. 5.17 shows the schematic for the two modes of operation: Mode I is drawn in solid lines and Mode II is drawn in dotted lines. The reactive power reference signal is always set to zero in order to ensure that zero reactive power is transferred to/from the grid.

The following three criteria were used to obtain the optimum size of the storage device. First, the size of the storage device was set to infinity and the simulations were performed on a yearly basis. Second, the storage device is allowed to accumulate energy in the batteries as long as the power level of the previous time sample is equal to or higher than that of the current time sample. Once the generated power level decreases, the BSS is discharged so that the power level is maintained at its previous (higher) value. In this case, the power levels are thus maintained for a longer period. Third, the maximum size of the storage device (upper boundary) that is required in order to store all the energy lost due to leveling was set at the maximum energy level that the storage device attained in the entire year. Fig. 5.18 illustrates

these three criteria. The solid lines show the leveling technique before the storage device was installed, and the effect of adding the storage device is shown by the dotted lines.

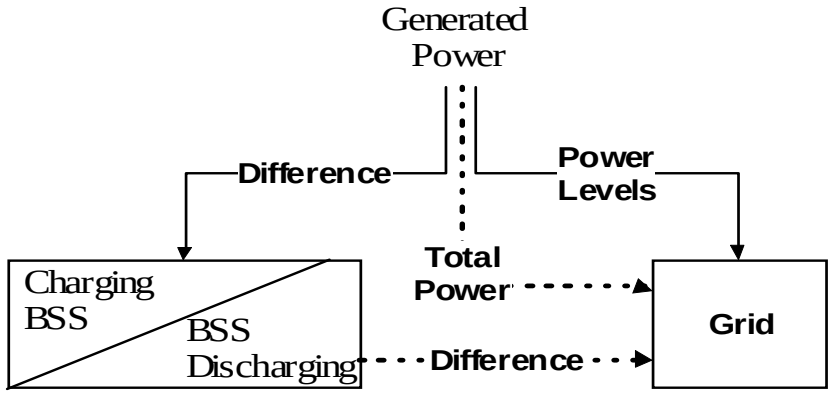

Fig. 5.17: Modes of operation

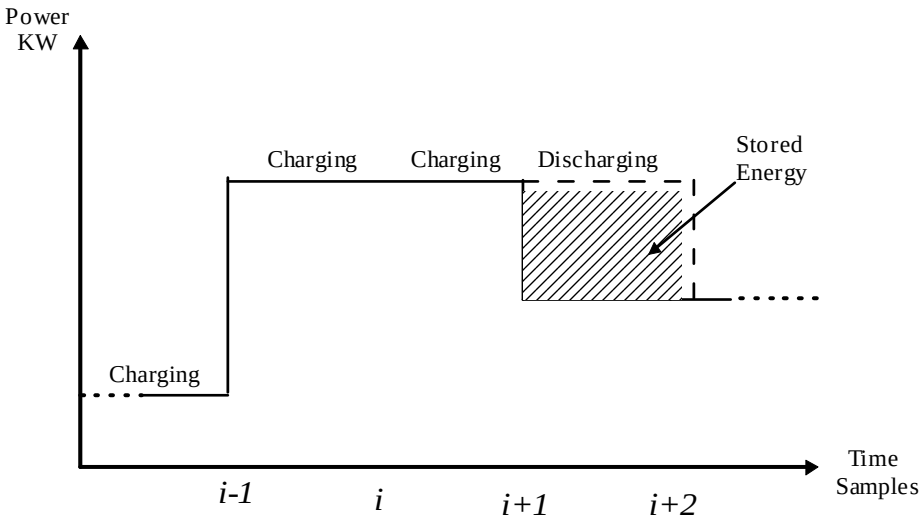

Fig. 5.18: Criteria for selecting the optimum size of the storage device

The size of the storage device was also evaluated relative to available BSS technologies and their corresponding costs so that the benefits to the ownerts can be maximized, as discussed below.

The objective function for maximizing the owner's benefits is given by

$$Max \sum_{i=1}^{8760} (C_e \times E_i(x)) - C_f(x) - C_v(x) \qquad \forall\, x = 0.1, 0.2 \ldots E_{max} \qquad (5.18)$$

where $E_i(x)$ is the hourly energy captured for a given storage size x in KWhr, C_e is the energy price in \$/KWhr, $C_f(x)$ is the fixed costs of the storage for a given size x in \$, $C_v(x)$ is the variable costs of the storage for a given size x in \$, and E_{max} is the maximum size of the BSS that is required in order to store the power loss due to leveling.

5.4.3 Energy Storage Costs

Energy capital (initial) storage costs are divided into two main categories: energy cost and power cost. The energy cost, expressed in \$/KWhr, is the cost of the equipment used to store the energy, e.g., batteries, and it can be charged and discharged a number of times. The rated KWhr of a storage device is the total amount of energy that can be stored in the device. On the other hand, the power cost, expressed in \$/KW, is the cost of the auxiliary equipment attached to the storage unit, e.g., the power electronic converter in a battery storage system. The rated KW of the storage device represents the amount of power that can be stored in the storage unit.

In addition to the capital storage costs, two other costs are time-dependent: the operation and maintenance cost, and the replacement cost. This section presents a method for calculating the annual cost of a storage device attached to a wind energy conversion system.

Based on the previous discussion, the total annual cost of a storage device includes three costs: the annual capital cost (ACC), the operation and maintenance cost (OMC), and the replacement cost (RC). The ACC is the summation of three costs [93, 94]:

- The total cost of the power electronics components (PEC):

$$PEC = PECU \times P_{SD} \qquad (5.19)$$

- The total cost of the storage units (SUC):

$$SUC = SUCU \times \frac{E_{SD}}{\eta_{SD}} \tag{5.20}$$

- The total cost of the balance of plant (BPC):

$$BPC = BPCU \times \frac{E_{SD}}{\eta_{SD}} \tag{5.21}$$

where P_{SD}, E_{SD}, and η_{SD} are the rated power of the storage device, the rated energy, and the efficiency, respectively, while *PECU*, *SUCU*, and *BPCU* are the unit cost of the power electronics in $/KW, the unit cost of the storage unit in $/KWhr, and the unit cost of the balance of the plant in $/KWhr, respectively.

The total capital cost (TCC) is thus expressed by

$$TCC = PEC + SUC + BPC \tag{5.22}$$

and the annualized total capital cost (ATCC) is given by

$$ATCC = TCC \times CRF \tag{5.23}$$

where *CRF* [94] is the capital recovery factor, which is expressed by

$$CRF = \frac{i_r(1+i_r)^z}{(1+i_r)^z-1} \tag{5.24}$$

where i_r and z are the interest rate and the planning horizon, respectively.

When batteries are used in a storage device, they should be replaced one or more times during the life of the storage device. This cost is annualized as follows:

$$A = F \times CRF \times [(1+i_r)^{-r} + (1+i_r)^{-2r} + \cdots] \tag{5.25}$$

where F and r are the future value of the replacement cost in \$/KWhr, and the battery replacement period, respectively.

Each type of battery has a limited number of charging/discharging cycles. The replacement period in years is calculated as follows [93]:

$$r = \frac{C}{n \times D} \tag{5.26}$$

where C is the number of charge/discharge cycles in the life of a battery storage, and D is the annual operating days of the storage device.

The annual replacement cost (ARC) of a battery is therefore

$$ARC = A \times \frac{E_{SD}}{\eta_{SD}} \tag{5.27}$$

The annual operation and maintenance cost can be found through multiplication of the fixed operation and maintenance cost in \$/KW (OM) by the rated power of the storage device:

$$OMC = OM \times P_{SD} \tag{5.28}$$

Finally, the total annual cost of the storage device (TAC) is given by [93, 94]:

$$TAC = ATCC + OMC + ARC \tag{5.29}$$

The most promising commercial and near-commercial BSS technologies were considered for use in our study: lead-acid (LA), valve-regulated lead-acid (VRLA), sodium sulfur (Na/S), zinc bromine (Zn/Br), and vanadium redox (VRB) [94]. These storage technologies are all commercially available. In 2007, the manufacturers of each type provided price quotes and performance information for bulk storage applications [95, 96]. The 2007 prices are listed in Table 5.5.

TABLE 5.5: BSS PARAMETERS FOR TRANSMISSION AND DISTRIBUTION APPLICATIONS

Parameters	LA	VRLA	Na/S	Zn/Br	VRB
Round-trip energy efficiency	0.75	0.75	0.77	0.7	0.7
Unit cost for power electronics ($/KW)	175	175	1000	175	0
Unit cost for storage unit ($/KWhr)	305	360	500	225	740
Unit cost for balance of plant ($/KWhr)	50	50	0	0	30
Fixed O&M cost ($/KW)	15	5	20	20	20
Future amount of replacement cost ($/KWhr)	305	360	500	225	222
Number of charge/discharge cycles in life	3200	1000	2500	10000	10000

5.4.4 Simulation Results after the Addition of the Storage Device

Wind speed data were collected from two sites for consecutive years, so that chronological simulations could be performed as a means of verifying the wind power leveling technique after the installation of the BSS. The technical specifications of the 2.0 MW wind turbine were also selected for the simulations. The values listed in Tables 5.3 and 5.4 were used to develop the active power reference signal for the voltage source converter (VSC), as explained earlier. Figs. 5.19, 5.20, and 5.21 show the wind speed, with and without the installation of the BSS, for the first day of 2005, 2006 and 2007, respectively.

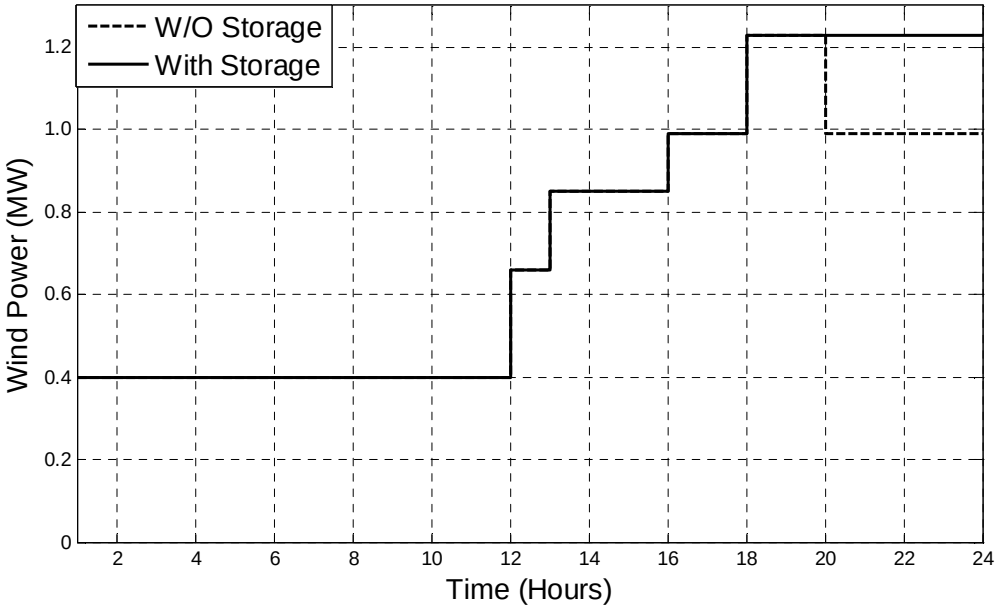

Fig. 5.19: Wind power without and with the installation of the storage device (BSS) for the first day of 2005

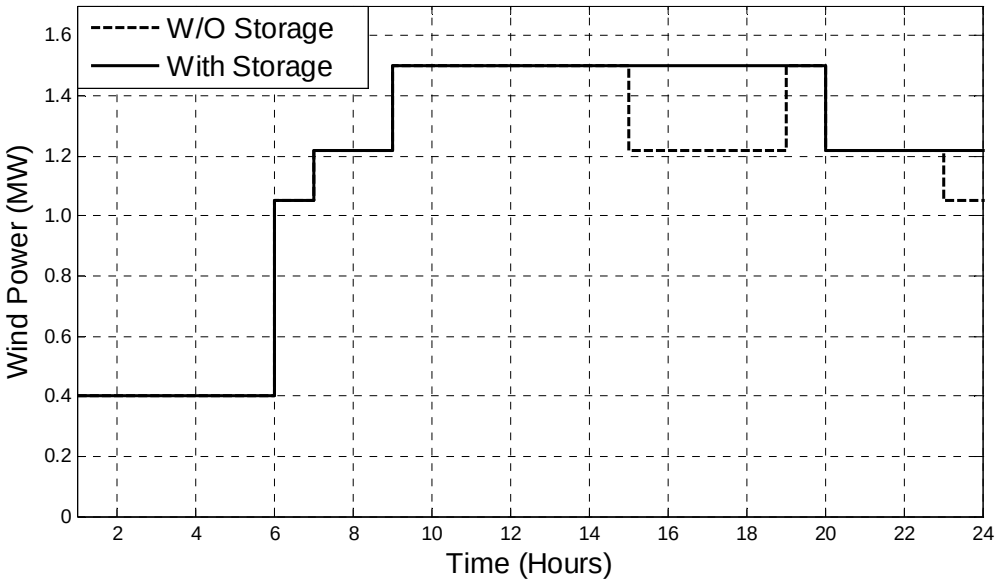

Fig. 5.20: Wind power without and with the installation of the storage device (BSS) for the first day of 2006

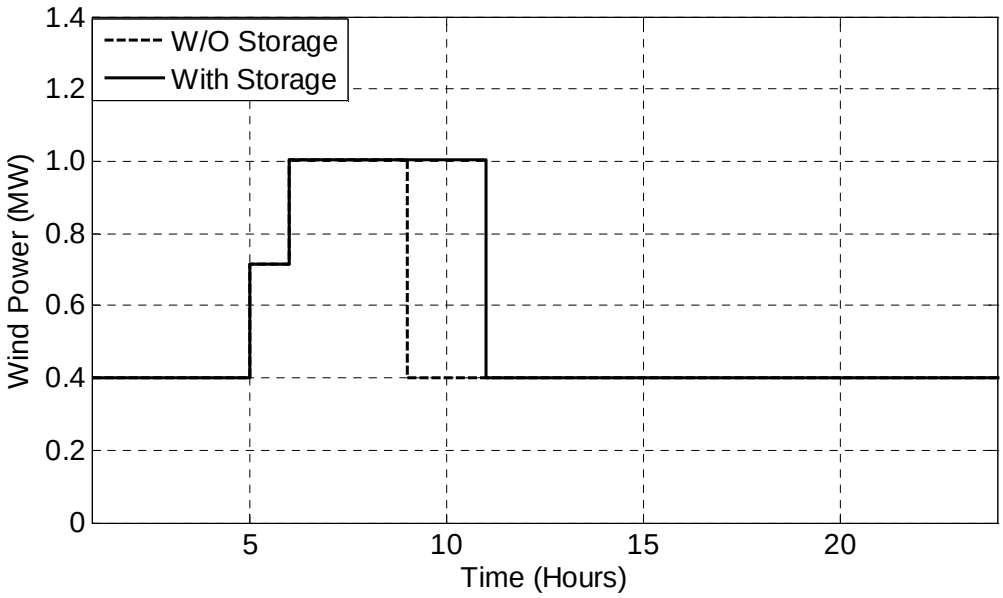

Fig. 5.21: Wind power without and with the installation of the storage device (BSS) for the first day of 2007

As can be seen in Figs. 5.19, 5.20, and 5.21 the power levels are maintained at a constant level for longer periods after the installation of the storage device. Because of this advantage, the leveling technique provides three benefits for a power system. First, the error involved in predicting output power will certainly be reduced because the backup energy in the storage device keeps the power level from dropping instantaneously, which gives the system operator more time to find an alternative source of power. Second, the power fluctuation and hence the voltage fluctuation will definitely be reduced. Third, installing a storage device will recover most of the energy lost through leveling, which is very important from the owner's point of view.

As a first step, in the selection of the optimum size of storage device, Table 5.6 shows the maximum size of storage device that is required for storing all of the energy lost due to leveling. These values were used to specify the upper boundary for the optimization problem, i.e., E_{max} in Equation (5.18).

TABLE 5.6: MAXIMUM SIZES OF THE BSS FOR 2005, 2006, AND 2007

Year	Maximum BSS Size (MWhr)
2005	1.46 MWhr
2006	1.34 MWhr
2007	1.58 MWhr

The final step is to determine the optimum size of the storage device. Since the sizes of the storage devices are available in the market in discrete values, a step of 200 KWhr was assumed for this study. Equations (5.19) to (5.29) were applied to the parameters for the BSS technologies listed in Table 5.5 in order to determine the total annual cost of each type of storage device. This analysis was repeated for the different sizes of storage devices from 200 KWhr up to 1600 KWhr. To calculate the net income for the owner, the total annual cost of the storage device was subtracted from the total savings, which is defined as the total energy captured for a given storage size, multiplied by the price of energy. Table 5.7 shows the net income for the range of storage device sizes for each BSS technology.

TABLE 5.7: NET INCOME ASSOCIATED WITH THE BSS TECHNOLOGIES

	Income (k$) for Each Technology				
Size of the Storage Devices	**LA**	**VRLA**	**Na/S**	**Zn/Br**	**VRB**
200 KWhr	-7.13	-21.46	-0.99	-1.95	-8.26
400 KWhr	-15.98	-50.63	-3.65	-2.61	-15.24
600 KWhr	-20.76	-75.74	-2.27	0.791	-18.15
800 KWhr	-24.38	-96.95	0.792	5.37	-19.89
1 MWhr	-27.5	-123	3.32	10.43	-21.14
1.2 MWhr	-33.23	-149	**3.76**	12.89	-25
1.4 MWhr	-40.28	-176.5	2.87	14.03	-30.17
1.6 MWhr	-51.11	-207.7	-1.8	11.38	-39.14

As can be seen in Table 5.7, not all BSS technologies are suitable for this application. The Na/S and Zn/Br are the only possible candidate technologies, because they produce positive net incomes for specific sizes. Within those two candidate technologies, a 1.2 MWhr Na/S BSS and a 1.4 MWhr Zn/Br BSS are the optimum sizes and are highlighted in Table 5.7. However, the globally optimal BSS is a 1.4 MWhr BSS with a Zn/Br battery bank.

5.5 Conclusions

Applying the new leveling technique to a Type A WECS controller provides several advantages. It ensures that power fluctuations are minimized because the generator produces constant amounts of power at the same speed levels for longer periods. It will also enhance the accuracy of predictions since it predicts only the range of the speed and not the exact value of the speed. Finally, since the output power generated can be predicted accurately, the system operator can reduce the assigned reserves, and the operation of the generation pool for the power system becomes more manageable. For example, for a 10 MW wind farm and without the leveling technique, the assigned reserves should match the wind farm rating. However, the application of the leveling technique will limit the assigned reserves to maximum difference between two adjacent levels which corresponds to an error in predicting the wind power level. Therefore, the leveling technique facilitates the reduction of assigned reserves by a large amount. On the other hand, the main limitation of the new control methodology is the amount of energy lost due to the decrease in the effective speed, which results in a reduction in output power.

Chapter 6
Applying the Leveling Technique on Type C WECS

6.1 General

The leveling technique explained in Chapter 4 was successfully applied to Type A WECS as presented in Chapter 5. This chapter describes the application of the developed control technique to Type C WECS with a storage device connected to the DC bus of a back-to-back converter. The controller of the back-to-back converter connected in the rotor circuit of a doubly-fed induction generator (DFIG) was modified in order to accommodate the new leveling technique.

6.2 System Description and Modeling

The underlying configuration of the WECS is illustrated in Figure 6.1. The developed WECS is comprised of a wind turbine coupled with a DFIG, a gearbox, an energy storage system connected to the DC bus of the back-to-back converter, and an interface transformer. The basic purpose of the storage device is to facilitate the application of the leveling technique. This configuration allows the maximum power tracking control to be maintained. Unlike the leveling technique for the Type A WECS, which was explained in Chapter 5, the energy loss due to power leveling does not occur with Type C WECS. When Type C WECS is operating at a specific power level and the generator suddenly toggles to a lower power level due to a decrease in wind speed, the storage device begins to inject energy into the grid in order to retain the preceding power level, which has the effect of maintaining a constant output power. The power management mechanism in the new configuration is explained in details in the following sections.

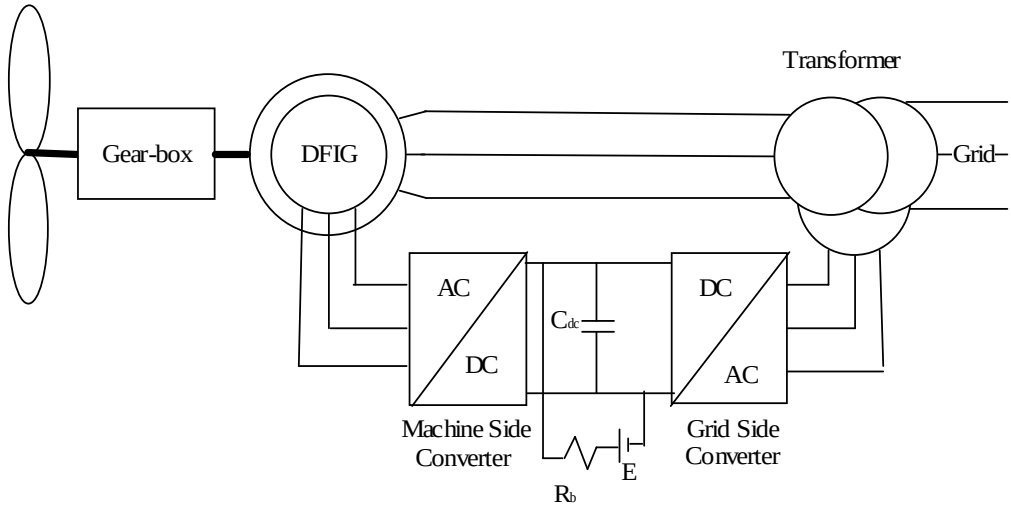

Fig. 6.1: Configuration of the developed wind energy conversion system

6.2.1 Wind Turbine Modeling

The model of the wind turbine explained in Chapter 2 was considered in this simulation.

6.2.2 DFIG Modeling

A doubly-fed induction generator (DFIG), as shown in Fig. 6.1, consists of a wound rotor induction generator with the rotor connected to the grid via a back-to-back converter. The power electronic converter is designed to handle 25 %-35 % of the total power of the machine. The back-to-back converter consists of two converters, a machine-side converter and a grid-side converter with their DC link connected to the DC link capacitor (C_{dc}) and a battery storage device. An inductor is connected in series with the battery storage in order to smooth the current. The battery storage was modeled as a voltage source (E) in series with an internal resistance (R_b). The main objective of the machine-side converter is to control the torque or the speed of the DFIG as well as the power factor at the stator terminals. The grid-side converter, however, is used to keep the DC link voltage constant and to control the output power.

6.2.3 DFIG Controller

To control both the mechanical parameters (torque and speed) and the electrical parameters (active and reactive power delivered to the grid) of the machine, two back-to-back voltage source converters are connected in the rotor circuit. The machine-side converter, which is connected directly to the rotor terminals, is responsible for controlling the DFIG parameters: DFIG speed, torque, and currents. On the other hand, the grid-side converter, which is connected to the grid terminals, is responsible for controlling the active and the reactive power delivered from the rotor to the grid.

6.2.3.1 Machine Side Converter

One control subsystem of the DFIG is the torque controller, whose purpose is to regulate the DFIG output torque to maximize its output power, i.e., to provide maximum power tracking. The governing equations of the torque controller are as follows [97]:

$$T_{ref} = k_{opt}\,\omega_r^2 \tag{6.1}$$

where T_{ref} is the DFIG torque command and ω_r is the rotor speed. k_{opt} is described as [97]

$$k_{opt} = \frac{0.5\rho A r^3 C_{p\max}}{\lambda_{opt}^3} \tag{6.2}$$

where ρ is the air density, A is the turbine swept area, r is the turbine radius, $C_{p\,max}$ is the maximum of the power coefficient, and λ_{opt} is the turbine tip-speed ratio corresponding to $C_{p\,max}$ [89].

The DFIG is controlled in the stator reference frame in which the electrical torque is expressed as [98]

$$T_e = \frac{1.5 V_{sp} i_{rq}}{(1+\sigma_s) f_o} \tag{6.3}$$

where σ_s is the stator leakage factor, V_{sp} is the peak value of the grid phase voltage, i_{rq} is the quadrature component of the rotor current, and f_o is the grid nominal frequency.

To maximize the DFIG output power, $i_{re\ ref}(t)$ is therefore determined to be

$$i_{rq\ ref}(t) = \frac{(1+\sigma_s) f_o}{1.5 V_{sp}} T_{ref}(t) \tag{6.4}$$

where T_{ref} is determined using (6.4). Due to the large turbine inertia, T_{ref} varies relatively slowly and hence:

$$T_e \approx T_{ref} = k_{opt} \omega_r^2 \tag{6.5}$$

Multiplying both sides by ω_r enables the DFIG output power to be expressed as

$$P_e \approx k_{opt} \omega_r^3 \tag{6.6}$$

The control law (6.5) results in a constant tip-speed ratio [98], and ω_r becomes proportional to the wind speed V so that Equation (6.6) can be written as

$$P_e \approx \left(\frac{\lambda_{opt}}{r} \right)^3 k_{opt} V^3 \tag{6.7}$$

The direct component of the rotor current i_{rd} can control the stator reactive power Q_s, as follows [98]:

$$Q_s = -\frac{1.5 V_{sp}^2}{(1+\sigma_s) L_m f_o} - \frac{1.5 V_{sp} i_{rd}}{(1+\sigma_s)} \tag{6.8}$$

where *Lm* is the generator magnetizing inductance.

6.2.3.2 Grid-Side Converter

The main purpose of a grid-side converter is to control the DC-link voltage and hence control the real and reactive power components. The real power is controlled to regulate the DFIG output power, to manage the state of the battery charge, and to maintain the DC link voltage.

The real and reactive powers P_o and Q_o are proportional and can be controlled by i_{sd}, and i_{sq} as follows [98]:

$$P_o = 1.5\, V_{sp}\, i_{sd} \tag{6.9}$$

$$Q_o = -1.5\, V_{sp}\, i_{sq} \tag{6.10}$$

where $P_{o\,ref}$ and $Q_{o\,ref}$ are determined by the power management controller that is explained in section 6.3.

6.2.4 Storage Device

The storage device is connected at the DC bus between the two converters in the rotor circuit. This arrangement helps reduce the total system cost, as only a single-stage converter (a DC/AC or a DC/DC converter) is required in order to control the storage device versus a complete AC/DC/AC converter in the case of connecting a storage device to the AC terminals of the wind turbine generator. The storage device is able to store extra power for later use to help smooth the DGIF output power and to ensure steadier power levels. The modeling of the storage device, the selection of the approperiate type, and the determination of the optimum size are explained in section 6.4.

6.3 Power Management Control Methodology

This section clarifies the power management control used to generate the reference commands $P_{o\,ref}$ and $Q_{o\,ref}$ explained in Section 6.2. In this control methodology, $Q_{o\,ref}$ is set to 0 at all times, i.e., the DFIG operates at a unity power factor. However, $P_{o\ ref}$ is determined through the power management controller. The power management controller has

three basic types of input: 1) the mechanical power input to the generator; 2) the storage energy level; and 3) the generator power output from the previous sample (i-1). The controller utilizes all types of input to generate the reference command $P_{o\ ref}$ which is send to the grid-side converter. Five scenarios are used to explain the power management control. Which scenario is selected depends on the wind speed and the status of the storage device as follows:

First Scenario: When the wind speed is too low (3m/s to 5 m/s), the slip factor is positive (sub-synchronous mode), and some amount of power (sP_g) circulates in the rotor circuit. In this scenario, the storage device should be disconnected.

Second Scenario: When the wind speed exceeds 5 m/s, the DFIG is in super-synchronous mode, the slip factor is negative; and power is transferred through both circuits, i.e., rotor and stator, to the grid ($(1- s)P_g$ is transferred through the stator and sP_g through the rotor). The second scenario is applied if and only if the storage is not fully charged. In this case, depending on the wind speed, the power management controller determines the appropriate power reference signal that corresponds to one of the power levels. This power level (value) is transferred to the grid through the stator circuit. However, the difference between the stator power and the power level is transferred through the grid-side converter to the storage device. The total amount of the rotor power is transferred to the storage device through the machine-side converter. The power reference command of the grid-side converter is therefore set to the negative of the difference between the power level and the stator power (i.e., the power flow direction is from the AC side to the DC bus). Fig. 6.2 shows a schematic diagram of the second scenario.

Third Scenario: If the operating power level drops (power dip), the storage supplies a portion of its stored energy through the grid-side converter in addition to the rotor power in order to develop the total DFIG power of the previously working level. The entire stator power is transmitted to the grid. The power reference command of the grid-side converter is therefore set to the difference between the power level and the stator power (i.e., the power flow direction is from the DC bus to the AC side). This scenario was designed to compensate

for speed dips that occur for short periods of time. However, if the speed increases again to the previous level, the second scenario is retained. Fig. 6.3 shows a schematic diagram of the second scenario.

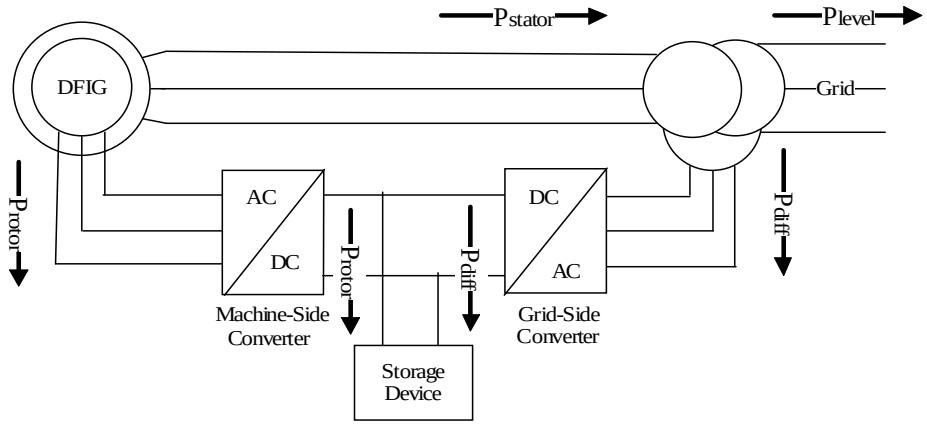

Fig. 6.2: The second scenario

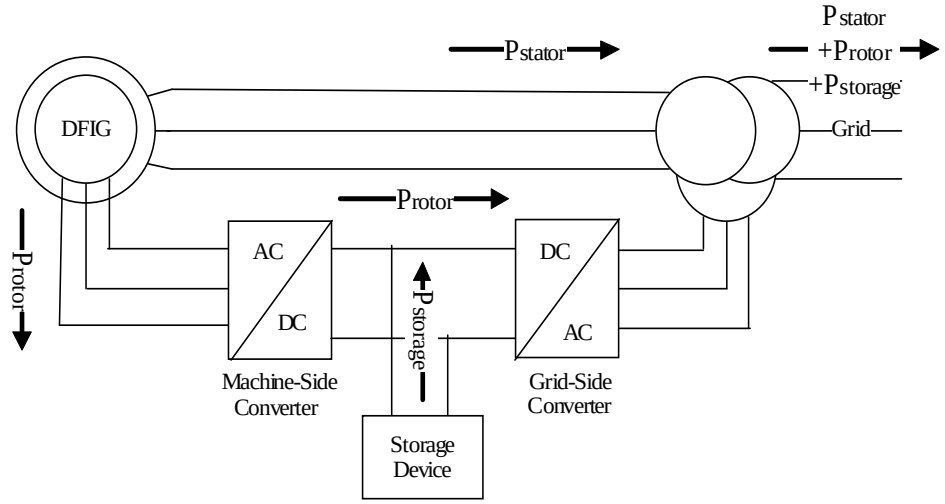

Fig. 6.3: The third scenario

Fourth Scenario: If the storage device is fully charged, the DFIG output power is boosted to the upper level by means of the stator, the rotor, and the storage. The power reference command of the grid-side converter is therefore set to the difference between the upper (next)

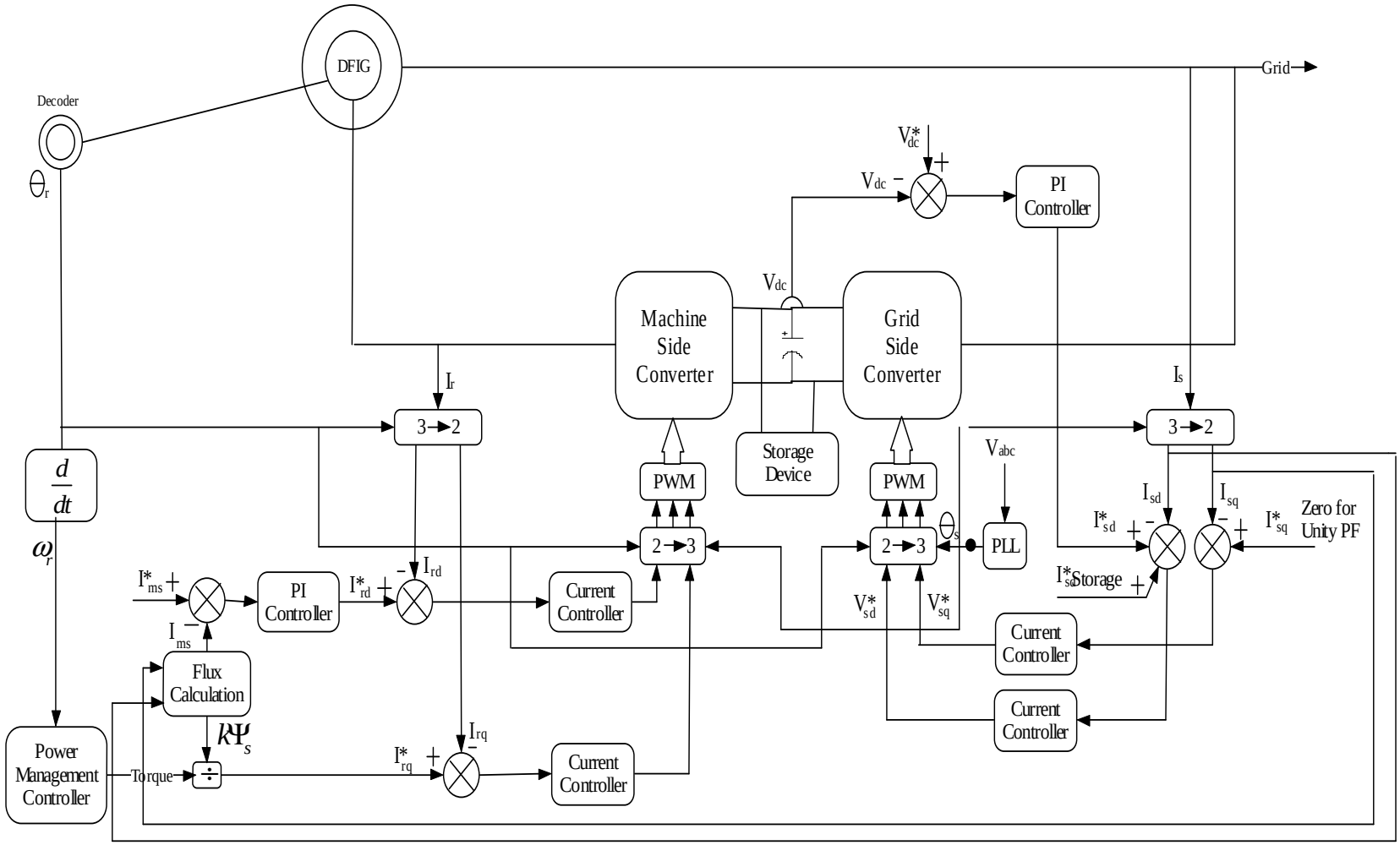

Fig. 6.4 Modified block diagram of the DFIG controller

power level and the stator power. The third and fourth scenarios are illustrated by the same schematic diagram.

Fifth Scenario: If the storage device is fully charged and the DFIG output power reaches its rated conditions (final power level), the pitch angle control is activated in order to limit the active power to the rated DFIG power.

The modified block diagram of DFIG controller after the application of the power management control methodology is given in Fig. 6.4. The three major modifications in the developed DFIG controller are the storage device, the power management controller and storage device reference signal. The power management controller selects one of the five scenarios according to the available wind power, the current power level, and the storage device status and it generates the storage device reference signal accordingly. The storage device and its controller are explained in the next section.

6.4 Storage Device

As with Type A WECS, a battery storage system (BSS) was also chosen for Type C WECS for the reasons previously explained in subsection 5.4.1. In addition, the existing DC bus between the two converters in the rotor circuit reduces the cost of the BSS by eliminating the need of a DC to AC converter [56-58].

6.4.1 System Description and Modeling

As illustrated in Fig. 6.1, the storage device was connected to a DC bus. The components of a BSS are a converter, a converter controller, and a storage element (battery bank). Fig. 6.5 shows a schematic diagram of the BSS. The following subsections illustrate the modeling of the BSS.

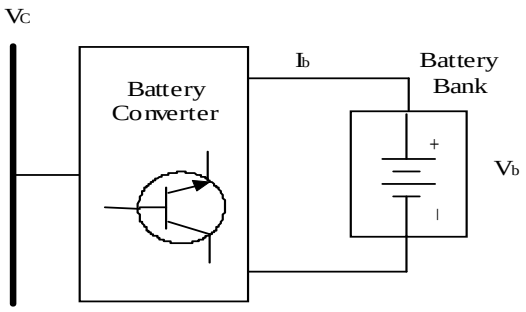

Fig. 6.5: Battery storage system (BSS)

6.4.1.1 Battery Converter

The battery converter is used to support the DC-Link voltage (V_{DC}). The rotor-side and stator-side converters draw currents I_1 and I_2, respectively. Neglecting the converter losses, the battery converter and the DC-link dynamics are governed by the following equations [43]:

$$v_b = L_b \frac{dI_b}{dt} + (1 - d_b)\, v_C \tag{6.11}$$

$$I_c = I_{DC} - I_1 - I_2 = (1 - d_b)I_b - I_1 - I_2 = C \frac{dv_C}{dt} \tag{6.12}$$

As shown in Fig. 6.6, the battery converter was modeled as a voltage-controlled current source, where L_b is the smoothing inductor.

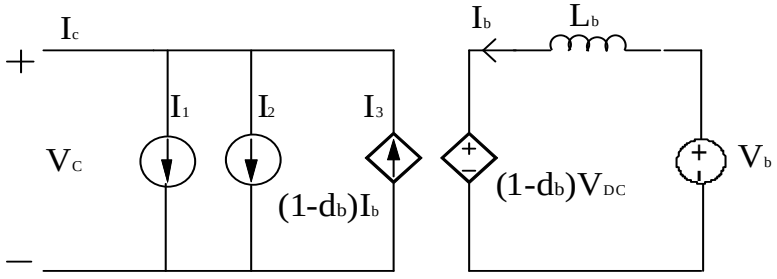

Fig. 6.6: Battery converter model

6.4.1.2 Battery Model

The battery model described in Chapter 5 was also used for Type C WECS.

6.4.1.3 Controller Design

Neglecting the battery converter losses, the power balance of the integrated wind power generation and energy converter system is governed by the following equations [43]:

$$P_b = P_r - P_g = V_C I_c = V_C C \frac{dv_C}{dt} \tag{6.13}$$

where P_b, P_r, and P_g are the battery power, the rotor-side converter power, and the grid-side converter power, respectively.

The active power transmitted into/from the battery storage is controlled using a PI controller, as given by

$$d_b = \left(k_{bp} + \frac{k_{bi}}{s}\right)(I_b^* - I_b) \tag{6.14}$$

where d_b is the PWM control signal, and k_{bp} and k_{bi} are the PI current controller gains.
Fig. 6.7 shows the structure of the controller of the battery converter.

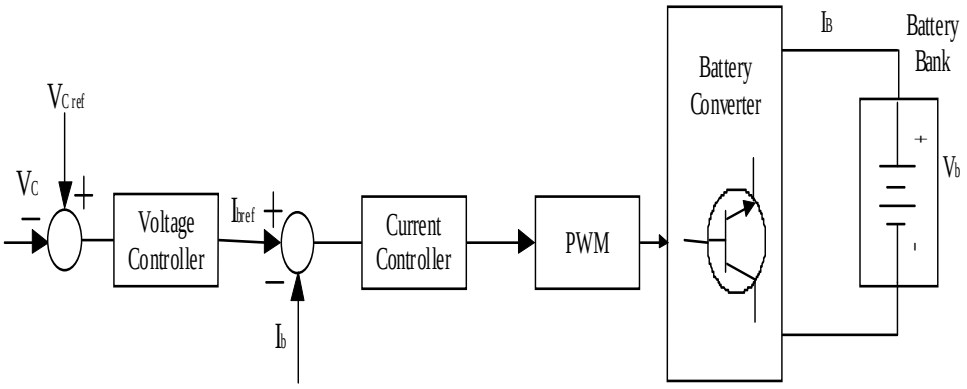

Fig. 6.7: Battery converter controller

In this simulation, the reactive power reference signal was set to zero so that reactive power would be neither absorbed nor transmitted to the grid. The active power reference signal was set to a value based on the scenarios explained in section 6.3. The active power reference signal can be positive or negative, depending on the desired power direction. In the second scenario, the active power signal is positive (charging mode); however, in the third,

fourth, and fifth scenarios, the active power signal is negative (discharging mode). The active power signal is set to zero in first and fifth scenarios.

6.4.2 Methodology

The following two criteria were used to obtain the optimum size of storage device. First, the size of the storage device was set to a very large value and the simulations were conducted on a yearly basis; the storage device is thus allowed to accumulate energy in the batteries as long as the power level of the previous time sample is equal to or higher than the current time sample, i.e., the fifth scenario is disabled. Once the generated power level decreases, the BSS is discharged to maintain the power level at its previous (higher) value. In this case, maintaining the power levels for a longer period is thus ensured. Second, the maximum size of the storage device (upper boundary) that is required to store all the energy for the entire year was set to be equal to the maximum energy level that the storage device reaches by the end of the year.

The size of the storage device was also evaluated relative to the available BSS technologies and their corresponding costs so that the benefit to the owner can be maximized. The evaluation was performed on a discrete basis to reflect the available sizes of the BSS in the market.

The objective function for maximizing the owner's benefits is given by

$$Max \sum_{i=1}^{8760} (C_e \times E_i\,(x)) - C_f(x) - C_v(x) \qquad \forall\, x = 0.1,0.2 \ldots E_{max} \tag{6.15}$$

The same procedure introduced in Chapter 5 was used to calculate the cost associated with the storage device.

6.5 Simulation Results

The first step was to calculate the optimum size of the storage to be used in the simulation results of the DFIG. As mentioned, the maximum size of the battery storage system was determined by adjusting its size to a very large number, running the simulation for a

complete year, and then taking the final value as the maximum value for the BSS. Table 6.1 shows the maximum size of the battery storage system. This value was then used to specify the upper boundary for the optimization problem, i.e., E_{max} in Equation (6.15).

TABLE 6.1: MAXIMUM SIZES OF THE BSS FOR 2005, 2006, AND 2007

Year	Maximum BSS Size (MWhr)
2005	0.83 MWhr
2006	0.901 MWhr
2007	0.953MWhr

The next step was to investigate the optimum size of the battery storage system, which led to a determination of whether the maximum storage size (i.e., to capture the total available wind energy) is also the most economical storage size. The answer was obtained through the evaluation of the cost of a range of incrementally larger storage device, which was compared to the amount of energy captured by each storage size. It is worth mentioning that a smaller battery storage system can capture a smaller amount of energy. Since BSSs are available in the market in discrete values, a step of 100 kWhr was assumed for this study. Equations (5.19) to (5.29) were applied to the parameters of the BSS technologies listed in Table 6.1 in order to determine the total annual cost of the available battery storage systems. This analysis was repeated for the range of BSS sizes, from 100 kWhr to the maximum storage size for all years/sites: 1000 kWhr. To calculate the net income for the owner, Equation (6.15) was applied, i.e., the total annual cost of the battery storage system was subtracted from the total savings, which is defined as the total energy captured for a given storage size multiplied by the price of energy. The total energy captured was calculated by adjusting the storage size in the simulations to the values of 100 kWhr to 1000 kWhr. Table 6.2 shows the net income for the various storage device sizes for each BSS technology.

TABLE 6.2: NET INCOME ASSOCIATED WITH THE BSS TECHNOLOGIES

	LA	VRLA	Na/S	Zn/Br	VRB
100 kWhr	-4.68	-9.94	-5.99	-1.95	-5.77
200 kWhr	-7.13	-21.46	-3.65	-2.61	-8.26
300 kWhr	-11.28	-33.33	-2.27	0.791	-12.44
400 kWhr	-15.98	-50.63	0.792	3.37	-15.24
500 kWhr	-18.35	-66.57	3.12	8.43	-16.27
600 kWhr	-20.76	-75.74	4.21	10.89	-18.15
700 kWhr	-22.45	-84.25	2.87	11.03	-19.23
800 kWhr	-24.38	-96.95	1.8	9.38	-19.89
900 kWhr	-26.01	-111.96	-1.36	4.84	-20.97
1000 kWhr	-27.5	-123	-3.32	2.15	-21.14

As can be seen in Table 6.2, not all BSS technologies are suitable for this application. As with Type A WECS, the Na/S and Zn/Br are the only possible candidate technologies because they produce positive net incomes. Within those two candidate technologies, a 600 kWhr Na/S BSS and a 700 kWhr Zn/Br BSS are the most economical sizes and are highlighted in Table 6.2. However, the globally optimal BSS is a 700 kWhr BSS with a Zn/Br battery bank.

Throughout the following simulation, the 700 kWhr battery storage system was attached to the DC link of the back-to-back converter in the rotor circuit of the DFIG in order to investigate the effect on the power levels of the addition of the storage device.

As discussed in Chapter 5, wind speed data that was collected over entire years collected from two different sites (Site A and B) was selected in order to include the seasonal effect.

The technical specifications of the 2.0 MW wind turbine are listed in Table 6.3, and these values were used in the simulation.

TABLE 6.3: SPECIFICATION OF A 2.0 MW DFIG-BASED WIND TURBINE

ROTOR	DIAMETER	80 M
	Area swept	5027 m^2
	Nominal revolution	16.7 rpm
	Operational interval	9-19 rpm
	Number of blades	3
Tower	Hub height	60-100 m
Operational Data	Cut-in speed	4 m/s
	Rated speed	15 m/s
	Cut-out speed	25 m/s
Generator	Type	DFIG
	Nominal output	2000 KW
	Operational data	50/60 Hz, 690 v

Fig. 6.8, Fig. 6.10, and Fig. 6.11 show the wind power with and without the addition of the battery storage system for the first day of 2005, 2006 and 2007, respectively, and Fig. 6.9 shows the behaviour of the DFIG during the first day of 2005.

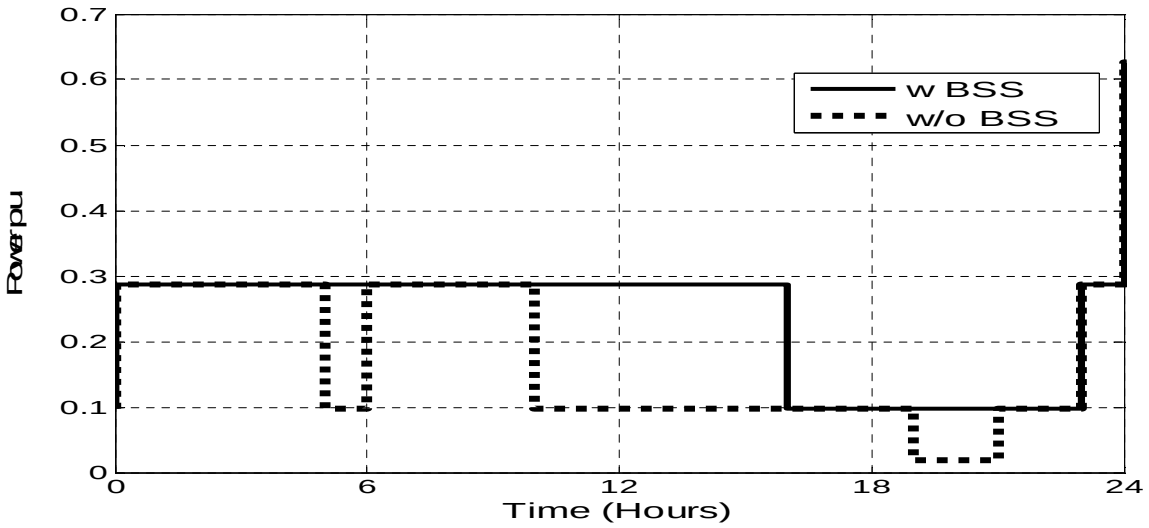

Fig. 6.8: Wind power levels without and with the BSS for the first day of 2005

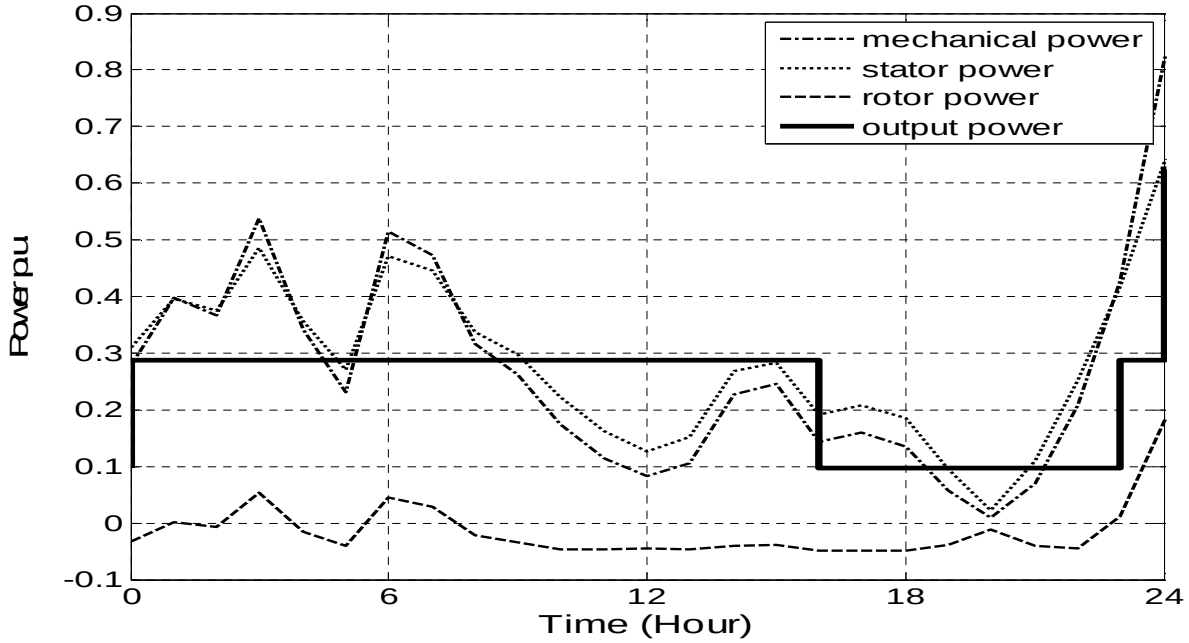

Fig. 6.9: Power management for the first day of 2005

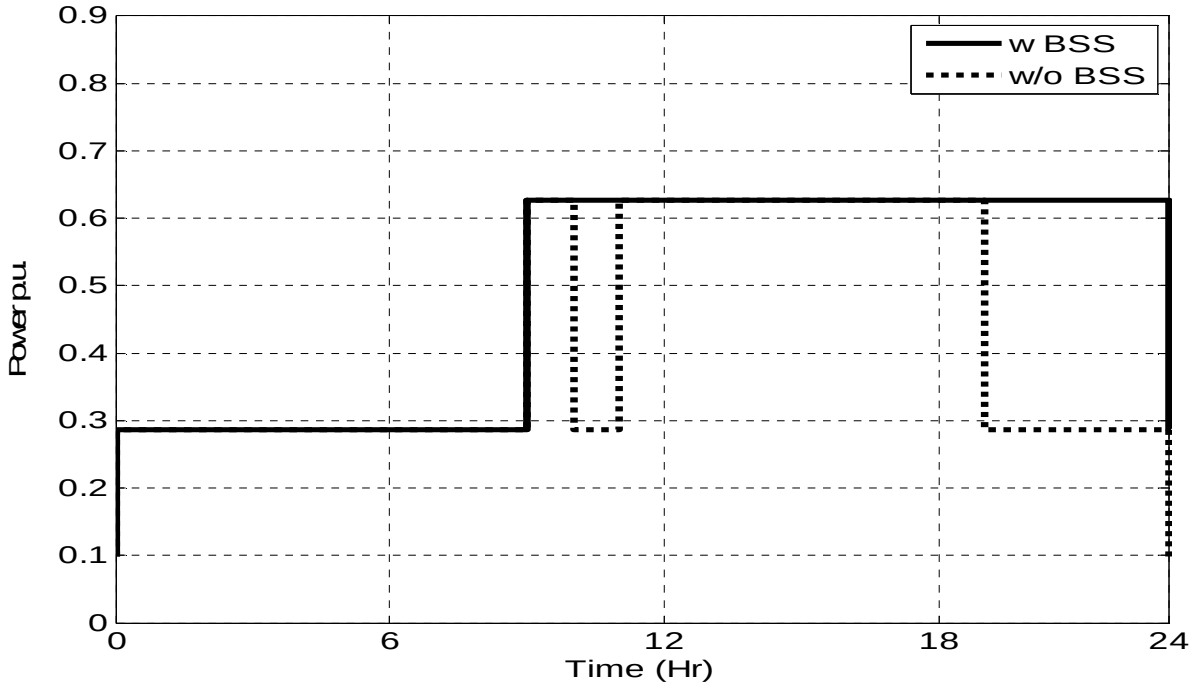

Fig. 6.10: Wind power levels without and with the BSS for the first day of 2006

In Figs. 6.8, 6.10, and 6.11 it can be noted that the continual variation in the output wind power has been greatly suppressed and that the output power is constant over a long period of time when the leveling technique is applied. Furthermore, when the WECS is operating at a specific power level and the generator suddenly toggles to a lower power level, the storage device injects energy into the grid in order to maintain the preceding power level, resulting in more constant output power. In addition, unlike Type A wind energy conversion system, Type C WECS exhibits no energy loss when the leveling technique is applied.

It can also be seen from Figs 6.8, 6.10, and 6.11 that not all power levels appear during every individual day; however, the daily levels are a subset of the levels selected for the entire year.

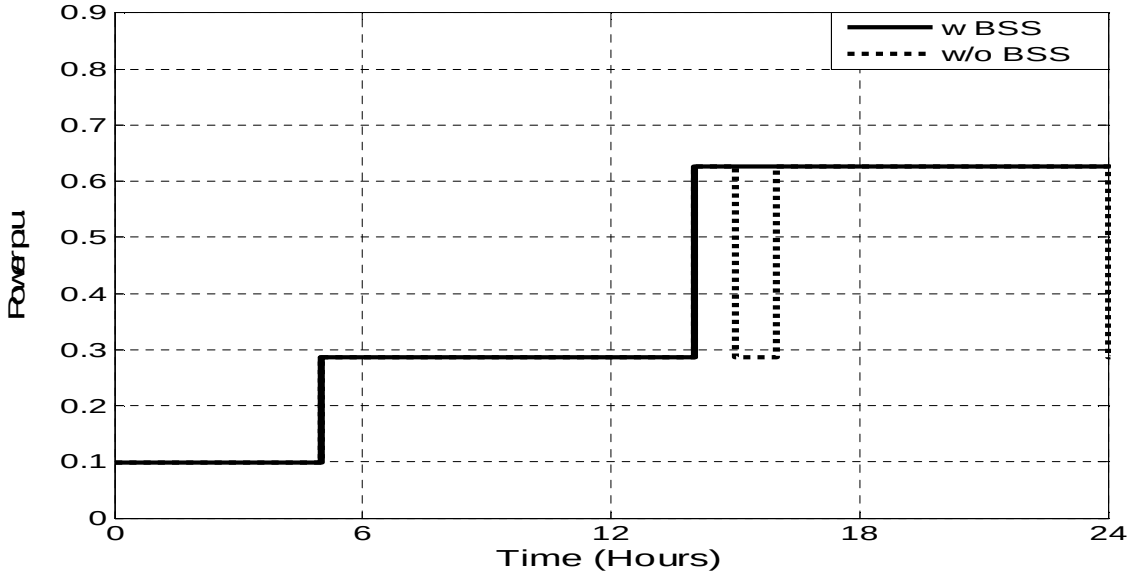

Fig. 6.11: Wind power levels without and with the BSS for the first day of 2007

6.6 Conclusion

Applying the leveling technique to a Type C WECS controller has several advantages. This technique ensures that power fluctuations are minimized because the generator produces constant amounts of power (i.e., same speed levels) for longer periods. It also enhances the

accuracy of wind speed (power) predictions since it predicts only the range of speed and not the exact speed value. In addition, no energy is lost due to power leveling, as occurs with Type A WECS. Finally, since the output power generated can be predicted accurately, the system operator can reduce the assigned reserves, and the operation of the power system generation pool becomes more manageable. On the other hand, the limitations of the proposed control methodology are the added costs due to the addition of the storage device and the modifications to the DFIG controller to accommodate the storage device.

Chapter 7
Optimum Sizing and Siting of Wind-Based DG in a Large Mesh Interconnected System

7.1 General

This chapter presents a new approach to the optimal determination of the appropriate size and location of wind-based distributed generation (WBDG) in a large mesh interconnected system. As mentioned in Chapters 5 and 6, applying the leveling technique converts the undispatchable wind generation to a reliable dispatchable source. In this chapter, wind-based distributed generation is treated as a power source with different fixed power levels, i.e., the leveling technique is used in WBDG. The chapter includes the description of a simple optimization technique in which the planner plays an important role in determining the optimal siting and sizing of the WBDG. Based on deficiencies in the system, the planner chooses appropriate weight factors for the parameters included in the optimization technique. Previous studies reported in the literature focused on determining the optimum size and/or site of the DG (dispatchable or non-dispatchable), with minimization of the system losses as the main target. However, in the developed algorithm, two additional new parameters are introduced: 1) voltage variations due to wind power fluctuation and 2) the percentage contribution of the WBDG to the short circuit current, which is introduced to represent the protective device requirements associated with the selection of the size and location of the WBDG. The new technique has been tested on the IEEE 24 - bus mesh interconnected test system. The results obtained clearly show that the optimal size and location can be easily determined using the developed approach.

7.2 Outline of the Approach and Objectives Outlines

The main objective of the work described in this chapter was to minimize the negative impact of installing wind-based DGs on the system performance, while maintaining the benefits of installing these DGs. This objective was achieved by preserving the following DG specifications:

- Optimal location of the WBDG
- Optimal size of the WBDG for a given location

For the purpose of this research, the impact of a WBDG can be categorized as either positive, because of the minimization of system losses, or negative, because of the voltage variations and the percentage contribution of the WBDG to the short-circuit current. The goal of the developed method is to maximize the positive impact and to minimize the negative ones. This approach is new because previous methods reported in the literature addressed only the positive impact of connecting wind energy: they determined optimal DG locations and ratings only by minimizing system losses.

7.3 Problem Formulation

As mentioned, the developed optimization technique is simple, flexible, and efficient. In the new algorithm each aspect of the impact of the WBDG is evaluated at all the generated power levels and then is multiplied by a weighting factor assigned to that aspect of the impact. The weighting factor is chosen by the planner to reflect the relative importance of each parameter in the decisions about the siting and sizing of the WBDG. The planner chooses the best weights depending on the deficiencies in the system. The location of the WBDG and its corresponding size in the electrical system can be optimally determined using the following objective function:

$$\max \quad f(P_{loss}, I_{SC}, V_{level}) \tag{7.1}$$

where

$$f(P_{loss}, I_{SC}, V_{level}) = \sum_{i=1}^{m} W_i \frac{F_i}{F_i^{\max}} \tag{7.2}$$

where F_i is the aspect of the impact of the WBDG, and W_i is the weighting factor selected by the planner to indicate the relative importance of that aspect of the impact, *i*. F_i^{max} is the maximum value of the aspect of the impact of the WBDG *i*, for all cases studied [99]. Three

aspect of the impact are expressed as F_P, F_I, and F_V. F_P, relates the percentage change in the power losses to the installation of the WBDG and F_P is given by

$$F_P = \frac{P_{loss}^{without\ DG} - P_{loss}^{with\ DG}}{P_{loss}^{without\ DG}} \tag{7.3}$$

where $P_{loss}^{without\ DG}$ is the summation of the system power loss before the installation of the WBDG, and $P_{loss}^{with\ DG}$ is the summation of the system power loss after the installation of the WBDG.

The second aspect of the impact, F_I, is the percentage increase in the short circuit current at each bus due to the installation of the WBDG. F_I is given by

$$F_I = \frac{I_{sc}^{without\ DG} - I_{sc}^{with\ DG}}{I_{sc}^{without\ DG}} \tag{7.4}$$

where $I_{sc}^{without\ DG}$ is the short circuit current before the installation of the WBDG, and $I_{sc}^{with\ DG}$ is the short circuit current after the installation of the WBDG. The value of F_I is always negative because the connection of any size WBDG at any location contributes to the short circuit current.

The third aspect of the WBDG impact introduced in this study, F_V, is the percentage change in the voltage level at each bus.

$$F_V = \frac{\left| V_{scheduled}^{without\ DG} - V^{with\ DG} \right|}{V_{scheduled}^{without\ DG}} \tag{7.5}$$

where $V_{scheduled}^{without\ DG}$ is the scheduled voltage level at each bus before the installation of the WBDG, and $V^{with\ DG}$ is the voltage level at each bus after the installation of the WBDG. The

sign of F_V is not important because any variation in voltage is considered a negative impact of the installation of a WBDG.

To determine the relative importance of each of the above aspects of the WBDG impact, each aspect is multiplied by a weighting factor, W_i. The weighting factor may be either negative or positive depending on the nature of the particular aspect of the impact. The sum of the absolute values of the weights assigned to all aspects of the impacts should add up to one, as shown in the following:

$$\left|W_{F_P}\right| + \left|W_{F_I}\right| + \left|W_{F_V}\right| = 1 \tag{7.6}$$

The objective function expressed as Equation (7.1) is subject to two main constraints: the bus voltage levels and the coordination limits of the protective devices. These constraints can be expressed as follows:

$$V_{\min} < V_{level}^{with\ DG} < V_{\max} \tag{7.7}$$

where $V_{\min}$ and $V_{\max}$ are the minimum and maximum permissible voltage limits at each bus, repectively.
and

$$I_{sc}^{with\ DG} < \textit{Short circuit level of the currently installed protective devices} \tag{7.8}$$

When the objective function, Equation (7.1), is subject to the constraints of Equations (7.7) and (7.8), the solution yields the optimum DG size and location as explained in the algorithm presented in the following subsection.

7.4 The Algorithm

Fig. 7.1 shows the flowchart of the developed algorithm, and Table 7.1 shows the procedure for the optimization technique used in this algorithm. Before the algorithm is run, the planner must input all of the data related to the system, including generation, transmission, transformers, and loads and must provide appropriate weights for the aspects of DG impact. The power flow analysis and short circuit analysis are then used in the analysis, which proceeds according to the following steps in the algorithm:

(1) Calculate the total system losses ($P_{loss}^{without\ DG}$), the short circuit current ($I_{sc}^{without\,DG}$) at all the available buses, and the voltage level ($V_{sheduled}^{without\,DG}$) at all the available buses as they exists prior to any DG placement (i.e., without DG).

(2) Consider the sizes of the WBDGs available in the market and determine the rated power of the ones that lie within the project budget. Calculate the power levels that correspond to the ratings of the suitable WBDGs.

(3) At the first available bus and using the first available WBDG rating, recalculate the following after the inclusion of the DG:

   (a) The short circuit current using the full rating of the WBDG (worst case scenario)

   (b) For each power level, the total system losses ($P_{loss}^{with\ DG}$) and the voltage level ($V_{level}^{with\ DG}$).

(4) Multiply the results from (3.b) by the density factor that corresponds to each power level, which is explained in Section 7.5.4.

(5) Calculate F_{11P}, F_{11I}, and F_{11V} according to Equations (7.3), (7.4), and (7.5). The results are tabulated as shown in Table 7.1, where the suffix (ijk) indicates the available bus i, the available rating j, and the level k, respectively.

TABLE 7.1: THE OPTIMIZATION TECHNIQUE

BUS No	RATING	LEVEL	$\alpha F_{ijk}(P)$	$\beta F_{ijk}(I)$	$\gamma F_{ijk}(V)$	Σ
BUS 1	Rating 1	Level 1	$\alpha F_{111}(P)$	$\beta F_{111}(I)$	$\gamma F_{111}(V)$	$\alpha F_{111}(P)+\beta F_{111}(I)+\gamma F_{111}(V)$
		Level 2	$\alpha F_{112}(P)$	$\beta F_{112}(I)$	$\gamma F_{112}(V)$	$\alpha F_{112}(P)+\beta F_{112}(I)+\gamma F_{112}(V)$
		…	…	…	…	…
		Level k	$\alpha F_{11k}(P)$	$\beta F_{11k}(I)$	$\gamma F_{11k}(V)$	$\alpha F_{11k}(P)+\beta F_{11k}(I)+\gamma F_{11k}(V)$
	Rating 2	Level 1	$\alpha F_{121}(P)$	$\beta F_{121}(I)$	$\gamma F_{121}(V)$	$\alpha F_{121}(P)+\beta F_{121}(I)+\gamma F_{121}(V)$
		Level 2	$\alpha F_{122}(P)$	$\beta F_{122}(I)$	$\gamma F_{122}(V)$	$\alpha F_{122}(P)+\beta F_{122}(I)+\gamma F_{122}(V)$
		…	…	…	…	…
		Level k	$\alpha F_{12k}(P)$	$\beta F_{12k}(I)$	$\gamma F_{12k}(V)$	$\alpha F_{12k}(P)+\beta F_{12k}(I)+\gamma F_{112k}(V)$
	Rating j	Level 1	$\alpha F_{1j1}(P)$	$\beta F_{1j1}(I)$	$\gamma F_{1j1}(V)$	$\alpha F_{1j1}(P)+\beta F_{1j1}(I)+\gamma F_{1j1}(V)$
		Level 2	$\alpha F_{1j2}(P)$	$\beta F_{1j2}(I)$	$\gamma F_{1j2}(V)$	$\alpha F_{1j2}(P)+\beta F_{1j2}(I)+\gamma F_{1j2}(V)$
		…	…	…	…	…
		Level k	$\alpha F_{1jk}(P)$	$\beta F_{1jk}(I)$	$\gamma F_{1jk}(V)$	$\alpha F_{1jk}(P)+\beta F_{1jk}(I)+\gamma F_{1jk}(V)$
Bus 2	…	…	…	…	…	…
BUS i	Rating 1	Level 1	$\alpha F_{i11}(P)$	$\beta F_{i11}(I)$	$\gamma F_{i11}(V)$	$\alpha F_{i11}(P)+\beta F_{i11}(I)+\gamma F_{i11}(V)$
		Level 2	$\alpha F_{i12}(P)$	$\beta F_{i12}(I)$	$\gamma F_{i12}(V)$	$\alpha F_{i12}(P)+\beta F_{i12}(I)+\gamma F_{i12}(V)$
		…	…	…	…	…
		Level k	$\alpha F_{i1k}(P)$	$\beta F_{i1k}(I)$	$\gamma F_{i1k}(V)$	$\alpha F_{i1k}(P)+\beta F_{i1k}(I)+\gamma F_{i1k}(V)$
	Rating 2	Level 1	$\alpha F_{i21}(P)$	$\beta F_{i21}(I)$	$\gamma F_{i21}(V)$	$\alpha F_{i21}(P)+\beta F_{i21}(I)+\gamma F_{i21}(V)$
		Level 2	$\alpha F_{i22}(P)$	$\beta F_{i22}(I)$	$\gamma F_{i22}(V)$	$\alpha F_{i22}(P)+\beta F_{i22}(I)+\gamma F_{i22}(V)$
		…	…	…	…	…
		Level k	$\alpha F_{i2k}(P)$	$\beta F_{i2k}(I)$	$\gamma F_{i2k}(V)$	$\alpha F_{i2k}(P)+\beta F_{i2k}(I)+\gamma F_{i12k}(V)$
	Rating j	Level 1	$\alpha F_{ij1}(P)$	$\beta F_{ij1}(I)$	$\gamma F_{ij1}(V)$	$\alpha F_{ij1}(P)+\beta F_{ij1}(I)+\gamma F_{ij1}(V)$
		Level 2	$\alpha F_{ij2}(P)$	$\beta F_{ij2}(I)$	$\gamma F_{ij2}(V)$	$\alpha F_{ij2}(P)+\beta F_{ij2}(I)+\gamma F_{ij2}(V)$
		…	…	…	…	…
		Level k	$\alpha F_{ijk}(P)$	$\beta F_{ijk}(I)$	$\gamma F_{ijk}(V)$	$\alpha F_{ijk}(P)+\beta F_{ijk}(I)+\gamma F_{ijk}(V)$

(6) Switch to the next available WBDG rating and perform the same calculations as in steps 3, 4, and 5. The results of this load bus are tabulated for all available WBDG sizes, i.e., F_{12P}, F_{13P} … F_{1NP}; F_{12I}, F_{13I} … F_{1NI}; and F_{12V}, F_{13V} … F_{1NV}. N is the number of available WBDG ratings.

(7) Switch to the next available bus and repeat steps 3, 4, 5, and 6 until all the available buses M are considered. The results for each bus for different WBDG sizes are tabulated and normalized. Normalizing the results entails dividing each type of result by the value of the maximum corresponding result, i.e., F_{11P}', F_{12P}' … F_{MNP}'; F_{11I}', F_{12I}' … F_{MNI}'; and F_{11V}', F_{12V}' … F_{MNV}'.

(8) Multiply each entry type by its corresponding weighting factor (α, β, and γ), and then add the resultant values of every row (Sum_{MN}).

The maximum of the summed weighted normalized value ($\sum_{i=1}^{m} W_i \frac{F_i}{F_i^{\max}}$) gives the optimum size (row) and the optimum site (column) for the WBDG. It is possible that one of the power levels is also the optimum size of the WBDG; in this case, the optimum size is the full rating of the WBDG that corresponds to that power level.

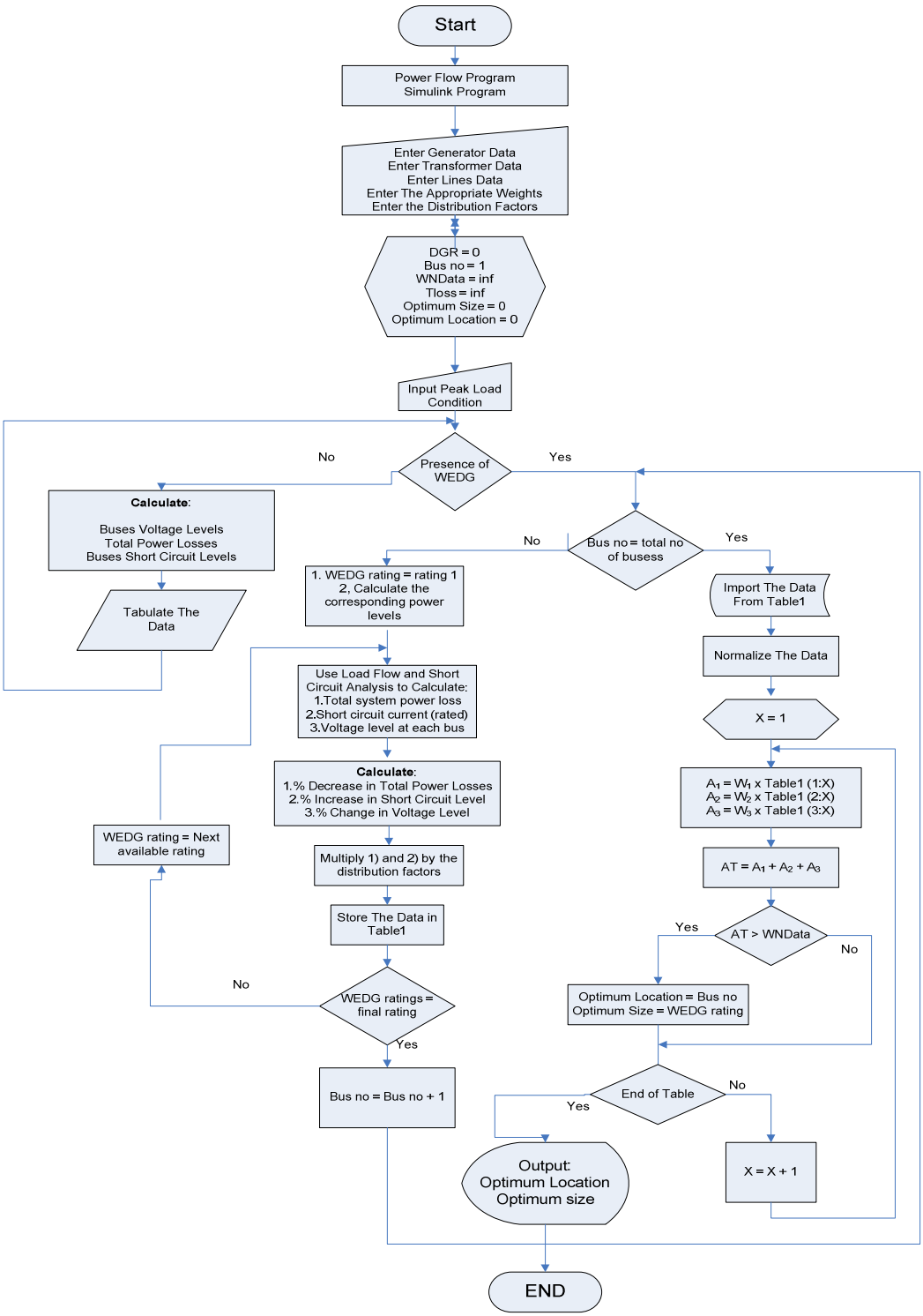

Fig. 7.1: The algorithm

7.5 System Description

The IEEE 24-bus meshed system [100] was used to test the developed method.

7.5.1 Load Model

The system was assumed to be heavily loaded. The annual peak load for the test system was set at 2850 MW. The load factor for this system is 61.4 %. A peak loading condition with a load diversity factor of one was considered in the analysis.

7.5.2 Generating System

Table 7.2 gives the number of each generating unit installed on the IEEE 24-bus test system, its corresponding bus number and the rating of each generating unit.

TABLE 7.2: NUMBER AND RATINGS OF GENERATORS

Bus	Unit 1 MW	Unit 2 MW	Unit 3 MW	Unit 4 MW	Unit 5 MW	Unit 6 MW
1	20	20	76	76	-	-
2	20	20	76	76	-	-
7	100	100	100	-	-	-
13	197	197	197	-	-	-
15	12	12	12	12	12	155
16	155	-	-	-	-	-
18	400	-	-	-	-	-
21	400	-	-	-	-	-
22	50	50	50	50	50	50
23	155	155	350	-	-	-

7.5.3 Network System

The network consists of 24 bus locations connected by 38 lines and transformers, as shown in Fig. 7.2. The transmission lines were set at two different voltage levels.

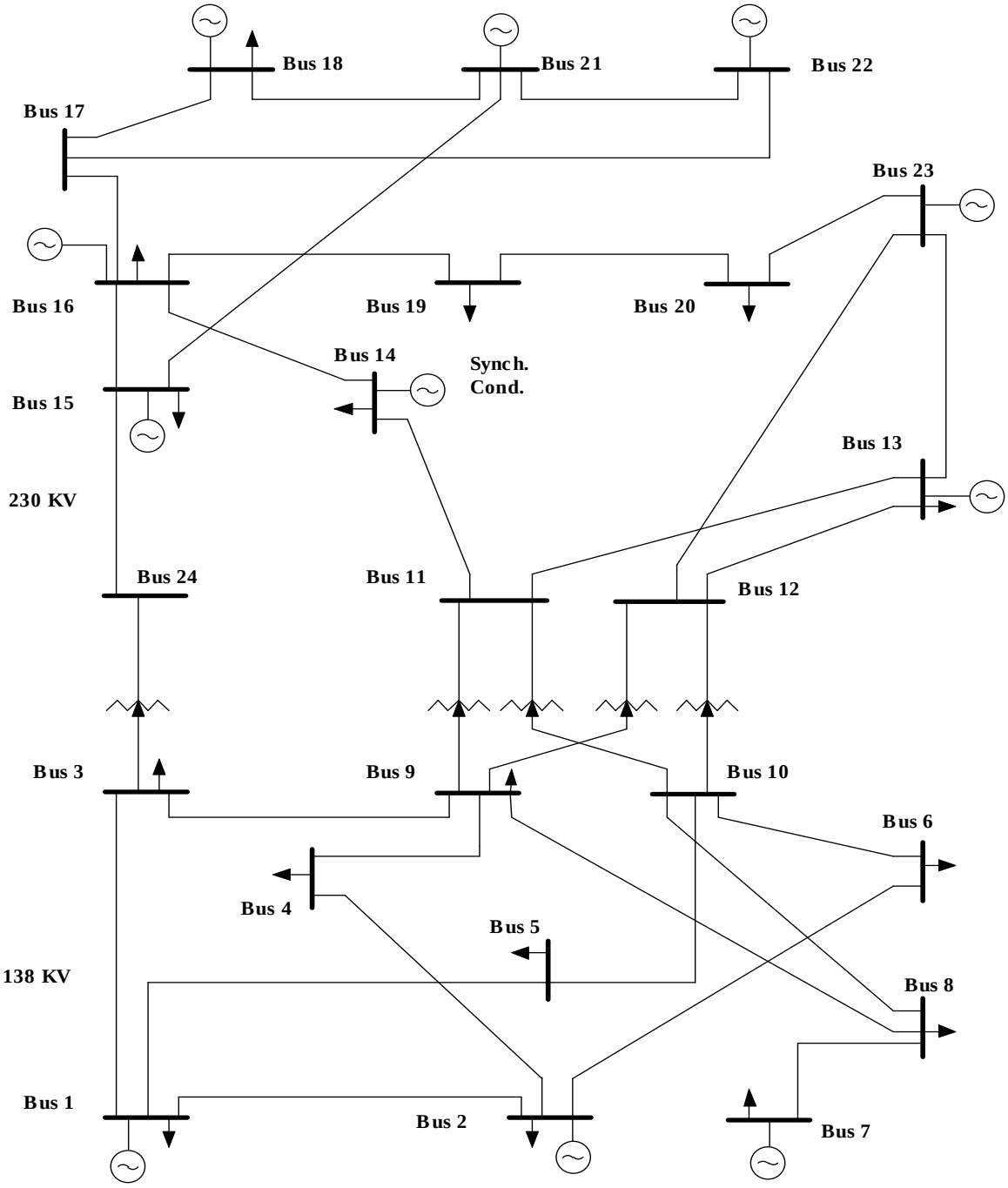

Fig. 7.2: The IEEE 24-bus test system

Impedance and rating data for lines and transformers can be found in [100]. All the data are in per unit on a base of 100 MVA. The data given assumes the transmission line to be modeled as a Π equivalent circuit.

7.5.4 Wind-Based Distributed Generation (WBDG)

Wind-based distributed generation is a wind generator with the new leveling technique applied to its controller, i.e., it could be either Type A or Type C WECS. The optimization algorithm described in Section 7.4 calculates the system parameters, (e.g., short circuit level, system power losses, and voltage variations) that correspond to each power level of every available WBDG rating. It is possible that the solution of the optimization problem could result in an optimum size corresponding to a power level that lasts for only a relatively short time during the year. To solve this problem, a density factor was introduced into the optimization algorithm. This density factor acts like the weighting factor selected by the planner, i.e., a density factor is assigned for each level such that the sum of the factors is unity. The wind-based distributed generation density factor is very similar to the load density factor used in examining power system security [101] and is calculated as follows:

$$DF_{level} = \frac{Duration\ of\ power\ level}{Total\ duration} \tag{7.9}$$

Fig. 7.3 shows a graphical representation of the distribution factor, indicating the values of the distribution factor for each level.

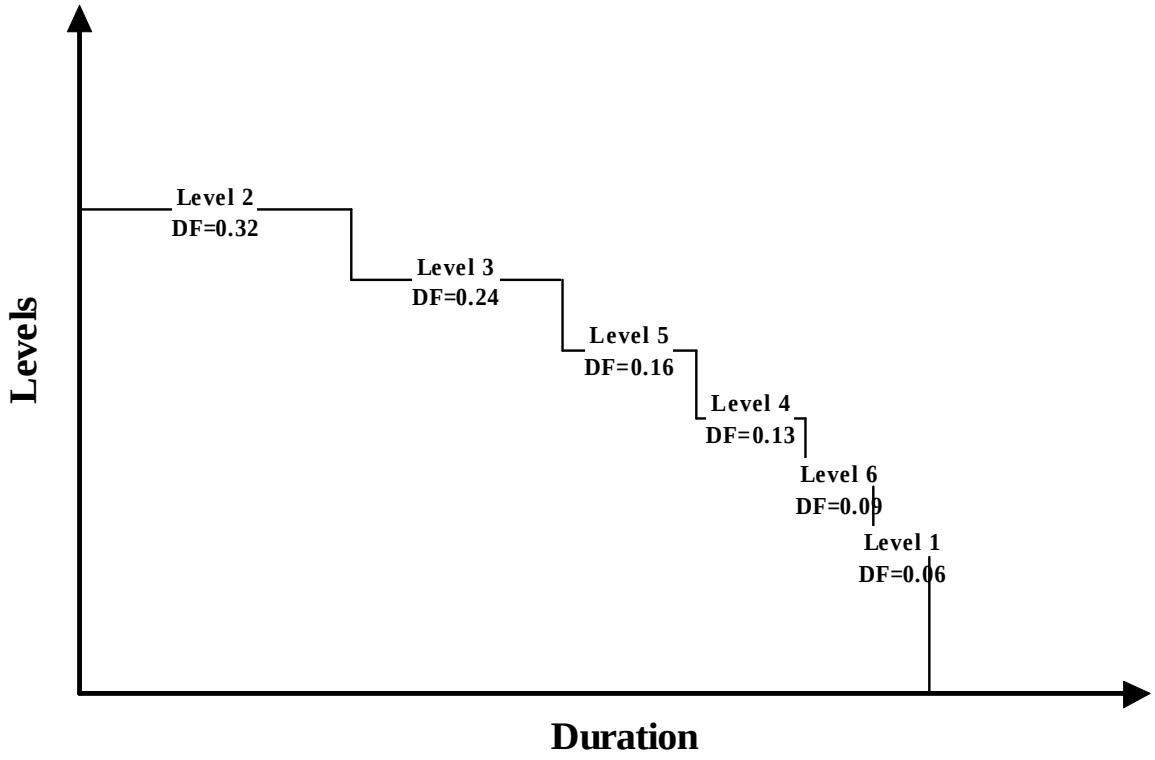

Fig. 7.3: The WBDG distribution factor

In the optimization algorithm to reflect the duration factor (distribution factor) of each level, the distribution factors are multiplied by the normalized value of the voltage variation and by the system power loss corresponding to each level.

7.6 Simulation Results

The wind speed data for 2005 were used in the simulation. Table 7.3 shows the optimal number of power levels, the optimal values of the wind speed levels, the per unit developed power for each power level, and the associated distribution factor for each power level calculated over a period of one year (2005). In the developed optimization algorithm, three WBDG sizes were considered: 50 MW, 100 MW, and 300 MW. The algorithm was tested on the IEEE 24-bus mesh interconnected test system. The data obtained were tabulated and then

normalized by dividing each element in a specific column by the maximum positive value in that column. The maximum value of each parameter in each column is thus one.

After the data are normalized, the planner should select the appropriate weighting factors based on his own experience. To represent a negative impact on system performance, the weighting factor of the absolute value of the voltage fluctuations should be negative; however, the percentage increase in the short circuit level has an inherent negative sign ($I_{sc}^{without\ DG} < I_{sc}^{with\ DG}$) and hence requires a positive weighting factor. The final consideration was that the weighting factor of the percentage decrease in losses should be positive (positive impact). Three equal weighting factors were selected for the first case study representing the assumption that the planner has no specific problem to solve. These weighting factors were set at 0.33 for the system power losses, 0.33 for the increase in the short circuit level, and -0.33 for the voltage variations. Table 7.4 shows the weighted normalized results obtained for equal weighting factors.

TABLE 7.3: OPTIMAL SPEED AND POWER LEVEL VALUES AND ASSOSIATED DISTRIBUTION FACTORS FOR 2005

LEVEL	**SPEED LEVEL VALUES**	**POWER LEVEL VALUES**	**DISTRIBUTION FACTORS**
1	4 m/s	0.2 p.u.	0.041
2	6.6 m/s	0.33 p.u.	0.229
3	8.51 m/s	0.43 p.u.	0.336
4	9.9 m/s	0.5 p.u.	0.192
5	12.3 m/s	0.62 p.u.	0.117
6	15 m/s	1 p.u.	0.085

TABLE 7.4: WEIGHTED NORMALIZED RESULTS WITH EQUAL WEIGHTING FACTORS (0.3, 0.3, AND -0.3 RESPECTIVELY)

BUS No	RATING	LEVEL	αF_{ijP}	βF_{ijI}	γF_{ijV}	Σ
BUS 3	50 MW	Level 1	0.0457	-0.16258	-0.3039	-0.42078
		Level 2	0.0601	-0.16258	-0.3075	-0.40998
		Level 3	0.0658	-0.16258	-0.3111	-0.40788
		Level 4	0.0829	-0.16258	-0.3145	-0.39418
		Level 5	0.0868	-0.16258	-0.329	-0.40478
		Level 6	0.0995	-0.16258	-0.33	-0.39308
	100 MW	Level 1	0.0992	-0.16556	-0.3304	-0.39676
		Level 2	0.0883	-0.16556	-0.3369	-0.41416
		Level 3	0.0757	-0.16556	-0.3374	-0.42726
		Level 4	0.069	-0.16556	-0.3378	-0.43436
		Level 5	0.0688	-0.16556	-0.3389	-0.43566
		Level 6	0.0634	-0.16556	-0.34	-0.44216
	300 MW	Level 1	-0.0536	-0.17457	-0.3426	-0.57077
		Level 2	-0.0898	-0.17457	-0.345	-0.60937
		Level 3	-0.2228	-0.17457	-0.3478	-0.74517
		Level 4	-0.3455	-0.17457	-0.3528	-0.87287
		Level 5	-0.3546	-0.17457	-0.3582	-0.88737
		Level 6	-0.4975	-0.17457	-0.36	-1.03207
BUS 4	50 MW	Level 1	-0.3606	-0.2401	-0.3573	-0.958
		Level 2	-0.2933	-0.2401	-0.3548	-0.8882
		Level 3	-0.1027	-0.2401	-0.3423	-0.6851
		Level 4	-0.0102	-0.2401	-0.3357	-0.586
		Level 5	0.0722	-0.2401	-0.3089	-0.4768
		Level 6	0.13385	-0.2401	-0.263	-0.36925
	100 MW	Level 1	-0.3643	-0.2444	-0.2635	-0.8722
		Level 2	-0.3375	-0.2444	-0.2637	-0.8456
		Level 3	-0.3197	-0.2444	-0.2638	-0.8279
		Level 4	0.0374	-0.2444	-0.2638	-0.4708
		Level 5	0.0526	-0.2444	-0.2639	-0.4557
		Level 6	0.1158	-0.2444	-0.264	-0.3926
	300 MW	Level 1	0.0946	-0.28611	-0.264	-0.45551
		Level 2	-0.3688	-0.28611	-0.2642	-0.91911
		Level 3	-0.3723	-0.28611	-0.2642	-0.92261
		Level 4	-0.4234	-0.28611	-0.2644	-0.97391
		Level 5	-0.6227	-0.28611	-0.2649	-1.17371
		Level 6	-0.6521	-0.28611	-0.265	-1.20321

BUS 5	50 MW	Level 1	-0.6322	-0.07721	-0.1599	-0.86931
		Level 2	-0.377	-0.07721	-0.1267	-0.58091
		Level 3	-0.2894	-0.07721	-0.0982	-0.46481
		Level 4	-0.1627	-0.07721	-0.0777	-0.31761
		Level 5	0.1093	-0.07721	-0.042	-0.00991
		Level 6	0.11837	-0.07721	-0.0212	0.01996
	100 MW	Level 1	0.1143	-0.07812	-0.0219	0.01428
		Level 2	0.1122	-0.07812	-0.0221	0.01198
		Level 3	0.1077	-0.07812	-0.0221	0.00748
		Level 4	0.1057	-0.07812	-0.0237	0.00388
		Level 5	0.1019	-0.07812	-0.0247	-0.00092
		Level 6	0.0986	-0.07812	-0.0255	-0.00502
	300 MW	Level 1	-0.0446	-0.08514	-0.0258	-0.15554
		Level 2	-0.0748	-0.08514	-0.026	-0.18594
		Level 3	-0.2965	-0.08514	-0.0264	-0.40804
		Level 4	-0.4625	-0.08514	-0.0269	-0.57454
		Level 5	-0.5145	-0.08514	-0.027	-0.62664
		Level 6	-0.582	-0.08514	-0.02706	-0.6942
BUS 6	50 MW	Level 1	-0.5373	-0.2998	-0.0249	-0.862
		Level 2	-0.3172	-0.2998	-0.0201	-0.6371
		Level 3	-0.1608	-0.2998	-0.0199	-0.4805
		Level 4	0.0157	-0.2998	-0.018	-0.3021
		Level 5	0.3283	-0.2998	-0.0167	0.0118
		Level 6	0.33	-0.2998	-0.0144	0.0158
	100 MW	Level 1	0.3303	-0.3003	-0.0145	0.0155
		Level 2	0.3304	-0.3003	-0.0147	0.0154
		Level 3	0.3305	-0.3003	-0.0147	0.0155
		Level 4	0.3307	-0.3003	-0.0149	0.0155
		Level 5	0.3309	-0.3003	-0.0149	0.0157
		Level 6	0.33	-0.3003	-0.0151	0.0146
	300 MW	Level 1	0.3241	-0.2574	-0.0151	0.0516
		Level 2	0.2602	-0.2574	-0.0152	-0.0124
		Level 3	0.2595	-0.2574	-0.0153	-0.0132
		Level 4	0.241	-0.2574	-0.0154	-0.0318
		Level 5	0.2306	-0.2574	-0.0154	-0.0422
		Level 6	0.1977	-0.2574	-0.01551	-0.07521

BUS 8	50 MW	Level 1	0.1842	-0.33	-0.0794	-0.2252
		Level 2	0.1723	-0.33	-0.0857	-0.2434
		Level 3	0.1244	-0.33	-0.1316	-0.3372
		Level 4	0.1063	-0.33	-0.1412	-0.3649
		Level 5	0.0903	-0.33	-0.2076	-0.4473
		Level 6	0.08366	-0.33	-0.23211	-0.47845
	100 MW	Level 1	0.126	-0.33	-0.2313	-0.4353
		Level 2	0.2258	-0.33	-0.2311	-0.3353
		Level 3	0.2385	-0.33	-0.2309	-0.3224
		Level 4	0.2772	-0.33	-0.2307	-0.2835
		Level 5	0.2874	-0.33	-0.2306	-0.2732
		Level 6	0.293	-0.33	-0.23039	-0.26739
	300 MW	Level 1	0.2465	-0.33	-0.2312	-0.3147
		Level 2	0.2346	-0.33	-0.2317	-0.3271
		Level 3	0.2229	-0.33	-0.2319	-0.339
		Level 4	0.2006	-0.33	-0.2322	-0.3616
		Level 5	-0.0895	-0.33	-0.2324	-0.6519
		Level 6	-0.1339	-0.33	-0.23331	-0.69721
BUS 9	50 MW	Level 1	-0.1244	-0.18991	-0.2348	-0.54911
		Level 2	-0.113	-0.18991	-0.2357	-0.53861
		Level 3	0.012	-0.18991	-0.2363	-0.41421
		Level 4	0.0904	-0.18991	-0.2371	-0.33661
		Level 5	0.1089	-0.18991	-0.2375	-0.31851
		Level 6	0.1104	-0.18991	-0.24	-0.31951
	100 MW	Level 1	0.1176	-0.20254	-0.2401	-0.32504
		Level 2	0.1193	-0.20254	-0.2403	-0.32354
		Level 3	0.1257	-0.20254	-0.241	-0.31784
		Level 4	0.1267	-0.20254	-0.2412	-0.31704
		Level 5	0.1286	-0.20254	-0.2418	-0.31574
		Level 6	0.1294	-0.20254	-0.24222	-0.31536
	300 MW	Level 1	0.1306	-0.25344	-0.2423	-0.36514
		Level 2	0.1446	-0.25344	-0.2423	-0.35114
		Level 3	0.151	-0.25344	-0.2424	-0.34484
		Level 4	0.1543	-0.25344	-0.2425	-0.34164
		Level 5	0.1546	-0.25344	-0.2432	-0.34204
		Level 6	0.1582	-0.25344	-0.24322	-0.33846

BUS 10	50 MW	Level 1	0.1586	-0.02746	-0.2346	-0.10346
		Level 2	0.1587	-0.02746	-0.231	-0.09976
		Level 3	0.1597	-0.02746	-0.1914	-0.05916
		Level 4	0.1605	-0.02746	-0.1799	-0.04686
		Level 5	0.1608	-0.02746	-0.0683	0.06504
		Level 6	0.1619	-0.02746	-0.01147	0.12297
	100 MW	Level 1	0.1623	-0.0337	-0.0119	0.1167
		Level 2	0.1657	-0.0337	-0.012	0.12
		Level 3	0.1729	-0.0337	-0.0126	0.1266
		Level 4	0.1778	-0.0337	-0.013	0.1311
		Level 5	0.1788	-0.0337	-0.0134	0.1317
		Level 6	0.1881	-0.0337	-0.0139	0.1405
	300 MW	Level 1	0.2319	-0.04785	-0.0139	0.17015
		Level 2	0.2337	-0.04785	-0.01397	0.17188
		Level 3	0.2445	-0.04785	-0.014	0.18265
		Level 4	0.2902	-0.04785	-0.0141	0.22825
		Level 5	0.3084	-0.04785	-0.0142	0.24635
		Level 6	0.33	-0.04785	-0.01419	0.26796
BUS 11	50 MW	Level 1	0.3192	-0.13479	-0.0298	0.15461
		Level 2	0.2137	-0.13479	-0.0317	0.04721
		Level 3	0.1977	-0.13479	-0.0641	-0.00119
		Level 4	0.1504	-0.13479	-0.069	-0.05339
		Level 5	0.1378	-0.13479	-0.0887	-0.08569
		Level 6	0.0983	-0.13479	-0.09112	-0.12761
	100 MW	Level 1	0.0984	-0.15486	-0.0918	-0.14826
		Level 2	0.0998	-0.15486	-0.0945	-0.14956
		Level 3	0.1038	-0.15486	-0.0949	-0.14596
		Level 4	0.1084	-0.15486	-0.0953	-0.14176
		Level 5	0.1165	-0.15486	-0.0967	-0.13506
		Level 6	0.1206	-0.15486	-0.0989	-0.13316
	300 MW	Level 1	0.1248	-0.16896	-0.0995	-0.14366
		Level 2	0.1385	-0.16896	-0.1007	-0.13116
		Level 3	0.151	-0.16896	-0.1064	-0.12436
		Level 4	0.1546	-0.16896	-0.1091	-0.12346
		Level 5	0.1651	-0.16896	-0.1093	-0.11316
		Level 6	0.1772	-0.16896	-0.11154	-0.1033

BUS 12	50 MW	Level 1	0.1647	-0.1273	-0.1088	-0.0714
		Level 2	0.1598	-0.1273	-0.0899	-0.0574
		Level 3	0.1508	-0.1273	-0.0822	-0.0587
		Level 4	0.1487	-0.1273	-0.075	-0.0536
		Level 5	0.1123	-0.1273	-0.0557	-0.0707
		Level 6	0.09996	-0.1273	-0.05118	-0.07852
	100 MW	Level 1	0.1001	-0.144	-0.0521	-0.096
		Level 2	0.1007	-0.144	-0.0529	-0.0962
		Level 3	0.1065	-0.144	-0.0534	-0.0909
		Level 4	0.1213	-0.144	-0.0547	-0.0774
		Level 5	0.1226	-0.144	-0.0562	-0.0776
		Level 6	0.1237	-0.144	-0.0574	-0.0777
	300 MW	Level 1	0.1719	-0.15213	-0.0588	-0.03903
		Level 2	0.1729	-0.15213	-0.0622	-0.04143
		Level 3	0.1897	-0.15213	-0.0641	-0.02653
		Level 4	0.2023	-0.15213	-0.0646	-0.01443
		Level 5	0.2076	-0.15213	-0.0651	-0.00963
		Level 6	0.2162	-0.15213	-0.06897	-0.0049
BUS 14	50 MW	Level 1	0.1796	-0.15746	-0.0695	-0.04736
		Level 2	0.1551	-0.15746	-0.0703	-0.07266
		Level 3	0.1445	-0.15746	-0.0948	-0.10776
		Level 4	0.1435	-0.15746	-0.1154	-0.12936
		Level 5	0.0796	-0.15746	-0.1337	-0.21156
		Level 6	0.0665	-0.15746	-0.15286	-0.24382
	100 MW	Level 1	0.0663	-0.2088	-0.1531	-0.2956
		Level 2	0.0621	-0.2088	-0.1538	-0.3005
		Level 3	0.062	-0.2088	-0.1542	-0.301
		Level 4	0.059	-0.2088	-0.1544	-0.3042
		Level 5	0.0577	-0.2088	-0.1549	-0.306
		Level 6	0.0574	-0.2088	-0.1551	-0.3065
	300 MW	Level 1	-0.0146	-0.2145	-0.1552	-0.3843
		Level 2	-0.0307	-0.2145	-0.1555	-0.4007
		Level 3	-0.1104	-0.2145	-0.1559	-0.4808
		Level 4	-0.1112	-0.2145	-0.156	-0.4817
		Level 5	-0.1292	-0.2145	-0.15601	-0.49971
		Level 6	-0.1529	-0.2145	-0.15609	-0.52349

BUS 17	50 MW	Level 1	-0.1748	-0.01937	-0.1466	-0.34077
		Level 2	-0.1832	-0.01937	-0.1036	-0.30617
		Level 3	-0.184	-0.01937	-0.0595	-0.26287
		Level 4	-0.184	-0.01937	-0.0453	-0.24867
		Level 5	-0.1928	-0.01937	-0.0388	-0.25097
		Level 6	-0.1941	-0.01937	-0.01237	-0.22584
	100 MW	Level 1	-0.2052	-0.0259	-0.0124	-0.2435
		Level 2	-0.2213	-0.0259	-0.0126	-0.2598
		Level 3	-0.225	-0.0259	-0.0128	-0.2637
		Level 4	-0.2688	-0.0259	-0.0131	-0.3078
		Level 5	-0.2823	-0.0259	-0.014	-0.3222
		Level 6	-0.2978	-0.0259	-0.01453	-0.33823
	300 MW	Level 1	-0.6913	-0.04224	-0.0143	-0.74784
		Level 2	-0.998	-0.04224	-0.0142	-1.05444
		Level 3	-1.3427	-0.04224	-0.0141	-1.39904
		Level 4	-1.456	-0.04224	-0.014	-1.51224
		Level 5	-1.5263	-0.04224	-0.0138	-1.58234
		Level 6	-1.5375	-0.04224	-0.01353	-1.59327
BUS 19	50 MW	Level 1	-1.4893	-0.07689	-0.0149	-1.58109
		Level 2	-1.2606	-0.07689	-0.0171	-1.35459
		Level 3	-1.2339	-0.07689	-0.0335	-1.34429
		Level 4	-0.5371	-0.07689	-0.0554	-0.66939
		Level 5	-0.4077	-0.07689	-0.064	-0.54859
		Level 6	-0.00878	-0.07689	-0.06941	-0.15508
	100 MW	Level 1	-0.011	-0.0847	-0.0694	-0.1651
		Level 2	-0.0124	-0.0847	-0.0695	-0.1666
		Level 3	-0.0173	-0.0847	-0.07	-0.172
		Level 4	-0.022	-0.0847	-0.0701	-0.1768
		Level 5	-0.0237	-0.0847	-0.0703	-0.1787
		Level 6	-0.0327	-0.0847	-0.0804	-0.1978
	300 MW	Level 1	-0.2393	-0.09075	-0.081	-0.41105
		Level 2	-0.272	-0.09075	-0.0813	-0.44405
		Level 3	-0.2879	-0.09075	-0.0817	-0.46035
		Level 4	-0.2934	-0.09075	-0.0817	-0.46585
		Level 5	-0.297	-0.09075	-0.0818	-0.46955
		Level 6	-0.3947	-0.09075	-0.08184	-0.56729

BUS 20	50 MW	Level 1	-0.3579	-0.06321	-0.0814	-0.50251
		Level 2	-0.3232	-0.06321	-0.0726	-0.45901
		Level 3	-0.3022	-0.06321	-0.0703	-0.43571
		Level 4	-0.1877	-0.06321	-0.0666	-0.31751
		Level 5	-0.0415	-0.06321	-0.057	-0.16171
		Level 6	0.01686	-0.06321	-0.0545	-0.10085
	100 MW	Level 1	0.0156	-0.0755	-0.0561	-0.116
		Level 2	0.0152	-0.0755	-0.0586	-0.1189
		Level 3	0.015	-0.0755	-0.0601	-0.1206
		Level 4	0.0147	-0.0755	-0.0634	-0.1242
		Level 5	0.0145	-0.0755	-0.0672	-0.1282
		Level 6	0.0142	-0.0755	-0.0675	-0.1288
	300 MW	Level 1	0.0095	-0.07656	-0.0672	-0.13426
		Level 2	-0.0007	-0.07656	-0.0664	-0.14366
		Level 3	-0.018	-0.07656	-0.0652	-0.15976
		Level 4	-0.033	-0.07656	-0.0643	-0.17386
		Level 5	-0.0613	-0.07656	-0.0619	-0.19976
		Level 6	-0.0671	-0.07656	-0.06303	-0.20669
BUS 24	50 MW	Level 1	-0.0325	-0.1116	-0.0678	-0.2119
		Level 2	-0.0265	-0.1116	-0.0704	-0.2085
		Level 3	-0.0256	-0.1116	-0.0781	-0.2153
		Level 4	0.0043	-0.1116	-0.0815	-0.1888
		Level 5	0.0261	-0.1116	-0.0864	-0.1719
		Level 6	0.04557	-0.1116	-0.08642	-0.15245
	100 MW	Level 1	0.0426	-0.1458	-0.0911	-0.1943
		Level 2	0.0331	-0.1458	-0.1046	-0.2173
		Level 3	0.0242	-0.1458	-0.1048	-0.2264
		Level 4	0.0162	-0.1458	-0.1053	-0.2349
		Level 5	0.0195	-0.1458	-0.1064	-0.2327
		Level 6	0.0038	-0.1458	-0.1085	-0.2505
	300 MW	Level 1	-0.1809	-0.1881	-0.1224	-0.4914
		Level 2	-0.2939	-0.1881	-0.1388	-0.6208
		Level 3	-0.2951	-0.1881	-0.1743	-0.6575
		Level 4	-0.3239	-0.1881	-0.1754	-0.6874
		Level 5	-0.4942	-0.1881	-0.1794	-0.8617
		Level 6	-0.5874	-0.1881	-0.198	-0.9735

The developed procedure results in an abundance of data regarding the bus number and the WBDG size. The candidate buses for WBDG installation are only the load buses and the connecting buses; i.e., no generator buses were considered.

During the analysis, it was noted that the maximum voltage variations (fluctuations) appear on the bus at which the WBDG is installed. It was also noted that, based on the above results, changing the size and location of the WBDG has a significant impact on the total system losses. In this example the losses vary from a worst case of a 24.2 % increase in total losses, when no WBDG is connected to the system, to the best case of a 0.5 % decrease in total losses, when a WBDG's full rating of 300 MW is installed. The results also show that both the voltage profile and the short circuit level are only slightly changed due to changes in the WBDG size, compared to the considerable changes that occur in the total system losses.

As can be seen in Table 7.4, the summation of all the weighted impact is at a maximum at bus (10) with the full 300 MW rating of the WBDG installed (the highlighted cell); i.e., the optimum location for the installation of a DG is bus (10), and of the three sizes available, the optimum full size of the WBDG is 300 MW.

For the second test, it was assumed that the planner has a serious problem with voltage fluctuation in the system, while the other two impacts, i.e., the total losses and the short circuit level, are of less importance. The weighting factors selected therefore will differ from the ones in the previous scenario and were given the following values: 0.2 for the system power losses, 0.2 for the short circuit level, and -0.6 for the voltage fluctuations. The application of these weighting factors in the algorithm results in changes to both the optimum size and location of the DG. The new optimum size was found to be 50 MW, with the optimum location being bus (3).

These results can be refined if the number of WBDG sizes available is increased and/or if other impact is added to the optimization problem.

7.7 Conclusion

This chapter has presented a simple, efficient, and flexible method of optimally determining the size and location of a wind-based DG to be installed in a large mesh interconnected system. The developed optimization technique has been proven to be highly practical for application in large systems, which could otherwise be computationally intensive. The new technique has been applied to a 24-bus distribution system. For the test system selected, it was found that the optimum size and location of the WBDG can be readily calculated using the developed procedure. The new technique incorporates the planner knowledge of the system through his selection of appropriate weighting factors. It has been shown that changing the weighting factors also changes the selection of the optimum size and location of the WBDG.

Total system losses, voltage drops and system short circuit levels were used in the formulation of the cost function for the optimization of the size and location of the wind-based distributed generation. This work can easily be extended to include additional parameters in the optimization problem.

Chapter 8
Contributions and Future Work

8.1 Contributions of the Research

The main contributions of the research presented in this thesis can be summarized as follows:

1. This thesis has presented a comprehensive overview of the current state of the art with respect to the technology associated with of wind energy conversion systems and also underlines research techniques in other areas related to this field. The positive and negative impact of integrating large-scale wind energy conversion systems into the electrical grid has been highlighted and analyzed in details. This focus was motivated by the current trend towards the integration of renewable sources of energy and by the global boom in wind power technologies.
2. The leveling technique introduced in this research is a novel control technique that overcomes the drawbacks of existing power fluctuation mitigation techniques, helps to elevate the performance of WECSs from a system point of view, and facilitates an increase in the penetration level of WECSs. This control technique utilizes available on-site wind speed data in a fast and efficient manner to, on one hand, reduce the wind power fluctuation and allow the system operator to make better operational decisions and, on the other hand, minimize energy losses throughout the year. The following are some advantages of the proposed leveling control technique:
    a. The developed control technique converts the non-dispatchable wind power generation to a disbatchable one.
    b. The developed control technique relies on actual on-site wind speed data, i.e., chronological data. Therefore, the controller outcome that consists of the number of levels and the value of these levels are efficient, reliable, and intelligent.
    c. The developed control technique integrates techniques from different fields of engineering, e.g., data mining, optimization, and power systems.

d. The developed control technique ensures that power fluctuations are minimized because the generator produces constant amounts of power for longer periods of time. As a result, the penetration level of the WECSs could be increased.
e. The developed control technique lowers the negative impact on the power system.
f. The new technique enhances the accuracy of predictions because it predicts only the speed range and not the exact value of the speed.
g. Since the output power generated can be predicted accurately, the system operator can reduce the assigned reserves, and the operation of the power system generation pool becomes more manageable; i.e., the system operator can make better operational decisions.
h. Modifications to the existing turbine and/or generator controller enable this control technique to be applied to all four types of wind energy conversion systems.
i. The developed control technique is applicable to the already installed WECSs because the required modifications are minimal.

3. The developed control technique was successfully applied to the two types of WECSs that represent the largest share of the current market; i.e., Type A and Type C.
4. This thesis has presented explicit analyses of the modifications required for the two types of WECSs, thus offering investors alternatives accompanied by a detailed economic study.
5. The developed leveling technique reduces the wind power fluctuation and hence facilitates the increase of wind penetration level.
6. This research was expanded to cover not only the operational planning that is enhanced by the leveling control technique and its application to the different types of WECSs, but also long-term planning that helps to determine the most appropriate location and the optimum size for the WECS. The long-term planning approach presented is superior to existing methods that rely on limited system parameters and

offers the advantages of simplicity, efficiency, and consideration of a wide range of system parameters. The following are some advantages of the proposed long-term planning criteria:

a. The developed planning criteria introduce two new parameters to the optimization problem, i.e., the voltage fluctuations due to the wind power fluctuations and the contribution of the wind generator to the short-circuit level.
b. The developed planning criteria establish the leveling technique in the optimization problem.
c. The developed planning criteria replace the black-boxed optimization techniques by a simple, flexible, and efficient technique.
d. The developed planning criteria incorporate the planners experience to optimally determine the site and size of the WBDG.

8.2 Scope of Future Work

This study has established a new direction for research related to wind energy conversion systems with respect to reducing or eliminating the power fluctuations, which are considered the main challenge in the integration of WECSs into electric networks. Based on the research presented in this thesis, the following is a summary of studies that could be conducted in the future:

1. Apply the power leveling technique to Type D WECS by modifying the converter controller.
2. Combine the leveling technique and the size of the storage device in a global optimization problem.
3. Investigate the wind power fluctuations over the proposed battery storage device.
4. Apply the leveling technique to photo-voltaic (PV) systems. This investigation could be performed by modelling a variety of PV system topologies, collecting irradiance and temperature data from the candidate site, entering the data collected into a two-

way unsupervised clustering technique in order to determine the number and values of the power levels, and modifying the controller of the PV system to accommodate the leveling technique.

Bibliography

[1] F. Blaabjerg, R. Teodorescu, M. Liserre, and A. V. A. T. A. V. Timbus, "Overview of Control and Grid Synchronization for Distributed Power Generation Systems," *IEEE Transactions on Industrial Electronics, ,* vol. 53, pp. 1398-1409, 2006.

[2] F. Blaabjerg, C. Zhe, and S. B. Kjaer, "Power electronics as efficient interface in dispersed power generation systems," *IEEE Transactions on Power Electronics,,* vol. 19, pp. 1184-1194, 2004.

[3] J. L. Del Monaco, "The role of distributed generation in the critical electric power infrastructure," in *IEEE-Power Engineering Society Winter Meeting*, 2001, pp. 144-145 vol.1.

[4] J. Gutierrez-Vera, "Use of renewable sources of energy in Mexico case: San Antonio Agua Bendita," *IEEE Transaction on Energy Conversion, ,* vol. 9, pp. 442-450, 1994.

[5] L. Philipson, "Distributed and dispersed generation: addressing the spectrum of consumer needs," in *IEEE Power Engineering Society Summer Meeting, ,* 2000, pp. 1663-1665 vol. 3.

[6] L. Soder, L. Hofmann, A. Orths, H. A. H. H. Holttinen, Y. A. W. Y. Wan, and A. A. T. A. Tuohy, "Experience From Wind Integration in Some High Penetration Areas," *IEEE Transaction on Energy Conversion, ,* vol. 22, pp. 4-12, 2007.

[7] T. Thiringer, T. Petru, and S. Lundberg, "Flicker contribution from wind turbine installations," *IEEE Transaction on Energy Conversion, ,* vol. 19, pp. 157-163, 2004.

[8] A. Feijoo and J. Cidras, "Analysis of mechanical power fluctuations in asynchronous WECs," *IEEE Transaction on Energy Conversion,,* vol. 14, pp. 284-291, 1999.

[9] L. Changling, H. G. Far, H. Banakar, A. P.-K. K. Ping-Kwan Keung, and A. B.-T. O. Boon-Teck Ooi, "Estimation of Wind Penetration as Limited by Frequency Deviation," *IEEE Transaction on Energy Conversion, ,* vol. 22, pp. 783-791, 2007.

[10] Y. J. Hsu and C. N. Lu, "Flicker measurements at an industrial power network with wind turbines," in *IEEE-Power Engineering Society General Meeting,*, 2006, p. 5 pp.

[11] T. Senjyu, R. Sakamoto, N. Urasaki, T. A. F. T. Funabashi, and H. A. S. H. Sekine, "Output power leveling of wind farm using pitch angle control with fuzzy neural network," in *IEEE-Power Engineering Society General Meeting,*, 2006, p. 8 pp.

[12] T. Senjyu, R. Sakamoto, N. Urasaki, T. A. F. T. Funabashi, H. A. F. H. Fujita, and H. A. S. H. Sekine, "Output power leveling of wind turbine Generator for all operating regions by pitch angle control," *IEEE Transaction on Energy Conversion, ,* vol. 21, pp. 467-475, 2006.

[13] C. Carrillo, A. E. Feijoo, J. Cidras, and J. A. G. J. Gonzalez, "Power fluctuations in an isolated wind plant," *IEEE Transaction on Energy Conversion,,* vol. 19, pp. 217-221, 2004.

[14] H. Banarkar, L. Changling, and O. Boon-Teck, "Power System Response to Wind Power Fluctuations," in *IEEE PES-Transmission and Distribution Conference and Exhibition,*, 2006, pp. 1445-1452.

[15] B. Mary and S. Goran, "Value of Bulk Energy Storage for Managing Wind Power Fluctuations," *IEEE Transaction on Energy Conversion, ,* vol. 22, pp. 197-205, 2007.

[16] L. Changling and O. Boon-Teck, "Frequency deviation of thermal power plants due to wind farms," *IEEE Transaction on Energy Conversion, ,* vol. 21, pp. 708-716, 2006.

[17] L. Changling, H. Banakar, S. Baike, and O. Boon-Teck, "Strategies to Smooth Wind Power Fluctuations of Wind Turbine Generator," *IEEE Transaction on Energy Conversion, ,* vol. 22, pp. 341-349, 2007.

[18] H. Banakar, L. Changling, and O. Boon Teck, "Impacts of Wind Power Minute-to-Minute Variations on Power System Operation," *IEEE Transactions on Power Systems, ,* vol. 23, pp. 150-160, 2008.

[19] P. Sorensen, N. A. Cutululis, A. Vigueras-Rodriguez, L. E. Jensen, J. Hjerrild, M. H. Donovan, and H. Madsen, "Power Fluctuations From Large Wind Farms," *IEEE Transactions on Power Systems,*, vol. 22, pp. 958-965, 2007.

[20] B. C. Ummels, M. Gibescu, E. Pelgrum, W. L. A. K. W. L. Kling, and A. J. A. B. A. J. Brand, "Impacts of Wind Power on Thermal Generation Unit Commitment and Dispatch," *IEEE Transaction on Energy Conversion, ,* vol. 22, pp. 44-51, 2007.

[21] S. Galloway, G. Bell, G. Burt, J. A. M. J. McDonald, and T. A. S. T. Siewierski, "Managing the risk of trading wind energy in a competitive market," *IEE Proceedings-Generation, Transmission and Distribution, ,* vol. 153, pp. 106-114, 2006.

[22] S. Roy, "Market constrained optimal planning for wind energy conversion systems over multiple installation sites," *IEEE Transaction on Energy Conversion,,* vol. 17, pp. 124-129, 2002.

[23] J. Matevosyan and L. Soder, "Minimization of imbalance cost trading wind power on the short-term power market," *IEEE Transactions on Power Systems, ,* vol. 21, pp. 1396-1404, 2006.

[24] C. Saniter and J. Janning, "Test Bench for Grid Code Simulations for Multi-MW Wind Turbines, Design and Control," *IEEE Transactions on Power Electronics, ,* vol. 23, pp. 1707-1715, 2008.

[25] E. Gomez-Lazaro, M. Canas, J. A. Fuentes, and A. Molina-Garcia, "Characterization of Measured Voltage Dips in Wind Farms in the Light of the New Grid Codes," in *2007 IEEE Lausanne on Power Tech, ,* 2007, pp. 2059-2064.

[26] "SIOUX VALLEY ENERGY INTERCONNECTION REQUIREMENTS FOR CUSTOMER-OWNED GENERATION," 2002.

[27] A. Murdoch, J. R. Winkelman, S. H. Javid, and R. S. A. B. R. S. Barton, "Control Design and Performance Analysis of a 6 MW Wind Turbine-Generator," *IEEE Transactions on Power Apparatus and Systems,* vol. PAS-102, pp. 1340-1347, 1983.

[28] P. D. Brown, J. A. Peas Lopes, and M. A. Matos, "Optimization of Pumped Storage Capacity in an Isolated Power System With Large Renewable Penetration," *IEEE Transactions on Power Systems, ,* vol. 23, pp. 523-531, 2008.

[29] X. Y. Wang, D. Mahinda Vilathgamuwa, and S. S. Choi, "Determination of Battery Storage Capacity in Energy Buffer for Wind Farm," *IEEE Transaction on Energy Conversion, ,* vol. 23, pp. 868-878, 2008.

[30] L. Meeus and R. Belmans, "Is the prevailing wholesale market design in Europe and North America comparable?," in *IEEE-Power Engineering Society General Meeting, ,* 2007, pp. 1-5.

[31] T. H. M. EL-Fouly, "Wind Farms Production: Control and Prediction," in *Electric and Computer Engineering*. vol. PhD Waterloo: University of Waterloo, 2007.

[32] A. M. De Broe, S. Drouilhet, and V. Gevorgian, "A peak power tracker for small wind turbines in battery charging applications," *IEEE Transaction on Energy Conversion, ,* vol. 14, pp. 1630-1635, 1999.

[33] E. S. Abdin and W. Xu, "Control design and dynamic performance analysis of a wind turbine-induction generator unit," *IEEE Transaction on Energy Conversion, ,* vol. 15, pp. 91-96, 2000.

[34] W. Xifan, D. Hui-Zhu, and R. J. Thomas, "Reliability Modeling of Large Wind Farms and Associateed Electric Utility Interface Systems," *IEEE transactions on power apparatus and systems,* vol. PAS-103, pp. 569-575, 1984.

[35] "LARGE SCALE INTEGRATION OF WIND ENERGY IN THE EUROPEAN POWER SUPPLY: analysis, issues and recommendations," The European Wind Energy Association 2006.
[36] C. Woei-Luen and H. Yuan-Yih, "Controller design for an induction generator driven by a variable-speed wind turbine," *IEEE Transaction on Energy Conversion, ,* vol. 21, pp. 625-635, 2006.
[37] L. L. Freris, "Wind Energy Conversion Systems," Englewood Cliffs, NJ: Prentice-Hall, 1990.
[38] J. L. Rodriguez-Amenedo, S. Arnalte, and J. C. Burgos, "Automatic generation control of a wind farm with variable speed wind turbines," *IEEE Transaction on Energy Conversion,,* vol. 17, pp. 279-284, 2002.
[39] P. Ledesma and J. Usaola, "Doubly fed induction generator model for transient stability analysis," *IEEE Transaction on Energy Conversion, ,* vol. 20, pp. 388-397, 2005.
[40] E. Muljadi and C. P. Butterfield, "Pitch-controlled variable-speed wind turbine generation," *IEEE Transactions on Industry Applications, ,* vol. 37, pp. 240-246, 2001.
[41] R. Pena, J. C. Clare, and G. M. Asher, "A doubly fed induction generator using back-to-back PWM converters supplying an isolated load from a variable speed wind turbine," *IEE Proceedings -Electric Power Applications,,* vol. 143, pp. 380-387, 1996.
[42] T. A. L. D. W. Novotny, *Vector Control and Dynamics of AC Drives*: Oxford University Press, 1996.
[43] J. Zhenhua and Y. Xunwei, "Modeling and control of an integrated wind power generation and energy storage system," in *IEEE Power & Energy Society General Meeting, 2009. PES '09.*, 2009, pp. 1-8.
[44] R. Datta and V. T. Ranganathan, "Variable-speed wind power generation using doubly fed wound rotor induction machine-a comparison with alternative schemes," *IEEE Transaction on Energy Conversion,,* vol. 17, pp. 414-421, 2002.
[45] A. Petersson, T. Thiringer, L. Harnefors, and T. Petru, "Modeling and experimental verification of grid interaction of a DFIG wind turbine," *IEEE Transaction on Energy Conversion, ,* vol. 20, pp. 878-886, 2005.
[46] J. N. Baker and A. Collinson, "Electrical energy storage at the turn of the Millennium," *Power Engineering Journal,* vol. 13, pp. 107-112, 1999.
[47] M. R. Rathi and N. Mohan, "A novel robust low voltage and fault ride through for wind turbine application operating in weak grids," in *31st Annual Conference of IEEE Industrial Electronics Society, 2005. IECON 2005. ,* 2005, p. 6 pp.
[48] G. O. Cimuca, C. Saudemont, B. Robyns, and M. M. A. R. M. M. Radulescu, "Control and Performance Evaluation of a Flywheel Energy-Storage System Associated to a Variable-Speed Wind Generator," *IEEE Transactions on Industrial Electronics, ,* vol. 53, pp. 1074-1085, 2006.
[49] G. O. Cimuca, C. Saudemont, B. Robyns, and M. M. Radulescu, "Control and Performance Evaluation of a Flywheel Energy-Storage System Associated to a Variable-Speed Wind Generator," *IEEE Transactions on Industrial Electronics, ,* vol. 53, pp. 1074-1085, 2006.
[50] R. Cardenas, R. Pena, G. Asher, and J. Clare, "Control strategies for enhanced power smoothing in wind energy systems using a flywheel driven by a vector-controlled induction machine," *IEEE Transactions on Industrial Electronics, ,* vol. 48, pp. 625-635, 2001.
[51] R. Cardenas, R. Pena, G. Asher, and J. Clare, "Power smoothing in wind generation systems using a sensorless vector controlled induction Machine driving a flywheel," *IEEE Transaction on Energy Conversion,,* vol. 19, pp. 206-216, 2004.
[52] J. P. Barton and D. G. Infield, "Energy storage and its use with intermittent renewable energy," *IEEE Transaction on Energy Conversion, ,* vol. 19, pp. 441-448, 2004.

[53] C. Abbey and G. Joos, "Supercapacitor Energy Storage for Wind Energy Applications," *IEEE Transactions on Industry Applications, ,* vol. 43, pp. 769-776, 2007.
[54] T. Kinjo, T. Senjyu, N. Urasaki, and H. Fujita, "Output levelling of renewable energy by electric double-layer capacitor applied for energy storage system," *IEEE Transaction on Energy Conversion, ,* vol. 21, pp. 221-227, 2006.
[55] D. V. Power, "Bath County Pumped Storage Station," Virginia 2008 Available online at: http://www.dom.com/about/stations/hydro/bath.jsp.
[56] B. S. Borowy and Z. M. Salameh, "Dynamic response of a stand-alone wind energy conversion system with battery energy storage to a wind gust," *IEEE Transaction on Energy Conversion, ,* vol. 12, pp. 73-78, 1997.
[57] L. Tsung-Ying, "Operating Schedule of Battery Energy Storage System in a Time-of-Use Rate Industrial User With Wind Turbine Generators: A Multipass Iteration Particle Swarm Optimization Approach," *IEEE Transaction on Energy Conversion,,* vol. 22, pp. 774-782, 2007.
[58] F. Giraud and Z. M. Salameh, "Steady-state performance of a grid-connected rooftop hybrid wind-photovoltaic power system with battery storage," *IEEE Transaction on Energy Conversion,,* vol. 16, pp. 1-7, 2001.
[59] A. Arulampalam, M. Barnes, N. Jenkins, and J. B. A. E. J. B. Ekanayake, "Power quality and stability improvement of a wind farm using STATCOM supported with hybrid battery energy storage," *IEE Proceedings-Generation, Transmission and Distribution, ,* vol. 153, pp. 701-710, 2006.
[60] J. Svensson, P. Jones, and P. Halvarsson, "Improved power system stability and reliability using innovative energy storage technologies," in *The 8th IEE International Conference on AC and DC Power Transmission, 2006. ACDC 2006. ,* 2006, pp. 220-224.
[61] G. Caralis and A. Zervos, "Analysis of the combined use of wind and pumped storage systems in autonomous Greek islands," *IET On Renewable Power Generation, ,* vol. 1, pp. 49-60, 2007.
[62] V. D. Hunt, "Wind Power: A Handbook on Wind Energy Conversion Systems," Van Nostrand Reinhold Company, 1981.
[63] J. S. Derk, "Compressed Air Energy Storage in an Electricity System With Significant Wind Power Generation," *IEEE Transaction on Energy Conversion, ,* vol. 22, pp. 95-102, 2007.
[64] C. Brunetto and G. Tina, "Optimal hydrogen storage sizing for wind power plants in day ahead electricity market," *IET On Renewable Power Generation, ,* vol. 1, pp. 220-226, 2007.
[65] G. Taljan, C. Canizares, M. Fowler, and G. Verbic, "The Feasibility of Hydrogen Storage for Mixed Wind-Nuclear Power Plants," *IEEE Transactions on Power Systems,,* vol. 23, pp. 1507-1518, 2008.
[66] K. Agbossou, M. Kolhe, J. Hamelin, and T. K. Bose, "Performance of a stand-alone renewable energy system based on energy storage as hydrogen," *IEEE Transaction on Energy Conversion, ,* vol. 19, pp. 633-640, 2004.
[67] M. Korpas and A. T. Holen, "Operation planning of hydrogen storage connected to wind power operating in a power market," *IEEE Transaction on Energy Conversion,,* vol. 21, pp. 742-749, 2006.
[68] E. B. Jack, "Wind Power Energy Storage for <emphasis emphasistype="italic">In Situ</emphasis> Shale Oil Recovery With Minimal CO₂ Emissions," *IEEE Transaction on Energy Conversion, ,* vol. 22, pp. 103-109, 2007.
[69] L. Dong-Jing and W. Li, "Small-Signal Stability Analysis of an Autonomous Hybrid Renewable Energy Power Generation/Energy Storage System Part I: Time-Domain Simulations," *IEEE Transaction on Energy Conversion, ,* vol. 23, pp. 311-320, 2008.

[70] S. Lemofouet and A. Rufer, "A Hybrid Energy Storage System Based on Compressed Air and Supercapacitors With Maximum Efficiency Point Tracking (MEPT)," *IEEE Transactions on Industrial Electronics, ,* vol. 53, pp. 1105-1115, 2006.
[71] L. Tsung-Ying and C. Nanming, "Optimal capacity of the battery energy storage system in a power system," *IEEE Transaction on Energy Conversion,,* vol. 8, pp. 667-673, 1993.
[72] C. Vilar Moreno, H. Amaris Duarte, and J. Usaola Garcia, "Propagation of flicker in electric power networks due to wind energy conversions systems," *IEEE Transaction on Energy Conversion, ,* vol. 17, pp. 267-272, 2002.
[73] D. Iannuzzi, L. Piegari, and R. Rizzo, "A filtering technique to solve flicker problems due to use of induction machines in wind power generation," in *31st Annual Conference of IEEE Industrial Electronics Society, IECON. ,* 2005, p. 6 pp.
[74] S. Tao, C. Zhe, and F. Blaabjerg, "Flicker study on variable speed wind turbines with doubly fed induction generators," *IEEE Transaction on Energy Conversion, ,* vol. 20, pp. 896-905, 2005.
[75] J. S. D. Brooks, E. Lo, S. Ishikawa, L. Dangelmaier, and M. Bradley,, "Development of a methodology for the assessment of system operation impacts of integrating wind generation on a small island power system," in *Proc. Eur. Wind Energy Conf.* London, U.K., 2004.
[76] M. J. Grubb, "Value of variable sources on power systems," *IEE Proc. Generation, Transmission and Distribution, ,* vol. 138, pp. 149-165, 1991.
[77] J. C. Smith, M. R. Milligan, E. A. DeMeo, and B. Parsons, "Utility Wind Integration and Operating Impact State of the Art," *IEEE Transactions on Power Systems, ,* vol. 22, pp. 900-908, 2007.
[78] E. A. DeMeo, W. Grant, M. R. Milligan, and M. J. Schuerger, "Wind plant integration [wind power plants]," *Power and Energy Magazine, IEEE,* vol. 3, pp. 38-46, 2005.
[79] Z. Chen and E. Spooner, "Grid power quality with variable speed wind turbines," *Energy Conversion, IEEE Transaction on,* vol. 16, pp. 148-154, 2001.
[80] R. S. Michalski, "Conceptual Clustering Versus Numerical Taxonomy," *Citeseer Journal,* 1983.
[81] Peter H. Sneath; Robert R. Sokal, *The First Decade of Numerical Taxonomy,* 1973.
[82] B. King, *Step-wise clustering procedures*, 1967.
[83] R. C. Dubes, "How many clusters are best?—an experiment," *Elsevier Science Inc.,* vol. 20, pp. 645 - 663, 1987.
[84] J. MacQueen, "Some methods for classification and analysis of multivariate observations," in *Fifth Berkeley Symposium on Mathematical Statistics and Probability*. vol. 1, J. N. Lucien M. Le Cam, Ed. Statistical Laboratory of the University of California, Berkeley, 1967, pp. 281-297.
[85] Zahn, " A New Graph-Theoretic Approach to Clustering and Segmentation," *Citeseer Journal,* 1971.
[86] L. A. Zadeh, "Fuzzy sets," *Information and Control,* vol. 8, pp. 338-353, 1965.
[87] M. Har-even and V. L. Brailovsky, "Probabilistic validation approach for clustering," *Pattern Recognition Letters,* vol. 16, pp. 1189-1196, 1995.
[88] D. a. M. Pelleg, A.W., "X-means: Extending K-means with efficient estimation of the number of clusters," in *pelleg2000xme,* 2000, pp. 727--734.
[89] T. Ackermann and J. W. Press, *Wind Power in Power Systems*: John Wiley & Sons Ltd, 2003.
[90] Z. Jie, Z. Buhan, M. Chengxiong, and W. Yunling, "Use of Battery Energy Storage System to Improve the Power Quality and Stability of Wind Farms," in *International Conference on Power System Technology, 2006. PowerCon 2006. ,* 2006, pp. 1-6.

[91] L. Hui, D. Cartes, M. Steurer, and T. Haibin, "Control design of STATCOM with superconductive magnetic energy storage," *IEEE Transactions on Applied Superconductivity*, vol. 15, pp. 1883-1886, 2005.
[92] Z. M. Salameh, M. A. Casacca, and W. A. Lynch, "A mathematical model for lead-acid batteries," *IEEE Transactions on Energy Conversion*, vol. 7, pp. 93-98, 1992.
[93] Y. M. Atwa and E. F. El-Saadany, "Optimal Allocation of ESS in Distribution Systems With a High Penetration of Wind Energy," *IEEE Transactions on Power Systems, ,* vol. PP, pp. 1-1.
[94] P. Poonpun and W. T. Jewell, "Analysis of the Cost per Kilowatt Hour to Store Electricity," *IEEE Transactions on Energy Conversion*, vol. 23, pp. 529-534, 2008.
[95] "Information from price quotes and performance data provided by energy storage device manufacturers."
[96] S. M. Schoenung and W. V. Hassenzahl, "Long- vs. short-term energy storage technologies analysis: A life-cycle cost study," *Sandia Natl. Lab.Albuquerque, NM, Sandia Rep. SAND2003-2783*, 2003.
[97] H. H. M. Zeineldin, "Distributed generation micro-grid operation : control, protection, and electricity market operation," in *Electric and Computer Engineering*. vol. PhD Waterloo: University of Waterloo, 2006.
[98] F. A. Bhuiyan and A. Yazdani, "Multimode Control of a DFIG-Based Wind-Power Unit for Remote Applications," *IEEE Transactions on Power Delivery, ,* vol. 24, pp. 2079-2089, 2009.
[99] M. M. A. Salama, R. Hackam, and A. Y. Chikhani, "Instructional design of multi-layer insulation of power cables," *Power Systems, IEEE Transactions on*, vol. 7, pp. 377-382, 1992.
[100] R. Billinton and R. N. Allan, *Reliability Assessment of Large Electric Power Systems*: Kluwer Academic Publishers, 1988.
[101] T. Gonen, *Electric Power Distribution System Engineering*, Second Edition ed., 2006.